Regulatory Aspects of DNA Double-Strand Break Repair in the Yeast *Saccharomyces cerevisiae*

Dissertation

zur

Erlangung der naturwissenschaftlichen Doktorwürde
(Dr. sc.nat.)

vorgelegt der

Mathematisch-naturwissenschaftlichen Fakultät

der

Universität Zürich

von

Sanja Kais

aus
Kroatien

Promotionskomitee
Prof. Dr. Josef Jiricny
Prof. Dr. Primo Schär
Prof. Dr. Michael Hengartner

Zürich, 2008

Table of contents:

SUMMARY

Genome stability is of primary importance for the survival and proper functioning of all organisms. Numerous endogenous and exogenous agents damage genomic DNA. Therefore, various systems have evolved to respond to DNA damage and enforce genomic stability.

DNA double-strand breaks (DSBs) are critical lesions that can give rise to genomic instability. They arise spontaneously during cell proliferation when replication polymerases encounter a damaged DNA template or upon impact of free radicals that are generated by the cell metabolism. They can also be created by external influence such as ionizing radiation or DNA-directed drugs. DSBs can be introduced into chromosomes on purpose and in those cases are important for genetic recombination associated with cell differentiation processes, such as meiosis or V(D)J maturation in lymphocytes.

In response to even a single DSB, organisms must trigger a series of events to promote repair that allows survival and restoration of chromosomal integrity. DSBs can be repaired in two fundamentally different ways: homologous recombination (HR) and non-homologous end joining (NHEJ). In HR, undamaged homologous donor sequence is used as a template for repair, while in NHEJ direct ligation of broken ends is performed without the need for sequence homology. Both processes are conserved in evolution. To ensure accurate repair, cells must regulate and/or balance these potentially competing DSB repair pathways. The mechanism underlying coordinated engagement of these pathways are poorly understood.

The aim of this thesis was to provide insight into how yeast cells discriminate between HR and NHEJ. For that purpose, two approaches were pursued. (I) a functional characterization of Ntr1, a newly discovered NHEJ protein with putative regulatory function in NHEJ, and (II) evaluation of the role of HR and NHEJ in the generation and repair of DSBs occurring at the naturally stalled replication forks in yeast ribosomal DNA (rDNA) locus.

Ntr1 was identified through a yeast two-hybrid screening for Lif1-interacting partners. This interaction was confirmed by co-immunoprecipitation and the interaction domains of both proteins were mapped. This mapping revealed that Ntr1 binds to the Dnl4-interacting domain of Lif1. Yeast three-hybrid experiments further showed that Lif1 forms two mutually exclusive complexes involving either Dnl4 or Ntr1. As disruption of *NTR1* was incompatible with cell viability and conditional "knock-out" strategies failed, I addressed possible effects of Ntr1 on DSB repair by overexpression of the protein. This showed that an overabundance of Ntr1 reduced NHEJ efficiency but not accuracy of NHEJ. Localization studies using EGFP-Ntr1 demonstrated a nuclear localization of Ntr1 with a distinct focal pattern. This localization was not dependent on presence of either Lif1 or DNA damage. EGFP-Ntr1 foci colocalized with telomeric protein Rap1 and partially with nucleolar Nop1. Furthermore, Ntr1 interacts with PinX1, another G-patch protein that has dual functions in the regulation of telomerase activity and telomere stability. Taken together, our data allowed us to propose a function for Ntr1 in inhibiting NHEJ by sequestering Lif1 in inactive complex or mediating the disassembly of active Lif1-Dnl4 complex at the sites where Ntr1 is enriched, namely in the nucleolus or at the telomeres.

To directly study the contribution of NHEJ and HR to replication fork stability, we monitored the generation and repair of DSBs occurring at a natural fork-pausing site in the yeast rDNA. S-phase- and Fob1-dependent DSBs arise at these sites during unperturbed growth conditions (Burkhalter and Sogo 2004) and are most probably a consequence of fork stalling at the replication fork barrier (RFB). To examine the processes involved in generation and/or repair of those breaks, we monitored DSB levels in cells deficient for factors influencing replication fork stability (*sgs1* and *top3*) and/or DSB repair (*rad52* and *dnl4*). We used 2D DNA gel electrophoresis and electron microscopy to characterize and quantify molecular transactions at the RFB. We detected increased levels of DSBs in *sgs1* and *top3* mutant cells. Surprisingly, the highest levels of DSBs were measured in a *dnl4* mutant background, establishing for the first

time an involvement of this DNA ligase and thus, presumably NHEJ, in the repair of S-phase dependent DSBs. By contrast, *rad52* mutant cells had wild-type levels of DSBs and Rad52 defect suppressed the effects observed in *sgs1* and *dnl4* mutant cells. This suggested a novel Rad52 role in the generation of DSBs occurring at the RFB. Our data allow to propose a model postulating a role for Rad52-dependent process in the generation of aberrant replication structures that can break either spontaneously or through the action of structure-specific nucleases such as Mus81-Mms4. Once broken, the replication fork can be re-established through HR (BIR) or, in situations where two forks converge at the RFB, by NHEJ.

ZUSAMMENFASSUNG

Die Erhaltung der Stabilität des Zellgenoms ist für das Überleben und einwandfreie Funktionieren aller Organismen von absoluter Notwendigkeit. Zahlreiche endogene und exogene Einflüsse beschädigen die genomische DNS (Desoxyribonukleinsäure). Daher haben sich verschiedene Systeme entwickelt, die auf diese Schäden reagieren und zur Genom-Stabilität beitragen können.

DNS Doppelstrangbrüche (*engl.* double strand breaks=DSBs) stellen kritische Läsionen dar, die zur Genom-Instabilität führen können. Sie entstehen spontan während der Zellproliferation, wenn Replikationspolymerasen auf beschädigte DNS-Matrizen treffen, oder nach der Reaktion der DNS mit reaktiven Zwischenprodukten des normalen Zellmetabolismus. Ausserdem können äussere Einflüsse wie ionisierende Strahlen oder chemische Substanzen, die mit der DNS interagieren (z.B. Chemotherapeutika), DSBs verursachen. DSBs werden jedoch physiologischerweise von der Zelle auch selbst generiert, beispielsweise im Rahmen der genetischen Rekombination während Zelldifferenzierungsprozessen wie Meiose oder der Reifung von Lymphozyten (V(D)J-Rekombination).

Als Antwort auf nur einen einzigen DSB müssen Organismen eine Serie von Prozessen auslösen können, die die Reparatur begünstigen und in der Folge das Überleben und die Wiederherstellung der chromosomalen Integrität sicherstellen. DSBs werden auf zwei fundamental verschiedene Arten repariert: Durch homologe Rekombination (*engl.* homologous recombination=HR) und nicht-homologes Zusammenfügen der gebrochenen DNS-Enden (*engl.* non-homologous end joining=NHEJ). Im Laufe der homologen Rekombination wird die unbeschädigte homologe DNS-Sequenz als Vorlage für die Reparatur des beschädigten DNS-Stranges genutzt, während der NHEJ-Prozess eine direkte Ligation der gebrochenen DNS-Enden umfasst, ohne dass die Notwendigkeit eines homologen intakten DNS-Stranges besteht. Beide Prozesse blieben während der Evolution konserviert. Denn um eine genaue Reparatur zu garantieren, müssen Zellen einen Weg finden, diese zwei potentiell

konkurrierenden DSB-Reparatur-Prozesse zu regulieren und/oder zu koordinieren. Der diesem koordinierten Eingreifen beider Prozesse zugrunde liegende Mechanismus versteht man heute kaum.

Das Ziel dieser Doktorarbeit bestand darin, herauszufinden, wie Hefe-Zellen zwischen den beiden zur Verfügung stehenden DSB-Reparaturwegen entscheiden. Zu diesem Zweck wurden zwei verschiedene Strategien verfolgt: (1.) Eine funktionelle Charakterisierung von Ntr1, eines neu entdeckten Proteins mit einer vermutlich regulatorischen Funktion im NHEJ-Prozess, und (2.) eine Untersuchung der Rollen, die HR und NHEJ während der Entstehung und Reparatur von DSBs an physiologisch blockierten Replikationsgabeln im ribosomalen DNS (rDNS)-Lokus in der Hefe spielen.

Ntr1 wurde in der Hefe mithilfe eines „Two-Hybrid-Screenings" für mit Lif1 interagierende Partner identifiziert. Diese chemische Interaktion wurde mittels Koimmunopräzipitation bestätigt und die miteinander in Wechselwirkung tretenden Domänen beider Proteine charakterisiert. Funktionelle Untersuchungen der Domänen ergaben, dass Ntr1 an die mit Dnl4 interagierend Domäne von Lif1 bindet. „Three-Hybrid"-Experimente in der Hefe zeigten weiter, dass Lif1, entweder mit Dnl4 oder Ntr1, zwei sich gegenseitig ausschliessende Komplexe bildet. Da das Ausschalten von *NTR1* mit dem Überleben der Zelle nicht vereinbar war und konditionelle „knock-out"-Strategien erfolglos blieben, untersuchten wir mögliche Effekte von Ntr1 auf die DSB-Reparatur mithilfe einer Überexpression des Proteins. Dabei konnte gezeigt werden, dass ein Überfluss an Ntr1 die Effizienz des NHEJ-Prozesses reduzierte, ohne jedoch seine Genauigkeit zu beeinflussen. Lokalisierungsstudien, die EGFP-markiertes Ntr1 benutzten, zeigten, dass Ntr1 im Zellnukleus nach einem ganz bestimmten fokalen Muster vorkommt. Diese Lokalisierung war von der Präsenz von entweder Lif1 oder einer DNS-Schädigung unabhängig. EGFP-Ntr1p-Foki konnten mit dem Telomer-Protein Rap1 und partiell auch mit dem nukleolären Nop1 kolokalisiert werden. Darüber hinaus interagierte Ntr1 mit PinX1, einem weiteren „G-patch"-Protein, welches mit der Regulation der Telomerase-Aktivität und -Stabilität eine Doppelfunktion besitzt. Zusammenfassend erlauben unsere Daten, Ntr1 eine Funktion in der Hemmung von NHEJ zuzuordnen. Diese Inhibition kommt durch

Sequestrierung von Lif1, was zu einem inaktiven Komplex führt, und durch Vermittlung der Auflösung des aktiven Lif1-Dnl4-Komplexes an Stellen, wo Ntr1 angereichert ist, namentlich im Nukleolus und an Telomeren, zustande.

Um den Beitrag von NHEJ und HR zur Stabilität von DNS-Replikationsgabeln direkt zu studieren, überwachten wir die Entstehung und Reparatur von DSBs an einem Ort, wo Replikationsbarrieren natürlicherweise vorkommen, in der rDNS der Hefe. S-Phasen- und Fob1p-abhängige DSBs entstehen an diesen Orten unter ungestörten Wachstumsbedingungen (Burkhalter und Sogo, 2004) und stellen höchst wahrscheinlich eine Konsequenz der Blockierung von Replikationsgabeln an der Replikations-Barriere (*engl.* Replication fork barrier=RFB) dar. Um die Prozesse, die an der Entstehung und/oder Reparatur solcher DNS-Brüche beteiligt sind, untersuchen zu können, überwachten wir die Anzahl der DSBs in Zellen, die für Faktoren, welche die Stabilität von Replikationsgabeln (*sgs1* und *top3*) und/oder die DSB-Reparatur (*rad52* und *dnl4*) beeinflussen, defizient sind. Zur Charakterisierung und Quantifizierung der molekularen Transaktionen an der RFB benutzten wir die 2D-DNS-Gel-Elektrophorese und die Elektronenmikroskopie. Wir detektierten eine erhöhte Anzahl von DSBs in *sgs1*- und *top3*-mutierten Zellen. Überraschenderweise wurde die grösste Anzahl DSBs vor dem Hintergrund einer *dnl4*-Mutante gemessen, was zum ersten Mal auf eine Involvierung dieser DNS-Ligase und damit wahrscheinlich NHEJ in der Reparatur von S-Phasen-abhängigen DSBs hinweist. Im Gegensatz dazu zeigten *rad52*-mutierte Zellen Wildtyp-entsprechende Mengen von DSBs und Defekte in Rad52 unterdrückten die Effekte, die in *sgs1*- und *dnl4*-mutierten Zellen beobachtet wurden. Diese Ergebnisse deuten auf eine neuartige Rolle von Rad52 in der Entstehung von DSBs, die sich an der RFB ereignen. Unsere Daten erlauben es, ein Modell vorzuschlagen, das ein Rad52-abhängiger Prozess bei der Entstehung von aberranter Replikationsstrukturen vorsieht, welche in der Folge entweder spontan oder aufgrund der Einwirkung strukturenspezifischer Nukleasen wie Mus81-Mms4 brechen. Einmal gebrochen kann die Replikationsgabel mithilfe von HR (BIR) oder, in Situationen, wo an der RFB zwei Gabeln konvergieren, mithilfe von NHEJ wiederhergestellt werden.

1. Introduction

The preservation of genomic integrity is crucial for all organisms. DNA, the carrier of genetic information, constantly acquires lesions. Current estimates say that, a single human cell encounters approximately 10^4 to 10^6 DNA-damage events per day (Friedberg et al 1995). These DNA modifications can lead to mutations and have severe effects if not repaired. To counter the consequences of DNA damage, various DNA repair systems have evolved, each of which is directed against specific types of lesions. If cells are not able to cope with the damage load, programmed cell death may be activated to avoid the proliferation of defective cells.

1.1. DNA double-strand breaks

Although DNA double-strand breaks (DSBs) are formed much less frequently than other forms of DNA damage, the consequences of DSBs can be very severe. If left unrepaired, DSBs result in broken chromosomes. Broken DNA ends cannot be transcribed or replicated, and misrepaired DNA ends can cause chromosomal rearrangements, which are associated with tumor formation in mammals, or cell death (Rothkamm and Lobrich 2002).

DSBs form as a consequence of exposure to external mutagens or as a result of natural cell metabolism. They can be induced by a variety of chemical and physical agents, either directly or indirectly. Topoisomerase inhibitors and DNA methylating agents (e.g. MMS) cause DSBs indirectly; the primary damage is a single-strand break which is converted to a DSB through replication or repair process. DNA inter- or intrastrand crosslinking agents like cisplatin (Fichtinger-Schepman et al 1995), an anti-cancer drug, can give rise to DSBs through repair processes (Frankenberg-Schwager et al 2005). Furthermore, ionizing radiation (X- and γ- irradiation and far UV light) or radiomimetic drugs like bleomycin, induce multiple damaged sites in close proximity in DNA and thus lead to

formation of DSBs. Under laboratory conditions DSBs can be induced in cells by expression of restriction endonucleases. Most commonly used are the yeast HO- or I-Sce-I endonucleases, which usually introduce a single cut in genomic DNA.

DSBs also occur spontaneously, as a result of normal cell metabolism. Reactive oxygen species i.e. free radicals that are formed as a byproduct of oxidative metabolism, are capable of directly inducing strand breaks as well as producing a broad range of oxidative DNA damage, which generates DSBs indirectly (Laval 1996). During the course of normal DNA replication, DSBs arise at sites where the template strand is damaged, either directly when the replication fork encounters a broken template strand (Southerland et al 2000, Leonce et al 2006), or as a consequence of a collapse of stalled replication forks (Burkhalter and Sogo 2004).

Despite the inherent risks, organisms have systems that intentionally induce DSBs. One of the well-characterized examples is mating-type switching in budding yeast where the HO-endonuclease induces a single cut at the MAT locus initiating mating-type cassette switching by HR (Strathern et al 1982). In mammals, DSBs are induced during B and T lymphocyte development, in the process of V(D)J recombination, to generate a diversity of antigen receptor genes (Lieber et al 2004). During meiosis, in both yeast and mammals, DSBs are generated throughout the genome to induce recombination and help proper chromosome segregation in meiosis I.

Repair of DSBs takes place in eukaryotes by two fundamentally different processes: non-homologous end joining (NHEJ) and homologous recombination (HR). NHEJ is a mechanism able to directly join DNA ends with no, or minimal, homology, whereas repair of DSBs by recombination requires a homologous sequence as a template.

1.2. DNA double-strand break repair

1.2.1. Homologous recombination

Homologous recombination (HR) is a process of exchange, or transfer, of information between homologous DNA molecules. It plays an important role in the maintenance of genome stability in prokaryotic and eukaryotic organisms. In mitotic cells, HR functions in the repair of DSBs or single-strand gaps (Fabre et al 2002), telomere maintenance (Tarsounas and West 2005) and proliferation in the absence of telomerase (Lundblad and Blackburn 1993). HR is also involved in re-initiation of replication forks after replication stalling (Osborn et al 2002). During meiosis, HR is essential to establish a physical connection between homologous chromosomes to ensure their correct disjunction in the first meiotic division (Roeder 1997). The associated high frequency of meiotic recombination contributes to diversity by creating new linkage arrangements between genes, or parts of genes, thus providing an evolutionary advantage. Herein, only mitotic recombination will be described in more detail.

The "classical" model. The process of mitotic HR can be divided in three basic steps (Figure 1): (1) pre-synapsis, preparation of DNA end for recombination; (2) synapsis, formation of a joint molecule intermediate between homologous DNA molecules; (3) resolution, separation and reconstitution of recombined DNA molecules. These steps need to occur in a highly coordinated manner.

Upon formation of a DSB, in the pre-synaptic phase of HR, a broken end of DNA is first processed to create a 3'-single-strand overhang (White and Haber 1990). This overhang will be subsequently loaded with a recombinase protein (Rad51 in eukaryotes, RecA in *E.coli*) to form a nucleoprotein filament. During the synaptic phase, the recombinase protein of the nucleoprotein filament, will mediate invasion and strand exchange between the resected end and an intact homologous DNA molecule. The joint molecule between the broken DNA and the intact

homologous template is a substrate for DNA polymerase and its accessory proteins, which re-incorporate missing nucleotides. At the end of this step, the recombining DNA molecules are connected through Holliday junctions (HJ) and need to be separated. This is accomplished during the resolution phase by the action of resolvase enzyme(s).

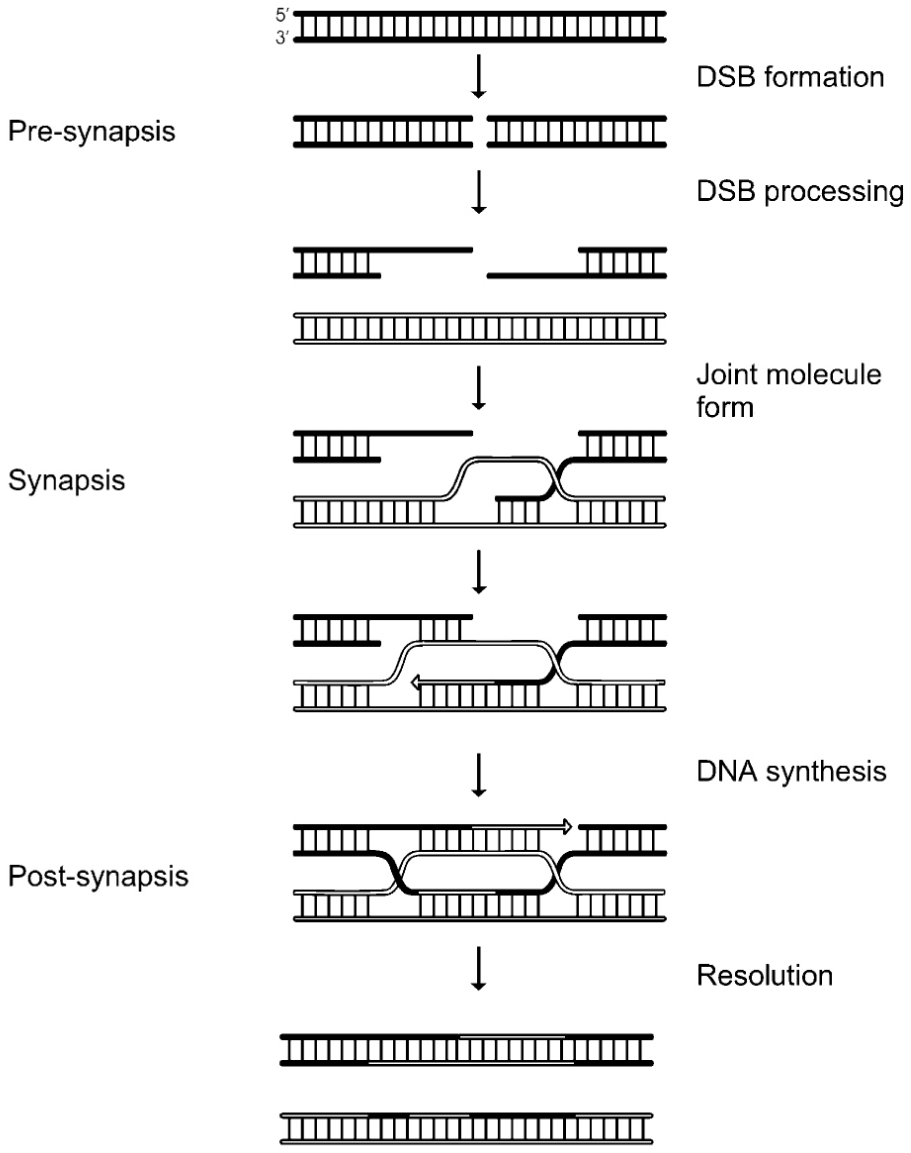

Figure 1. "Classical" HR model. After the formation of the DSB, DNA ends are resected in the pre-synaptic phase to expose ss-3'-overhangs. In the synaptic phase, the recombinase protein catalyzes a strand invasion reaction and formation of joint molecule between the resected end and an intact homologous DNA molecule. The homologous DNA molecule will then serve as a template for DNA synthesis. In the post-synaptic phase, two recombining molecules are connected through Holliday junctions and are subsequently separated in the resolution phase. Adapted from Wyman et al 2004.

There are several distinct sub-pathways of HR for DSB repair. Synthesis-dependent strand annealing (SDSA) is similar to "classical" HR in the initial steps of DSB-end processing and invasion into a homologous chromosome, but instead of capturing the second end of the DSB into the recombination intermediate, the invading strand is displaced after repair synthesis and re-anneals with the single-stranded tail on the other DSB end (Figure 2).

If a DSB occurs between closely repeated sequences, it can also be repaired by the HR process of single-strand annealing (SSA). In the SSA pathway, the DSB ends are processed to form ssDNA tails that can anneal with each other (Figure 2). SSA does not require the full repertoire of HR genes, as the repair process does not require strand invasion (Paques and Haber 1999). Furthermore, the resolution step of SSA doesn't involve HJ resolvases, but instead requires flap-endonuclease Rad1-Rad10 (Ivanov and Haber 1995).

Finally, when one-ended DSBs occur upon breakage, the single end can participate in an HR reaction that is known as break-induced replication (BIR) (McEarchen and Haber 2006). In this reaction, the DNA end is processed to give a single-stranded tail (pre-synapsis) that invades a homologous sequence (synapsis), followed by DNA synthesis to copy information from the donor chromosome (Figure 2). In this way HR serves to re-establish broken replication forks.

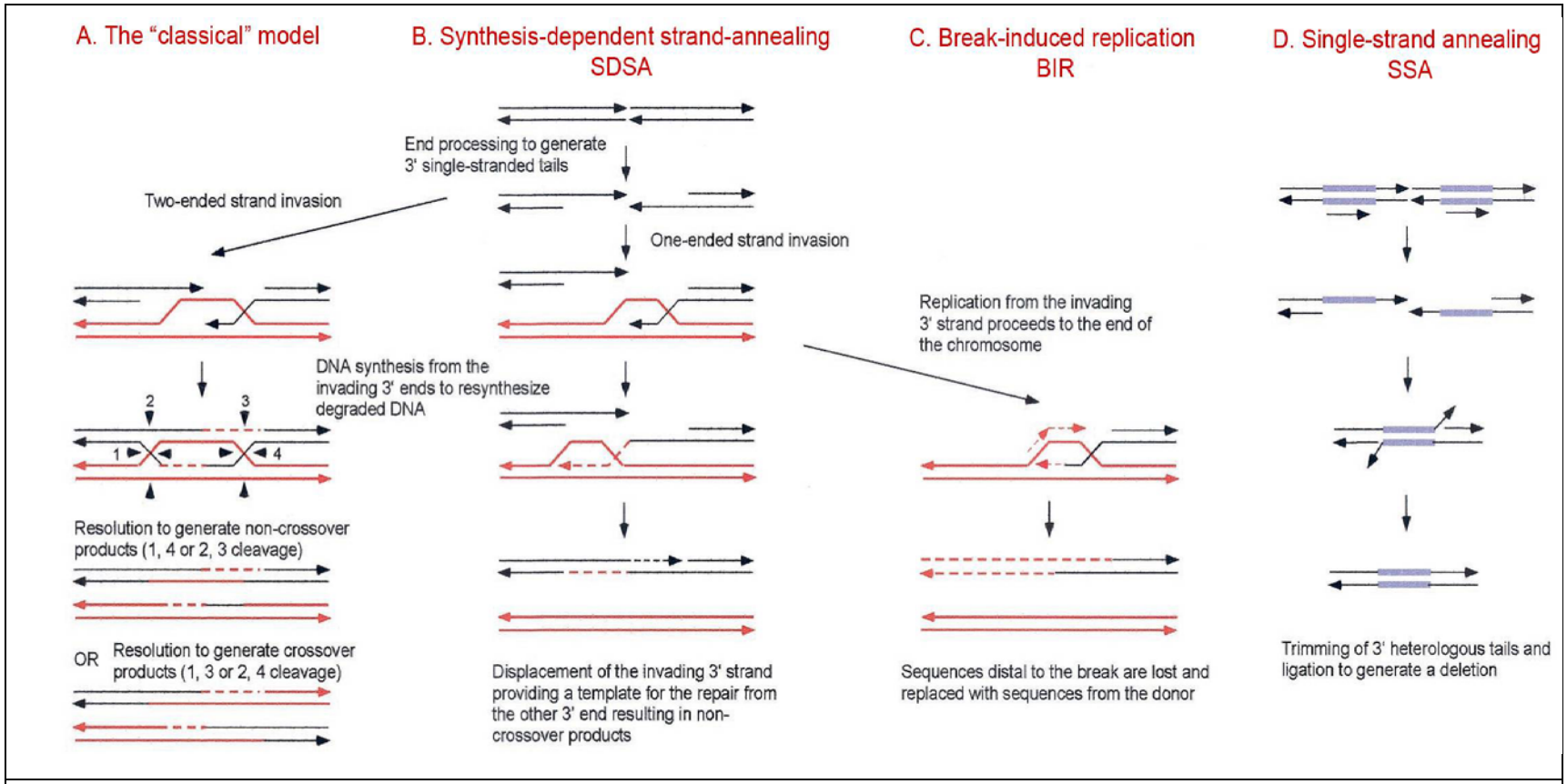

Figure 2. Models of different HR sub-pathways. **A**. The "classical" model. The dsDNA ends are processed to yield 3'-single-stranded tails. The 3'-ends invade the homologous duplex, priming the DNA synthesis. After ligation, a double HJ intermediate is formed, which can subsequently be resolved by endonucleolytic cleavage of the two HJs. **B**. In the SDSA model, the ends are processed to yield 3'-single-stranded tails, one of which invades the homologous duplex, priming the DNA synthesis. After displacament from the dononr duplex, the nascent strand pairs with the other 3'-single-stranded tail and DNA synthesis completes repair. **C**. The initial steps in the BIT model are the same as in the SDSA model, but DNA synthesis from the invading strand continues to the end of the DNA molecule. **D**. In the SSA model, a DSB made between direct repeats is subject to resection to generate 3'-single-stranded tails. When complementary sequences are revealed due to the extensive resection, the single stranded DNA anneals, resulting in deletion of one of the repeats and the intervening DNA. The 3'-tails are endonuleolytically removed, and the nicks are ligated. Adapted from Symington (2002). The 3'-ends are indicated by arrowheads.

Key factors. HR is an evolutionary conserved process. Model organisms, from bacteria to mammals, share a number of structurally and/or functionally conserved factors that build the core system of HR (Table 1). I will focus here on the description of key factors involved in HR in S. cerevisiae, most of which have orthologs in mammals.

Genes important for the HR were identified primarily as mutations sensitive to X-rays but not UV irradiation. These genes were classified as the *RAD52* epistasis group because of the epistatic of the Rad52 defect in double mutant analysis (Game and Mortimer 1974). Currently, 10 genes fall into this group: *RAD50*, *RAD51*, *RAD52*, *RAD53*, *RAD54*, *RAD55*, *RAD56*, *RAD57*, *MRE11* and *XRS2*.

RAD52 stands alone as the gene required for all HR pathways including DSBR, SDSA, BIR and SSA (Sugawara and Haber 1992, McEarchen and Haber 2006). By itself, Rad52 binds ssDNA and mediates DNA strand annealing (Mortensen et al 1996) in a reaction that is stimulated by single-strand binding protein RPA (Shinohara et al 1998). Thus, it will promote the efficient annealing of two complementary single strands of DNA but will not catalyze the invasion of a single strand of DNA into a double-stranded molecule of the same sequence. Yeast *rad52* mutant cells are extremely sensitive to X-rays and MMS. Repair of DSBs is hardly detectable in these mutants (Prakash et al 1980). Moreover, *rad52* strains are defective in spontaneous and induced mitotic recombination and mating-type switching. The formation of viable spores in meiotically dividing cells is almost completely blocked in a *RAD52*-deficient background (Game et al 1980).

DSBs chanelled to HR are most likely resected by the Rad50-Mre11-Xrs2 (MRX) complex, although other exonuclease activities (like Exo1 or Rad27) are able to compensate for the loss of the MRX complex (Moreau et al 2001). Rad51 forms a nucleoprotein filament on single-stranded DNA (ssDNA) (Sung and Robberson 1995), in reaction regulated by RPA, and mediates strand exchange of homologous double-stranded DNA (dsDNA). Strand invasion is promoted by Rad52 (New et al 1998). Rad55 and Rad57 share sequence similarities with Rad51 and form a heteromeric complex that stimulates Rad51-mediated strand exchange (Sung 1997). Rad54 and Rdh54, SWI/SNF family ATPases, stimulate the Rad51-

dependent homologous DNA pairing (Petukhova et al 2000), and thus assist proper strand exchange. The Holliday-junction resolvase has not been identified in yeast, although, several structure-specific endonucleases (Mus81-Mms4, Slx1-Slx4) have been implicated in resolution of HJs. There is, however a growing line of evidence that supports the role of Mus81 as a HJ resolvase (reviewed in Osman and Whitby 2007).

Table 1. Factors involved in homologous recombination in yeast, bacteria (*E.coli*) and human cells.

Yeast protein	Biochemical activity	*E.coli* ortholog	Human ortholog	Notable features
Rad50	DNA binding	SbcC	hRad50	Member of SMC family; forms complex with Mre11 and Xrs2
Mre11	ssDNA endonuclease 3'-5' exonuclease	SbcD	hMre11	Forms complex with Rad50 and Xrs2
Xrs2	Not known	-	NBS1	Forms complex with Rad50 and Mre11
Rad51	DNA pairing strand exchange ssDNA filament	RecA	hRad51	Forms nucleoprotein filaments; interacts with Rad52 and Rad54
RPA	ssDNA binding	SSB	hRPA	Binds ssDNa during pre-synaptic phase
Rad52	ssDNA binding and annealing	-	hRad52	Mediator of strand exchange
Rad55	ssDNA binding	-	XRCC2,3; Rad51B,C,D	Forms heterodimer with Rad57; facilitates strand exchange
Rad57	ssDNA binding	-	XRCC2,3; Rad51B,C,D	Forms heterodimer with Rad55; facilitates strand exchange
Rad54	DNA-dependent ATPase	-	hRad54	Promotes homologous DNA pairing by Rad51
Rdh54	DNA-dependent ATPase	-	hRad54	Member of Snf2 family DNA ATPases
Mus81	structure-specific endonuclease	RuvC	hMus81	Forms heterodimer with Mms4/Eme1; HJ resolvase

1.2.2. Non-Homologous End-Joining

Non-homologous end-joining (NHEJ) was discovered as illegitimate recombination in yeast and bacteria and V(D)J recombination in mammalian cells.

In yeast, genomic integration of transforming DNA with no homology to the genome was observed (Mezard and Nicolas 1994, Schiestl et al 1993). Later, with better characterization of the process it became known as NHEJ.

V(D)J recombination is the process by which the variable (V), diversity (D) and joining (J) segments of the immunoglobulin and T cell receptor genes are rearranged during development of the immune response (Gellert 2002). Recombination is initiated by the lymphoid-specific RAG1 and RAG2 proteins, which cooperate to make double-strand breaks at specific recognition sequences. Broken ends are then processed and joined with the help of NHEJ factors. Mutants lacking any of the core NHEJ components are impaired in their ability to perform V(D)J recombination and deficient mice display severe combined immunodeficiency (SCID) (Rooney et al 2002).

NHEJ stands for the direct rejoining of the ends from a DSB, without a need for an undamaged homologous template. In budding yeast HR plays a dominant role in the DSB repair and NHEJ appears to play only a minor role (Aylon and Kupiec 2004).

The current model. As opposed to HR, the DNA ends of DSB are not resected prior to processing by NHEJ factors. They are, rather, recognized and bound by Ku proteins (Ku70 and Ku80) (Figure 3). The Ku70/80 heterodimer is highly conserved in evolution and found in all NHEJ-proficient organisms. The heterodimer will protect the DNA end from unwanted degradation and lead to recruitment of further NHEJ factors. In the following step, DNA processing factor(s) (like Artemis), as well as signaling molecule(s) (like DNA-PK_{cs}) are localized to the DSB. Depending on the nature of the broken DNA end and the surrounding DNA context, different set of proteins will be engaged. The function of this step is to

form a scaffold which will hold the broken DNA ends together and, at the same time, prepare them for the ligation. Finally, the dsDNA ligase is recruited and, following ligation, NHEJ factors disassemble from DNA. Although NHEJ doesn't require the homologous undamaged template for efficient repair, in some situations, DNA ends are processed prior to repair initiation, to expose short stretches of microhomology, or simply to make ends compatible for ligation. Under such circumstances, NHEJ can lead to introduction of small insertions or deletions at the junction of repaired DNA ends.

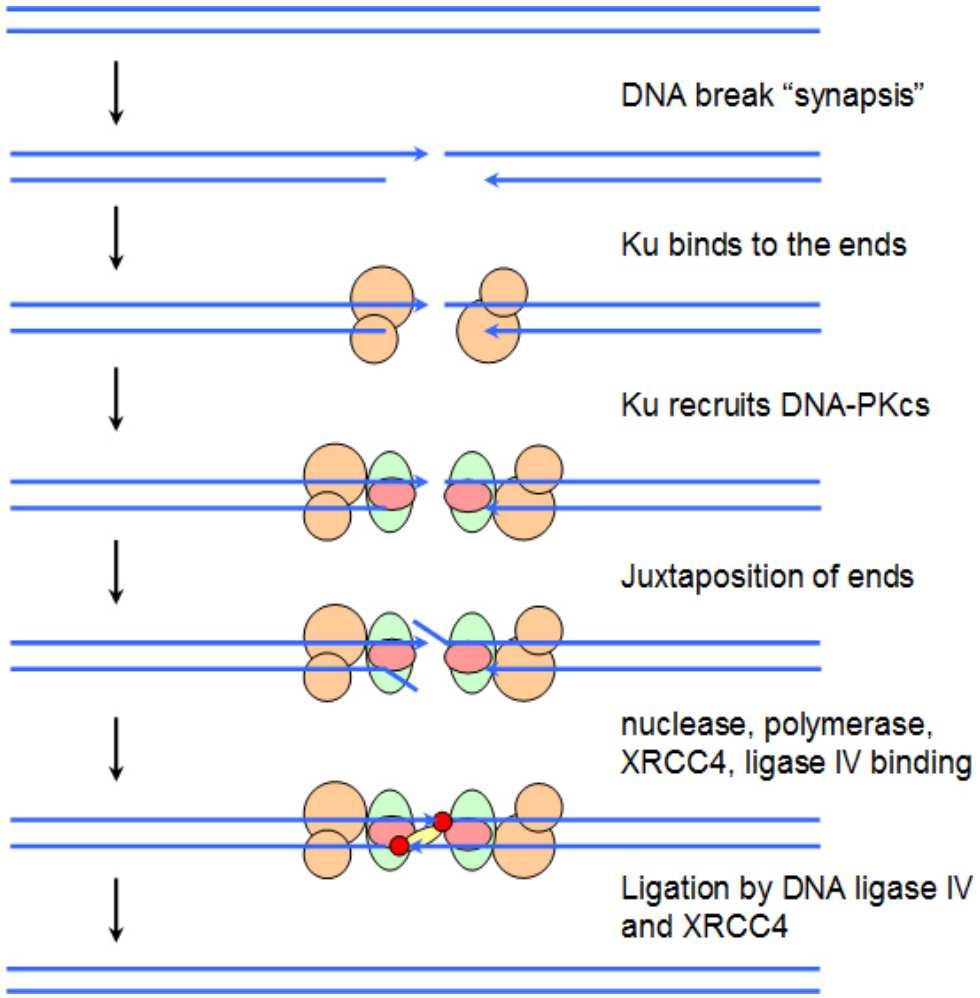

Figure 3. Model of NHEJ. In NHEJ, the DNA ends are not resected following DSB formation. Rather, they are bound by Ku heterodimer. Ku will protect the ends from nucleolytical degradation and recruit subsequent factors required for repair. DNA-PK_{cs} will bind the DNA-bound Ku and mediate juxtapositions of ends. In case the broken ends are not ligatable, nucleases and polymerases will be recruited, to resect the ends and fill the gaps prior to ligation. Finally DNA ligase will reseal the break.

The Ku70/80 heterodimer and the NHEJ ligase appear to be the only NHEJ components consistently found in all model organisms (Table 2), and are considered to be the core NHEJ factors. The key factors of *S.cerevisiae* NHEJ will be considered next.

Table 2. Factors involved in Non Homologous End-Joining in yeast, bacteria (*B.subtilis*) and human cells

Yeast protein	*B.subtilis* ortholog	Human ortholog	Notable properties
Yku70	YkoV	Ku70	Yku70-80 heterodimer binds free DNA ends and recruits downstream NHEJ factors
Yku80	YkoV	Ku80	Yku70-80 heterodimer binds free DNA ends and recruits downstream NHEJ factors
-	-	DNA-PK_{cs}	No yeast homolog; DNA-dependent protein-kinase; forms complex with Ku70/80
Lif1	-	XRCC4	Binds to and stabilizes Dnl4
Dnl4	YkoU	LIG4	dsDNA ligase, catalyzes a final step of NHEJ
Rad50	SbcC	hRad50	Member of SMC family; forms complex with Mre11 and Xrs2
Mre11	?	hMre11	Forms complex with Rad50 and Xrs2
Xrs2	-	NBS1	Forms complex with Rad50 and Mre11
Snm1	?	ARTEMIS	Nuclease; DNA hairpin-opening activity
Nej1	-	XLF	Cell-type specific regulator of NHEJ, affects Lif1 localization

The key factors. The first NHEJ component to bind to a DSB is Yku70/Yku80 (*S. cerevisiae* homolog of mammalian Ku70/Ku80 (Milne et al 1996)). In higher eukaryotes the Ku70/80 heterodimer is a subunit of a DNA-dependent protein kinase (DNA-PK) complex together with catalytic subunit DNA-PK_{cs}. DNA-PK_{cs} takes part in DNA end-to-end bridging (DeFazio LG et al 2002), signaling by phosphorylation of subsequent NHEJ factors (Meek et al 2004), and recruitment of the exonuclease Artemis (Drouet et al 2006). DNA-PK_{cs} is not strictly required for NHEJ. In V(D)J recombination, coding join formation required DNA-PK_{cs} but not signal join formation; both are NHEJ events. The same may apply to Artemis. In yeast, however, a homolog of DNA-PK_{cs} hasn't been identified yet. The MRX complex is recruited to DSBs following loading of the Yku70/80 heterodimer. This complex is believed to mediate DNA end-bridging and to provide a scaffold for recruitment of downstream factors (Chen et al 2001). In case DNA end-processing is needed, factors having nucleolytic and gap-filling activities are involved, most likely Rad27 and Pol4, respectively (Tseng and Tomkinson 2004). End-processing will generate ligatable structures for the final end-joining reaction. The Dnl4/Lif1 complex (ortholog of mammalian LIG4/XRCC4 complex) is then targeted to the repair intermediate to ligate the ends. Dnl4 is a dsDNA ligase that acts specifically in NHEJ (Wilson et al 1997) and is only stable in the presence of a cofactor Lif1 (Herrmann et al 1998, Teo and Jackson 2000). Upon ligation, NHEJ factors are believed to disassemble from the repaired DNA.

1.2.2.1. NHEJ core factors of *S.cerevisiae*

The Yku70/80 complex

Yku70 and Yku80 form a heterodimer that represents yeast equivalent of the human Ku70/Ku80 DNA end-binding complex. Although Ku proteins are quite conserved in size and function across species, the amino-acid sequence can differ substantially from organism to organism (Dynan and Yoo 1998). The Ku70/80 heterodimer is one of the most abundant DNA

end-binding proteins in mammalian cells. It was identified in patients with polymyositis-scleroderma overlap syndrome (Mimori et al. 1981) as a human nuclear autoantigen, that binds DSBs with great specificity. Following further investigation, the Ku complex was found to bind different discontinuities in dsDNA, including single-strand gaps and bubbles, but it has the strongest affinity for blunt dsDNA ends, 5'- or 3'-overhangs and hairpins (Featherstone and Jackson 1999). The crystal structure of the human Ku complex revealed a special feature - its central *β*-barrel ring structure (Walker et al. 2001). The Ku heterodimer binds DNA by forming a ring-like structure and slipping the dsDNA end through this ring. The Ku ring binds ends in single orientation and is able to translocate along the duplex DNA. In the repair reaction Ku is acting as a bridging factor as well as a recruitment and stimulating factor (McElhinny et al 2000, Kysela et al 2003). These essential features of the human Ku complex are conserved in yeast.

Yeast cells lacking either Yku70 or Yku80 display reduced recircularization efficiency of transformed linear plasmid DNA and an increased frequency of imprecisely joined products (Boulton and Jackson 1996). Compared to single mutants, the double *yku70 yku80* mutant shows no additional repair or growth defects, as expected. Loss of Yku70 or Yku80 sensitizes yeast cells to ionizing radiation only in the absence of functional HR, but doesn't affect sensitivity towards UV light or hydroxyurea (HU).

Apart from its function in DSB repair, the Yku70/80 complex has an important function in telomere length maintenance and silencing. The Yku70/80 complex is associated with chromosome ends of *in vivo* (Gravel et al 1998). In the absence of Yku70/80 complex, an enhanced shortening of chromosome ends was observed (Gravel et al 1998). Therefore, the complex was proposed to function in the protection of DNA ends from nucleolytic processing. In addition to telomere protection, Yku70/80 is involved in clustering of yeast telomeres and their anchoring to the nuclear periphery (Laroche et al 1998). In yeast, genes located in the close proximity to telomeres are subjected to transcriptional silencing, a phenomenon termed telomere positioning effect (TPE), that is dependent upon Sir2/3/4 proteins (Grunstein 1997). TPE is strongly diminished in Yku-deficient cells, although global silencing is not affected (Boulton and

Jackson 1998). An explanation of this phenomenon is provided by the fact that Yku70/80 recruits Sir2/Sir3/Sir4 complex, through its interaction with Sir4, which, in turn, induces chromatin condensation and repression of transcription (Tsukamoto et al 1997, Roy et al 2004). Thus, it is interesting to note that the role of Yku70/80 is different when it binds to internal DSBs or to chromosome ends. While it provides for coordinated end-processing and joining in one case, it mediates silencing and localization, and prevents joining in the other.

The Mre11/Rad50/Xrs2 complex (MRX)

Mre11/Rad50/Xrs2 complex is a second core factor of yeast NHEJ. As opposed to mammalian cells, where the evidence for involvement of Mre11/Rad50/Nbs1 in NHEJ is still inconclusive, genetic and biochemical analysis in *S. cerevisiae* clearly implicate MRX function in yeast NHEJ (Tsukamoto et al 1996, Chen et al 2001).

In vivo NHEJ assays showed that strains, from which *MRE11*, *RAD50*, or *XRS2* was deleted, exhibited a dramatic drop in NHEJ efficiency (Moore and Haber 1996). This phenotype was shown to be epistatic with Yku70/80 and Lig4/Lif1, thus implicating a function in NHEJ. *In vitro* experiments further showed that interaction between Xrs2 of MRX complex and Lif1 specifically stimulates intermolecular ligation by Lig4/Lif1, a process that is additionally stimulated by Yku70/80 (Chen et al 2001).

Unlike other NHEJ components, MRX is also involved in HR and was thus proposed to be involved in the regulation of DSB repair pathway utilization. MRX role in HR is still somewhat unclear. It could be involved in DNA end processing as well as channeling the repair towards sister chromatid-based recombination. Unlike the situation in mitotic cells, processing of DNA DSBs during meiotic recombination is largely dependent on the Mre11-associated nuclease activity. Genetic analyses have revealed that Rad50, Mre11, and Xrs2 work in conjunction with Spo11 to introduce meiosis specific DNA DSBs (D'Amours and Jackson 2002).

Yeast cells lacking any component of the MRX complex, exhibit very

similar phenotypes (D'Amours and Jackson 2002) namely defects in meiotic recombination (HR), premature senescence, suppression of gross chromosomal rearrangements, elevated rates of spontaneous mitotic recombination, and delayed mating-type switching (reviewed in Dudas and Chovanec 2004). As for Yku70/80, MRX also plays a role in telomere length maintenance. Cells deficient for MRX suffer telomeric erosion, losing approximately 65% of the terminal repeats (Moreau et al 1999). But, although MRX functions epistatically with Yku70/80 in telomere length maintenance, it doesn't affect TPE as TPE analysis in the *mre11*, *rad50*, or *xrs2* mutants didn't implicate MRX in this process (Boulton and Jackson 1998). Furthermore, MRX is important for initiation of intra-S phase checkpoint in response to DNA damage, requiring Mre11 nuclease activity and activation of Mec1/Tel1 signalling pathway (D'Amours and Jackson 2001).

Biochemical analysis of the MRX complex revealed a 2:2:1 stoichiometry (Chen et al 2001) of a purified complex. Rad50 is a large coiled coil protein, related to SMC family of proteins. It contains Walker A and B motifs, separated by the coiled coil, which are responsible for ATP binding and hydrolysis (Hopfner et al 2002). Crystal structure of Rad50 reveals that a hinge motif, present in the center of coiled coil region, promotes Zn^{2+}- dependent dimerization of Rad50. In the complex, the Rad50 dimer binds two distinct Mre11 dimers. The Mre11 dimer binds to the coiled-coils of two Rad50 molecules adjacent to the ATPase domain, forming a globular head, which is responsible for the DNA-binding and/or DNA end-processing activities of the complex. Hence, one Mre11/Rad50 heterodimer possesses two DNA-binding and end-processing active sites. This observation led to a model in which Mre11/Rad50 acts as a bridging factor during NHEJ in such way that its two active sites bind the two DNA extremities with Rad50 providing a flexible tether for subsequent NHEJ reactions (Hopfner et al 2002).

Mre11 is a SbcCD-family nuclease. It possesses Mn^{2+}-dependent 3' to 5' dsDNA and ssDNA endonuclease, ssDNA exonuclease and hairpin cleavage activities (Trujillo and Sung 2001). Xrs2 is the least characterized component of the complex with proposed regulatory functions. Through its DNA binding activity, Xrs2 facilitates Mre11 translocation to the nucleus

(Tsukamoto et al 2005) and helps targeting MRX to DNA ends (Trujillo et al 2003). Additionally, Xrs2 is engaged in protein-protein interactions with other factors, like Tel1 and probably serves to recruit those factors to the DSB (Nakada et al 2003).

The Dnl4/Lif1 complex

DNL4 and *LIF1* encode yeast orthologs of mammalian DNA ligase IV and XRCC4, respectively (Schär et al 1997, Teo and Jackson 1997, Herrmann et al 1998, Wilson et al 1997). The ligation step in yeast NHEJ strictly requires DNA ligase IV, the product of *DNL4*. The only other yeast ligase, DNA ligase I (Cdc9) cannot compensate for the loss of Dnl4. Conversely, Dnl4 is incapable of supporting replication and has no known role outside of end joining (Wilson et al 1997). Dnl4 and Lif1 form a strong heteromeric complex and can be co-purified from cell extracts (Chen et al 2001). Moreover, Dnl4 is not stable in the absence of Lif1 (Herrmann et al 1998).

The C-terminus of human LIG4 consists of two tandem BRCT domains (Teo and Jackson 2000), with the known XRCC4 binding domain mapping to the linker connecting those BRCT domains (Sibanda et al 2001). This interaction is conserved in yeast and enabled the identification of the XRCC4 ortholog, Lif1. The crystal structure of XRCC4 shows a globular head in the N-terminus (Junop et al 2000) followed by a coiled coil domain, which binds the ligase linker peptide. The mammalian complex shows a 1:2 (DNA ligase IV:XRCC4) stoichiometry and possesses DNA-binding and ATP-dependent dsDNA ligase activities. Although XRCC4 and Lif1 are only poorly conserved at the primary-structure level, the central Lif1 region that binds Dnl4 is predicted to fold as a coiled coil (Herrmann et al 1998).

Inactivation of the *DNL4* or *LIF1* gene does not lead to increased sensitivity of dividing cells to agents inducing DSB such as IR and MMS (Herrmann et al 1998). However, disruption of either of the genes, results in a dramatic reduction in the cellular ability to join restriction enzyme-generated DSB ends of a transformed linear plasmid. In the absence of Dnl4 or Lif1, plasmid-based DSB are repaired by an error prone mechanism (Schar et al 1997, Teo and Jackson 1997). A fraction of these

repair products was generated by a Rad52-dependent HR process, as judged from the phenotype of a *dnl4 rad52* double mutant and from characterizing the structures of joined molecules. Furthermore, Dnl4/Lif1 does not seem to have an essential function in telomere length maintenance (Herrmann et al 1998, Teo and Jackson 1997).

Additional NHEJ factors

When DNA termini of a DSB are damaged (displaying damaged bases and/or sugar moieties) or not fully compatible, DNA end-processing mediated by nucleases and DNA polymerases might be required. End-processing to reveal microhomologies; i.e. short tracks of DNA sequence homology close to the break site that facilitate DNA ends alignment, also employs factors in addition to core NHEJ proteins.

In *S. cerevisiae*, the gap-filling polymerase is likely to be Pol4, a member of Pol X family of nucleotidyl transferases. The N-terminal BRCT domain of Pol4 directly interacts with Dnl4 (Tseng and Tomkinson 2002). This interaction stimulates the DNA synthesis activity of Pol4 and, to a lesser extent, the ligation activity of Dnl4/Lif1.

Rad27 (FEN-1 in mammals) is a structure-specific nuclease that possesses flap endonuclease and 5’ to 3’ exonuclease activities (Harrington and Lieber 1994) and acts in a subset of NHEJ events that require processing of 5’ flaps (Wu et al 1999). Consistently, Rad27 also interacts physically and functionally with Pol4 and Dnl4/Lif1 (Tseng and Tomkinson 2004). The activities of Rad27 and the Pol4 are coordinated to achieve optimal filling and 5’ processing in NHEJ.

1.2.3. Elements influencing the choice of the DSB repair mechanism

HR and NHEJ are two fundamentally different processes for the repair of DSBs. In order to efficiently deal with DSBs, cells have to decide which pathway to utilize. Induction of DSBs will expose dsDNA ends and the first choice made in cells is whether to repair or not. While repair of endogenous dsDNA is advantageous, there is a risk of recognizing chromosome ends i.e. telomeres as DSBs. Erroneous "repair" of telomeres will lead to formation of dicentric chromosomes and will increase genome instability. As DSBs are the most toxic type of DNA lesions, even the inaccurate repair is advantageous over no repair at all. However, depending on the given (genetic) context i.e. cell type, cell cycle stage, availability of homologous sequences, a decision of pathway choice is made. The mechanistic details of the choice of DSB repair pathway are still poorly understood. Below, I will focus on the regulatory aspects of NHEJ.

1.2.3.1. Cell type regulation of NHEJ; Nej1

A first indication that NHEJ is under active control in *S. cerevisiae* appeared when it was demonstrated that this process is down-regulated by Mata1-Matα2 repressor, resulting in significantly reduced NHEJ efficiency in diploid cells compared to haploid cells (Astrom et al 1999, Lee et al 1999). Subsequently, the responsible target gene, *NEJ1*, was identified (Valencia et al 2001, Kegel et al 2001) and shown to be haploid-specific. Expression of *NEJ1* is virtually undetectable in the presence of diploid-specific repressor Mata1-Matα2, because of a consensus-binding site for this repressor in the *NEJ1* promoter (Valencia et al 2001, Kegel et al 2001). Nej1 is indispensable for NHEJ since *nej1* cells display a strong defect in plasmid repair assay as well as in the repair of HO endonuclease-induced chromosomal DSBs (Frank-Vaillant and Marcand 2001, Kegel et al 2001, Valencia et al 2001). It has been shown that the C-terminal part of

Nej1 strongly binds the N-terminal part of Lif1 (Frank-Vaillant and Marcand 2001). However, the molecular function of Nej1 still remains unclear. It has been implicated in Lif1 localization to the cell nucleus (Valencia et al 2001) but this effect was difficult to reproduce in different strain backgrounds. Whether Nej1 also has an impact on ligation by Dnl4 is still elusive. There are no clear structural features in Nej1 protein, although two putative transmembrane helices in the N-terminus could be predicted. One study (Liti and Louis 2003) implied Nej1 in maintenance of genomic stability, since, in the absence of telomerase, *nej1* mutant shows increased levels of end fusions at telomeres and increased occurrence of dicentric chromosomes. Recently, biochemical characterization of Nej1 revealed that the C-terminus of the protein possesses the DNA binding-activity which is required for efficient NHEJ *in vivo* (Sulek et al 2007). So, a possible role of Nej1 might be targeting Lif1 to the nucleus and facilitating tethering of Lif1/Dnl4 complex to DNA ends that need repair.

1.2.3.2. Cell cycle regulation of DSB repair processes

It has been postulated for a long time that in haploid cells NHEJ should predominate in G1 and HR in late S and G2/M solely on the basis of requirement and availability of homologous sequences. However, the supporting evidence for such a model came only quite recently, by showing that cells maintained in G1 cannot complete DSB repair by HR because DSB ends are not resected, i.e. the pre-synapsis step of HR is non-functional. Indeed, the Clb-CDK activity promotes HR by controlling the resection step of DSB repair (Aylon et al 2004). The mechanism of this control is not known, in part because the mechanism of resection itself is poorly understood. Although CDK activity is associated with decreased NHEJ, NHEJ can be completed in S/G2. It seems that NHEJ is also permitted in S/G2 if it can be rapidly completed, but resection will take over and commit a break to HR when NHEJ is delayed (Aylon et al 2004, Ira et al 2004). In addition, Ira and coworkers (2004) reported that CDK activity is necessary to activate the yeast checkpoint response,

because CDK-mediated DSB resection activates checkpoint by allowing the formation of RPA-ssDNA filaments. In the absence of resection in G1 cells, the MRX complex seems to accumulate at the broken ends. Sae2 in S. cerevisiae is involved in meiotic and mitotic recombinational pathways together with MRX complex (Rattray et al 2001,Clerici et al 2005).

After those initial observations, there is now also evidence from other organisms, that NHEJ is restricted to G1 phase of the cell cycle. For instance, V(D)J recombination by NHEJ during lymphoid development, is restricted to G1 cells by a tight regulation of the RAG2 gene and protein (Lee and Desiderio 1999). Also in *S. pombe* cells, in the absence of the telomere protein Taz1, telomeres undergo fusion through an NHEJ mechanism that is restricted to G1 (Ferreira and Cooper 2004). These results suggest that the restriction of NHEJ to G1 and HR to the rest of the cell cycle is a conserved feature of eukaryotic cells.

Apart from G1, NHEJ is also influenced by the nutritional status and/or by oxidative stress and is increased in G0/stationary haploid cells (Karathanasis and Wilson 2002). It is not known whether haploid spores formed during meiosis show a similar phenomenon.

1.2.3.3. Locus specific regulation of DSB repair at telomeres

Telomeres are ends of linear chromosomes and as such have a potential to be recognized DSBs, and serve as substrates for inappropriate repair. This could lead to the formation of dicentric chromosomes, either by fusion between telomeres of different chromosomes or the fusion of a telomere to a "real" DSB. However, under normal physiological conditions, telomeres fusions are prevented by telomere-binding proteins that form a protective structure named telomere cap. Paradoxically, many of NHEJ factors are bound near or at the telomeres and play an important role in telomere length homeostasis and chromosome end protection (reviewed in Riha et al 2006).

Telomere fusions have so far been observed and studied only in cells with dysfunctional telomeres i.e. shortened telomeres that have lost protective protein capping. Such dysfunction can arise either by depletion of a crucial

protein component of the telomere cap or by telomerase inactivation and the slow erosion of telomeric DNA that arises from the end replication problem. In cells with dysfunctional telomeres, the majority of telomere fusions are formed through NHEJ. For example, mammalian cells lacking TRF2 (telomeric repeat binding factor 2), carry dysfunctional telomeres that induce a DNA-damage response that is characterized by the formation of telomere damage-induced foci, consisting of γ-H2AX, Mre11, ATM, and other DNA repair factors (Takai et al 2003). Such cells also exhibit a high frequency of chromosome end-to-end fusions (Smogorzewska et al 2002). These findings suggest that defective telomeres are recognized as DNA damage and subject to repair by NHEJ. In fission yeast, cells lacking Taz1 (ortholog of mammalian TRF1 and TRF2) telomere fusions arise by either NHEJ or HR and the utilization of the DSB pathway depends on the stage of the cell cycle (Ferreira and Cooper 2004). NHEJ predominates in G1 phase of cell cycle, resulting in the formation of lethal interchromosomal fusions in *taz1*− strains (Ferreira and Cooper 2001). Inactivation of Rap1 (Repressor Activator Protein, binding telomere sequences and playing a role in telomere silencing and structure) in *S. cerevisiae* also results in telomere fusions and genetic analysis showed that all known core components of the yeast NHEJ pathway are required for fusion formation (Pardo and Marcand 2005). All of these examples show that NHEJ involvement in telomere fusions is conserved through evolution and implicate a necessity of adequate telomere protection mechanism. But the apparent paradox of NHEJ factors' involvement in both telomere protection and lethal fusions is still unresolved to date.

1.3. DSBs at stalled replication forks

1.3.1. Stalling of replication forks

DNA replication is a particularly sensitive moment in the cell cycle, as the cell needs to ensure faithful passage of the genetic material to the progeny, while many events interfere with the progression and the stability of the replication fork (RF). Once established, a single RF will replicate several tens of thousands of bases before meeting a converging fork. During this time, the progression of the replication forks can be compromised. When replication forks meet a replication barrier (in the form of a damaged template strand or a specific DNA secondary structure), they slow down or stall. Failure to protect arrested forks from collapsing results in breakage and genomic instability (Cobb et al 2005).

Replication progression can be compromised by different kinds of obstacles. Fork stalling can be caused by DNA damage that escaped detection and repair by an appropriate repair-system, prior to the arrival of a replisome. Such damage can block the polymerase progression leading to uncoupling between the replisome and the helicase (Katou et al 2003) or uncoupling leading and lagging strand synthesis (Pages and Fuchs 2003). Alternatively, damaged DNA template can block the progression of replicative helicase (Michel et al 1997). RFs also arrest at loci with specific secondary DNA structures like G-quadriplex DNA, hairpins and inverted repeats (Hyrien 2000). Stalling of RFs can be induced using replication inhibitors (drugs like hydroxyurea (HU) and aphidicolin). HU is a specific inhibitor of ribonucleotide reductase. The presence of HU leads to depletion of nucleotides and, consequently, blocks DNA synthesis. Aphidicolin is the reversible inhibitor of eukaryotic DNA polymerase α. Treatment with replication inhibitors leads to formation of stable, reversibly arrested forks (Lopes et al 2001).

Several protein-DNA complexes form natural barriers to fork progression. In *E. coli*, the Tus protein binds to Ter sequences forming a structure that will pause the replication fork and lead to replication termination upon arrival of converging RF (Rothstein et al 2000). In eukaryotes, the best

described example is the Fob1-dependent replication fork barrier (RFB) at the ribosomal DNA (rDNA) of *S. cerevisiae*. In this system, the RFB ensures quasi-unidirectional replication and prevents collision of replication and transcription machineries (Takeushi et al 2003).

1.3.2. Processing of stalled forks and restart of DNA replication

Failure to reactivate either arrested or collapsed replication forks is a source of genomic instability. Replication conflicts are solved through several pathways, which operate directly at the fork to enable fork reactivation outside the origin of replication (Michel et al 2004, Cox 2002). The existence of multiple such pathways reflects the importance of recovering from different types of damage that affect RF progression in different ways, to ensure that DNA replication is completed faithfully. There is a growing list of factors that have a role in the maintenance of RF stability and recovery of collapsed forks in budding yeast, although the mechanistic details of concerted action of these factors are still not very well understood. The most prominent factors are described below in detail.

1.3.3. Factors involved in maintenance of RF stability

Fob1. *FOB1* was identified as the gene required for RF pausing in the direction opposite to 35S rRNA transcription at the RFB site (Figure 4) (Kobayashi and Horiuchi 1996). Both *in vivo* and *in vitro* RFB site binding activity of Fob1 was demonstrated (Kobayashi 2003, Mohanty and Bastia 2004). It is believed that the Fob1/RFB system is required to avoid a head-to-head collision between replication and transcription by RNA polymerase I (Brewer and Fangman 1988, Kobayashi and Horiuchi 1996) and, thereby, to contribute to chromosome stability. *FOB1* is thought to be required for the maintenance of average copy number by increasing or decreasing copy number through the regulation of recombination events between the repeats (Kobayasi et al 1998). Furthermore, DNA strand

break formation around the RFB site was observed to be *FOB1* dependent (Burkhalter and Sogo 2004, Kobayashi et al 2004).

Sgs1 and Top3. Sgs1 is a RecQ type of helicase. Loss of *SGS1* function leads to increased rates of mitotic and meiotic recombination, gross chromosomal rearrangements, chromosomal loss and cellular senescence (Sinclair et al 1997, Myung et al 2001). *sgs1* cells are sensitive to DNA damaging agents (Frei and Gasser 2000) and hypersensitive to HU (Cobb et al 2003). Levels of Sgs1 peak in S-phase and the protein colocalizes with sites of DNA replication (Frei and Gasser 2000, Cobb et al 2003). Absence of Sgs1 reduces the stability of DNA polymerases α and ε at arrested RFs (Cobb et al 2003). Sgs1 interacts genetically and physically with DNA topoisomerase Top3. Top3 is a type IA topoisomerase that unlinks single-strand catenates (Gangloff et al 1994, Wu et al 2000). Deletion of *TOP3* results in slow growth phenotype that can be suppressed by deletion of *SGS1* (Gangloff et al 1994). *top3* cells also show high levels of recombination and chromosome loss (Myung et al 2001). A variety of biological roles have been proposed for the eukaryotic RecQ helicases either alone or in conjunction with Top3. These include roles in the termination of DNA replication (Wang 1991; Rothstein and Gangloff 1995), chromosome segregation (Watt et al. 1995), and the restart of stalled RFs (Rothstein et al. 2000; Kaliraman et al. 2001; Fabre et al. 2002).

Rrm3. Rrm3, a 5’ -to-3’ DNA helicase (Ivessa et al 2002), is a member of the Pif1 subfamily of DNA helicases that are highly conserved among eukaryotes. *RRM3* is not an essential gene, but in its absence, RFs pause at over 1,000 discrete sites, including sites in the rDNA repeats, tRNA genes, centromeres, telomeres, and the silent mating-type loci (Ivessa et al 2003, Ivessa et al 2000). Both fork breakage and recombination are increased at sites of Rrm3 pausing. Sites dependent on Rrm3 for normal fork progression are assembled into non-nucleosomal protein-DNA complexes (Ivessa et al 2003). *In vivo* Rrm3 associates with telomeres and rDNA (Ivessa et al 2002, Ivessa et al 2000). Thus, Rrm3 was proposed to act directly and catalytically to promote replication past

protein-DNA complexes.

Structure specific nucleases. Synthetic-lethal screens have been used to isolate genes that are functionally redundant with *SGS1* in *S. cerevisiae* (Mullen et al. 2001; Tong et al. 2001). Two complexes with structure-specific nuclease activities have been identified in this way: Mus81-Mms4 and Slx1-Slx4. Loss of *MUS81* or *MMS4* results in sensitivity to camptothecin and MMS and in sporulation defects (Interthal and Heyer 2000, Bastin-Shanower et al 2003). It has been suggested that Mus81 constitutes a part of a Holliday-junction resolvase (Boddy et al 2001, Chen et al 2001). The *SGS1–TOP3* and *MUS81–MMS4* pathways appear to intersect downstream of HR because a synthetic-lethal phenotype of *sgs1 mus81* mutants is suppressed in the absence of the *RAD52* epistasis-group genes (Fabre et al. 2002; Bastin-Shanower et al. 2003). *SLX1–SLX4* is likely to define a pathway distinct from *MUS81–MMS4* because the synthetic lethality of *sgs1 slx1* or *sgs1 slx4* double mutants is not suppressed in a *rad52* background (Fabre et al. 2002; Bastin-Shanower et al. 2003) and the loss of *SLX1* or *SLX4* results in no obvious growth or sporulation defects. The data available suggest that Slx1–Slx4 and Sgs1–Top3 play overlapping roles at the termination of rDNA replication (Kaliraman and Brill 2002).

Recombination factors. There are two recombination pathways that are proposed to restart broken replication forks. The first pathway is BIR, which is Rad52 and Rad59 dependent but largely Rad51 independent (Symington 2002). In BIR, broken replication forks can be reinitiated by strand invasion and replication can resume and continue to the end of the chromosome or until this replication complex converges with another replication fork (Kraus et al 2001). The second pathway is Rad51 and Rad52 dependent and involves downstream activation of either Sgs1/Top3 or Mus81/Mms4 for fork restart (Fabre et al 2002). Recombination factors are described in more details in the section 1.3.3.

1.3.4. Yeast rDNA locus as a model to study naturally stalling RFs

The ribosomal locus of budding yeast is an array of around 100-200 copies of rDNA units, located on chromosome XII (Warner 1989). Each rDNA unit (Figure 4, upper panel) has a size of 9137bp and consists of 35S and 5S genes separated by two non-transcribed spacer regions (NTS1 and NTS2). Spacer regions contain various elements influencing replication, transcription and recombination in the unit. NTS2 contains the rARS (yeast origin of bidirectional DNA replication) and a promoter for RNA polymerase I, located at the 5' end of 35S gene. NTS1 contains an enhancer (located near 3' end of 35S gene) that positively regulates transcription of both down- and upstream flanking 35S genes (Banditt et al 1999). The enhancer overlaps one major and two minor replication fork barriers (Gruber et al 2000). After initiation of replication, two replication forks move in opposite direction away from the origin (Figure 4, lower panel). Only the origin-upstream moving fork will get blocked at RFB, and this is dependent on the presence of Fob1 (Kobayashi and Horiuchi 1996 and see above). This fork will stay paused until it fused with a converging fork from an upstream origin. The termination of replication will, therefore, also happen in the RFB region and is shown to be dependant on Fob1 (Mohanty and Bastia 2004, Kobayashi 2003).

In terms of rDNA recombination, the RFB site is thought to be a recombination hot spot that induces DNA double-strand breaks (Kobayashi et al 2001). *FOB1* was shown to be essential for recombination in the rDNA (Johzuka and Horiuchi 2002, Merker and Klein 2002). *FOB1*-dependent recombination in the rDNA is known to be required for regulation of copy number, probably through unequal sister-chromatid recombination after a double-strand break at the RFB (Kobayashi et al 1998). Double-strand breaks also produce extrachromosomal rDNA circles, whose accumulation seems to be a cause of aging in yeast (Sinclair et al 1997, Rothstein and Gangloff 1999).

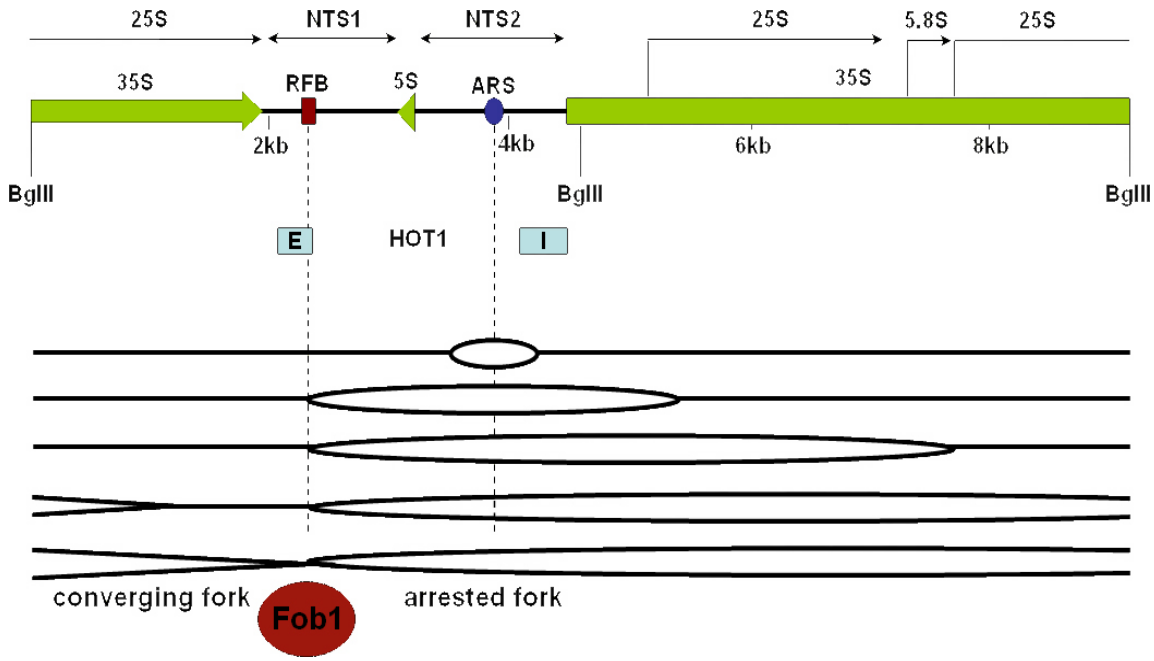

Figure 4. Organization and replication of rDNA locus of budding yeast. Yeast rDNA locus is a tandem array of about 150 rDNA repeat units. One of those units is depicted on upper panel. An rDNA unit consists of 2 transcription units (35S, 5S), and two non-transcribed spacer regions (NTS1,2). NTS2 harbors the bidirectional origin of replication (ARS); polar replication fork barrier (RFB) is located in the NTS1. Lower panel- after initiation of replication, two replication forks travel in opposite directions from ARS. Rightward moving fork is free to move, while leftward-moving fork is paused at the RFB and remains there until if fuses with another fork coming from the neighboring rDNA unit.

1.3.5. Stalled RFs as a source of DSBs during replication

In most cases during fork progression, the replisome remains stably associated with the stalled fork (Cobb et al 2003) and replication restart can occur once the block is alleviated. However, there are situations when arrested forks may experience replisome dissociation and collapse, which is accompanied by occurrence of DNA single- and double-strand breaks (Weitao et al. 2003, Burkhalter and Sogo 2004). The broken fork must be restored before replication is allowed to proceed, which usually involves some form of homologous recombination (Kraus et al 2001).

RFs stalled at RFB in yeast have a potential to collapse, which can lead to generation of S-phase specific breaks in DNA (Burkhalter and Sogo 2004) even in the absence of exogenous DNA damage or other forms of replication stress. The rDNA locus of *S. cerevisiae* is also very well characterized, which makes it a good model system to study processes associated with generation and repair of DNA DSBs at naturally stalling RFs.

2. Aims of the work

In eukaryotic cells, DNA double strand breaks (DSBs) represent the most disruptive form of DNA damage. If left unrepaired, they may lead to loss or alterations of genetic information, which can be associated with carcinogenesis and/or cell death. Therefore, cells posses two conceptually distinct DSB repair strategies, homologous recombination (HR) and non-homologous end-joining (NHEJ), to fix chromosomal breaks.
In *S. cerevisiae*, the biological function of NHEJ is still not very clear and how this process is regulated and coordinated with other DNA repair activities is poorly understood. It seems to be clear though that cells need to have means to decide whether breaks are to be repaired by HR or NHEJ.

The goal of this work was to provide more insight into the regulation of NHEJ, particularly with respect to the choice of repair pathway in situations where both HR and NHEJ pathways are able to act. Two different approaches were chosen to elucidate this problem.

Functional characterization of a newly identified NHEJ protein with putative regulatory function: Ntr1 was isolated in an yeast two-hybrid screen for interacting partners of a known NHEJ factor, Lif1. Initial experiments indicated that this protein acts as a negative regulator of NHEJ. Since no negative regulators of NHEJ have been described before, the function of this essential protein was further characterized. The aim was to understand under which circumstances and to which extent Ntr1 suppresses NHEJ in logarithmically growing yeast cells.

Investigation of DSB repair at naturally stalled replication forks, where pathway engagement has to be coordinated: For this purpose, DSBs arising at the replication fork barrier in the yeast rDNA locus, during unperturbed S-phase, served as a model. The role of HR and NHEJ in the maintenance of fork stability (both the generation and the repair of DSBs) was examined in mutants deficient in either one or both repair pathways.

Generation and repair of DSBs was monitored using 2D DNA electrophoresis and Southern blotting. The aim was to distinct the roles of HR and NHEJ in the repair of DSBs associated with naturally stalled forks or terminating replication molecules.

3. Results

3.1. Original research publication – Ntr1

Conserved interactions of the splicing factor Ntr1/Spp 382 with proteins involved in DNA double-strand break repair and telomere metabolism.

Gernot Hermann, **Sanja Kais**, Jak Hoffbauer, Kijwasch Shah-Hosseini, Nicole Brüggenolte, Heiko Schober, Margaret Fäsi and Primo Schär

reprinted from: Nucleic Acid Research, 2007, Vol 35, No 7, 2321-2332

Published online 27 March 2007

Nucleic Acids Research, 2007, Vol. 35, No. 7 ***2321–2332***
doi:10.1093/nar/gkm127

Conserved interactions of the splicing factor Ntr1/Spp382 with proteins involved in DNA double-strand break repair and telomere metabolism

Gernot Herrmann[1,*], Sanja Kais[2], Jan Hoffbauer[1], Kijwasch Shah-Hosseini[1], Nicole Brüggenolte[1], Heiko Schober[4], Margaret Fäsi[3] and Primo Schär[2]

[1]Department of Dermatology, University of Cologne, D-50924 Cologne, Germany, [2]Centre for Biomedicine, University of Basel, CH-4058 Basel, Switzerland, [3]Institute of Molecular Cancer Research, University of Zürich, CH-8008 Zürich, Switzerland and [4]Friedrich Miescher Institute for Biomedical Research, CH-4058 Basel, Switzerland

Received November 22, 2006; Revised February 14, 2007; Accepted February 15, 2007

ABSTRACT

The ligation of DNA double-strand breaks in the process of non-homologous end-joining (NHEJ) is accomplished by a heterodimeric enzyme complex consisting of DNA ligase IV and an associated non-catalytic factor. This DNA ligase also accounts for the fatal joining of unprotected telomere ends. Hence, its activity must be tightly controlled. Here, we describe interactions of the DNA ligase IV-associated proteins Lif1p and XRCC4 of yeast and human with the putatively orthologous G-patch proteins Ntr1p/Spp382p and NTR1/TFIP11 that have recently been implicated in mRNA splicing. These conserved interactions occupy the DNA ligase IV-binding sites of Lif1p and XRCC4, thus preventing the formation of an active enzyme complex. Consistently, an excess of Ntr1p in yeast reduces NHEJ efficiency in a plasmid ligation assay as well as in a chromosomal double-strand break repair (DSBR) assay. Both yeast and human NTR1 also interact with PinX1, another G-patch protein that has dual functions in the regulation of telomerase activity and telomere stability, and in RNA processing. Like PinX1, NTR1 localizes to telomeres and associates with nucleoli in yeast and human cells, suggesting a function in localized control of DSBR.

INTRODUCTION

Double-strand breaks (DSBs) can arise in DNA through genotoxic stress or as a consequence of DNA metabolic processes associated with DNA synthesis and cell differentiation. Such breaks are highly cytotoxic and will kill a cell, unless repaired. Inaccurate repair, however, will lead to the loss or alteration of genetic information, promoting tumorigenesis and aging. Nature has evolved two fundamentally different strategies for DSB repair (DSBR); homologous recombination (HR) and non-homologous end-joining (NHEJ). Although their relative biological significance varies across the phylogeny, HR and NHEJ are highly conserved repair systems that require a high level of coordination if genomic instability by misrepair is to be avoided (1,2).

NHEJ in mammalian and yeast cells requires a set of common core factors, including the DNA end-binding proteins Ku70 (Ku70p) and Ku80 (Ku80p), as well as the DNA ligase LIG4 (Dnl4p) and its associated factor XRCC4 (Lif1p) (3–6). Yeast Lif1p is detectable near DNA ends, suggesting that it binds DNA in cooperation with Ku and targets Dnl4p to the DSB (7). Similarly, Ku proteins together with the p460 kinase subunit of DNA-PK_{cs} are necessary to recruit the XRCC4-LIG4 complex to DNA ends in human cells (8). Additional factors that contribute to the synapsis and processing of double-stranded DNA ends, including the DNA-PK_{cs}, the MRE11/RAD50/NBS1 (Xrs2p) complex, or Artemis appear to be less conserved between single and multi-cellular organisms [e.g.(9,10)]. Several key components of the NHEJ pathway, e.g. Ku70/80, MRE11/RAD50/NBS1 and Sir proteins, associate with telomeres in lower and higher eukaryotes where they contribute to telomeric maintenance. Telomeres, the free ends of eukaryotic chromosomes, form specialized structures that distinguish them from internal chromosomal breaks and prevent undesired ligation by the NHEJ pathway (11,12).

With an objective to identify regulatory components of the NHEJ pathway, we set out to isolate proteins interacting with Lif1p in a two-hybrid screen in *Saccharomyces cerevisiae*. We isolated two interacting proteins. One of them, Nej1p, was then shown to be a

*To whom correspondence should be addressed. Tel: +49-221-478-7341; Fax: +49-221-478-5949; Email: gernot.herrmann@uni-koeln.de

cell-type-specific regulator of NHEJ in yeast (13–16). The majority of positive clones, however, contained a fragment of an open reading frame (ORF), denoted as YLR424W in the *S. cerevisiae* genome database. YLR424W encodes Ntr1p (Nineteen complex-related protein; standard name SPP382 at SGD), an essential protein with a G-patch domain, which was recently described as a factor involved in spliceosome disassembly (17–19). G-patches are short conserved sequences of ~40 amino acids containing seven highly conserved glycine residues that have been proposed to mediate RNA binding (20). G-patches have also been found in tumor suppressors and DNA-repair proteins (21–25). We show here that Ntr1p associates with Lif1p in a way that excludes binding of Dnl4p and, doing so, forms a stable ternary complex with Lif1p and Nej1p. An *ntr1*Δ disruption causes lethality, but overexpression in yeast affects NHEJ in a plasmid ligation assay and DSBR in a chromosomal context. Ntr1p and its interaction with Lif1p is conserved as we show that a human putative NTR1 ortholog, known as TFIP11 (tuftelin interacting protein), competes with LIG4 for the binding to XRCC4. Like the yeast counterpart, the human NTR1 has been implicated in RNA splicing (26,27). Both the yeast and the human NTR1 proteins further interact with the respective orthologs of PinX1 (PinX1p), another G-patch-containing protein. PinX1 localizes to the nucleolus and to telomeres and appears to have dual functions in RNA processing and the modulation of telomerase activity (22,28). Yeast and human NTR1 also appear to localize to telomeres and to nucleoli. Thus, our data suggest that yeast and human NTR1 are members of a newly emerging family of G-patch proteins that have multiple functions in RNA splicing, DNA repair and telomere maintenance, including also PinX1 (22,28–30), and the orthologs TgDRE of *Toxoplasma gondii* (23,24), DRT111 of *Arabidopsis thaliana* (21) or SPF45 of *Drosophila melanogaster* (25).

MATERIALS AND METHODS

Yeast strains and growth conditions

Saccharomyces cerevisiae strains FF18734, FF18984, FF18743 (*rad52*Δ) and PRSY003,1 (*dnl4*Δ) used in this study are isogenic derivatives of two closely related, congenic series in an A364A background (4). Yeast strains AH109 and Y187 (Clontech) were used for two- and three-hybrid analysis. The *ntr1*Δ deletion was a precise deletion of the ORF, marked by KAN-MX4 (Research Genetics). Cells were grown at 30°C in yeast complete medium or appropriate synthetic drop out media.

Plasmids, DNA manipulations and sequence analyses

For two-hybrid analysis, different fragments of *LIF1*, *DNL4* or human *LIG4* were PCR-amplified from pGEH019, pGEH009 or pGEH007, respectively (3) and subcloned into the Gal4-BD vector pAS2-1, or Gal4-AD vector pACT2 (BD Clontech). The entire *S. cerevisiae NTR1* or *PINX1* ORFs were amplified by PCR of genomic DNA from FF18743 and subcloned into pACT2 or pAS2-1 (BD Clontech). XRCC4 was PCR-amplified from a construct containing the entire ORF (31). Plasmids containing the full-length ORF of human NTR1 were obtained from DKFZ, Heidelberg, Germany (DKFZp434B194, Accession No. AL080147); PinX1 (MGC-8850) and TRF1 (3118244) cDNAs were from ATCC. All plasmids containing entire ORFs were then used as templates for further PCR amplification of fragments which were then cloned into appropriate yeast or bacterial expression vectors. For co-expression studies in bacteria and yeast, we used the IPTG-inducible expression vector pET-28(c) (Novagen) or pGEX-KG. For co-expression studies in yeast, we used the galactose-inducible expression vector pYes2 (Invitrogen). *LIF1* was co-expressed in yeast from pGEH014 (3). yEGFP-sc*NTR1* and yEGFP-hu*NTR1* were constructed by fusing the full-length *NTR1* genes to the MET25 promoter and yEGFP sequences in plasmid pUG36 (16). For transient expression in human cells, fragments of human NTR1 were fused to ECFP, and were then PCR-amplified and subcloned into the tetracycline-inducible vector pcDNA4/TO/*myc*-His (Invitrogen). TRF1 was fused with red fluorescent protein in pDsRed2-C1 or with green fluorescent protein in pDsGreenC1 (Clontech). All constructs were verified by sequencing using an ABI 377 DNA sequencer (Perkin Elmer). Primer sequences and details are available on request. For general database searches and comparisons, we used the BLAST, FASTA and ENTREZ services provided at NCBI's web page; for yeast genome database searches, we accessed MIPS and SGD through their web pages.

Two-hybrid and three-hybrid analysis

Two-hybrid screening was performed using the Matchmaker™ two-hybrid system from Clontech. A *S. cerevisiae* two-hybrid library was kindly provided by Dr N. Lowndes, Galway, Ireland. A pretransformed Human HeLa Matchmaker™ cDNA Library was obtained from Clontech. Three-hybrid analysis was carried out according to the manufacturer's recommendations (Clontech). In extension to two-hybrid analysis, three-hybrid analysis allows investigation of ternary protein complex formation by expression of a third protein cloned into vector pBridge (Clontech) under the control of a methionine-repressible promotor (32). Expression was induced by omitting methionine from the growth medium of the yeast cells. β-Galactosidase assays were carried out according to standard protocols (33).

NHEJ and chromosomal breakage assays

Ligation of restriction endonuclease-digested linearized plasmids and chromosomal breakage assays were carried out as described previously (4,34). Briefly, yeast strains were co-transformed with plasmids carrying the URA3 marker gene and either expressing HO, or EcoRI endonuclease (35) under the control of the inducible *GAL1* promoter and the plasmid-expressing NTR1. Four individual URA+ transformants of each strain were grown to late exponential phase (5×10^7 cells/ml) in liquid medium lacking uracil at 30°C before dropping 5 µl

of serial dilutions (2×10^7, 2×10^6, 2×10^5, 2×10^4, 2×10^3 cells/ml) onto media containing 2% of either glucose, raffinose or raffinose + galactose. The plates were incubated at 30°C for 3–5 days and then photographed. For quantitative analyses, c.f.u. of appropriate dilutions were counted and percentages of survival calculated from at least three independent experiments.

Protein purification and western blot analysis

Purification of 6× histidine-tagged Lif1p from *E. coli* and of 6× histidine-fused proteins from *S. cerevisiae* was performed as described elsewhere (3). GST-tagged fragments of human and yeast NTR1, or PinX1 were expressed alone or co-expressed in different combinations with Lif1p, XRCC4 or NTR1 [in pET28(c)], and purified from *E. coli* BL21(DE3) cells using glutathione sepharose beads. 6× histidine-fused yeast or human NTR1 were co-expressed with Lif1p in yeast strain FF18734 and purified as described elsewhere (3). Induction with galactose (2%) was performed for 10 h. To minimize unspecific binding to the corresponding columns and to increase stringency, washes were performed in a buffer that contained 637 mM NaCl, 2.7 mM KCl, 10 mM phosphate, 0.2% NP-40, 1 mM β-mercaptoethanol; pH 7.4. HeLa and WI26 VA4 cell extracts were prepared with RIPA buffer (supplemented with 4 mM EDTA, 0.2% *n*-dodecyl-β-maltoside, protease inhibitors and ethidium bromide) and 5 mg of extracts were incubated with glutathione sepharose-bound GST-fusion proteins or glutathione sepharose beads overnight at 4°C. Western blot analysis was carried out as described elsewhere (3). Affinity-purified anti-LIF1 antibody was used at a dilution of 1:1000 in PBS containing 1% (w/v) non-fat dried milk, 0.1% Tween-20 for 1 h at room temperature; anti-scNtr1p and anti-huNTR1 antibodies were used at dilutions of 1:200 and 1:2000, respectively, in the same buffer (details on antibody generation on request); anti-XRCC4 (ab2857, Abcam), anti-6× histidine (Cell Signaling) and anti-GFP antibodies (11E5 Invitrogen) were used at dilutions of 1:1000. Anti-PinX1 (ab2344, Abcam) was used at 1:100 overnight at 4°C. Secondary antibodies conjugated to horseradish peroxidase (Pierce, Rockford) were used at dilutions of 1:2000–1:7500.

Microscopic analyses of yeast and human cells

The interaction between Ntr1p and telomeric protein Rap1p was investigated following transformation of the FF18734 strain with plasmid constructs expressing EGFP-NTR1 under the control of the inducible Met25 promoter. Cells were incubated overnight in the liquid minimal medium supplemented with methionine to the final concentration of 1 mM. Cells were prepared for immunofluorescence according to a protocol described previously (36). The endogenous Rap1p was detected using rabbit polyclonal antibody (gift from Susan Gasser) diluted 1:200 in PBS and goat anti-rabbit-TRITC (Sigma) diluted 1:50 in PBS. The signals from EGFP and TRITC were visualized on the confocal Zeiss LSM 510 META microscope with ×63 Plan-Apochromat objective (1.4 oil). An argon laser at 488 nm was used to detect EGFP fluorochrome. To detect TRITC fluorochrome, a helium–neon laser was filtered at 543 nm, while for the DAPI fluorochrome a laser diode was filtered at 405 nm. For image capture, standardized conditions for the pinhole size, gain and offset were used. Each image is an average of eight scans. Images were deconvolved using the Huygens program. To visualize co-localization between Ntr1p and nucleolar protein Nop1, the FF18734 strain was co-transformed with plasmids pUG36-EGFP-NTR1 and pGVH45 (carrying NOP1-CFP; gift from Susan Gasser). The cells were grown overnight in liquid medium (to select for the both plasmids) supplemented with methionine to the final concentration of 1 mM (to keep the levels of EGFP-Ntr1p low). For the live cell imaging, cells were spread on SC agar patches containing 4% glucose. The Metamorph-driven Olympus IX70 microscope equipped with a Zeiss 100×/1.4 oil objective was used to capture 21 image stacks of 200-nm step size (two sequential wavelength 432/515 nm, Chromas filter cube CFP/YFP). The image stacks were deconvolved using the Metamorph program.

Transfections of human WI26 VA4 fibroblasts were performed with FuGENE^{TM} (Boehringer Mannheim) and the Tet-On expression system (BD Biosciences) according to the manufacturer's instructions. Tetracycline induction of ECFP-NTR1 was performed for 4 at 16 h after transfection. Cells were formaldehyde-fixed (3.7%, 15 min at room temperature). Confocal images were taken with an inverted Leica TCS-SP laser-scanning microscope with a ×3 PL Fluotar 1.32–0.6 oil immersion objective. The 488-nm argon ion laser line was used for excitation of ECFP and the 588-nm krypton ion laser line for DsRed2. DAPI was excited using a two-photon laser (772 nm, Spectra Physics). Under all imaging conditions used, no signal from one fluorochrome could be detected on the other filter set. Images were processed using the accompanying software. All images were prepared for publication using Adobe Photoshop.

RESULTS

Ntr1p interacts with Lif1p

We set out to identify interaction partners of the DNA ligase IV-associated protein Lif1p by two-hybrid screening of a yeast cDNA library. Full-length Lif1p and a C-terminal deletion variant consisting of the first 260 amino acids only served as baits. We isolated several clones containing parts of the ORF YLR424W that locates on chromosome XII. YLR424W encodes an 83-kDA protein of 708 amino acids that was recently described as a factor involved in spliceosome disassembly, Ntr1p (17–19). Two-hybrid-based mapping of the Ntr1p interaction site in Lif1p revealed that amino acids between 220 and 240 are essential for interaction (Figure 1A and B). This is the region also required for efficient interaction with Dnl4p (Figure 1B) (3), and where Lif1p shares the highest degree of sequence identity (52.4%) with its human ortholog XRCC4 (Figure 1A). The overall identity between Lif1p and XRCC4 is ~20%. *Vice versa*, examination of different fragments of Ntr1p in two-hybrid

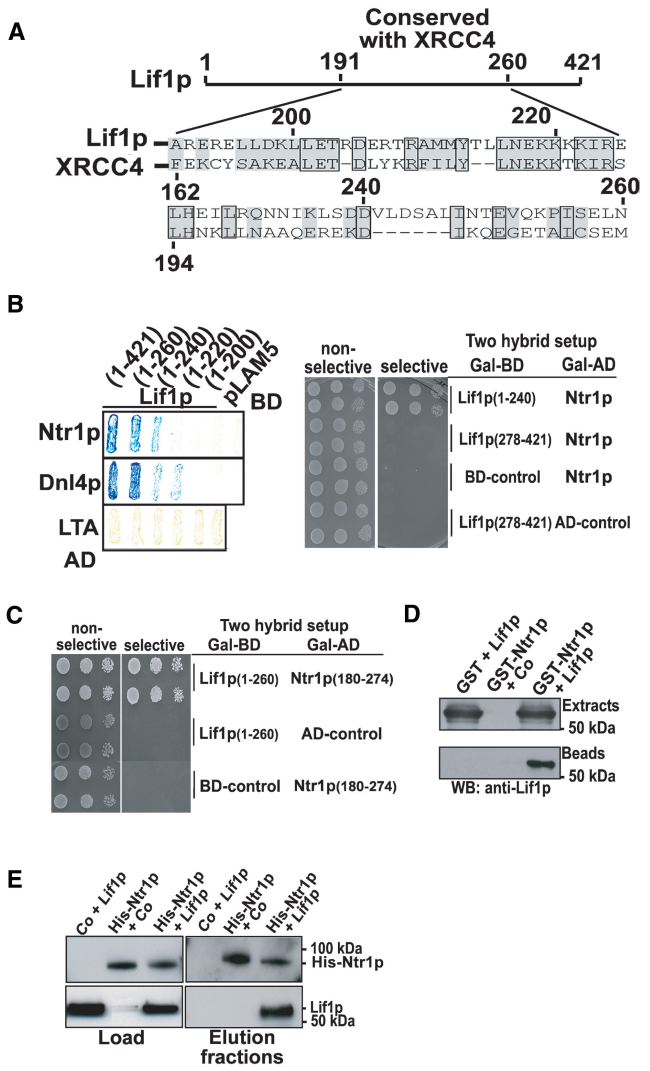

Figure 1. Ntr1p interacts with Lif1p. (**A**) Amino acid alignment of the conserved core region of *S. cerevisiae* Lif1p and human XRCC4. (**B**) Mapping of Ntr1p and Dnl4p interaction domains of Lif1p. Left panel: β-Galactosidase assays of yeast two-hybrid analyses; right panel: two-hybrid analyses with serial dilutions of two independent colonies plated on non-selective (-Leu-Trp) and selective (-Leu-Trp-His) media. Different fragments of Lif1p were expressed as BD (Gal4 DNA-binding domain) fusion proteins (numbers in brackets indicate amino acids). Gal4 activation domain (AD) constructs are fusions of the coding sequences for amino acids 89–509 of Ntr1p and the entire ORF of Dnl4p. LTA is SV40 large T-antigen, pLAM5 is human lamin C (66–230). (**C**) Mapping of Lif1p interaction domain of Ntr1p with the indicated fusion proteins of Lif1p and Ntr1p. Two-hybrid analyses were performed as described for the right panel of Figure 1B. (**D**) Copurification of Lif1p from bacteria expressing recombinant Lif1p and GST-fused Ntr1p. Western blot (WB) analysis of bacterial extracts and glutathione sepharose-bound proteins using anti-Lif1p antibody. Upper panel: 20 μg of extracts expressing Lif1p and GST-Ntr1p proteins as indicated. Lower panel: Lif1p copurification from 1 mg of soluble proteins after pull down of GST-tagged proteins and several washes at high salt stringency. Co indicates the vector control for Lif1p. Here, 5 μl out of 30 μl of proteins eluted from the beads were applied. (**E**) Copurification of Lif1p from *S. cerevisiae* expressing 6× histidine-fused Ntr1p (His-Ntr1). Co indicates the vector control. Proteins were co-expressed in yeast and histidine-fused proteins were purified using nickel agarose. Amounts of proteins used for affinity purification and WB analysis were the same as in (D). WB analysis of relevant elution fractions using anti-Lif1p or an antibody directed against 6× histidine (anti-His).

experiments located the Lif1p-interacting site between amino acids 180 and 274 of Ntr1p (Figures 1C and S1). This region of Ntr1p was previously shown to be involved in the interaction with Ntr2p, another spliceosome disassembly factor (17). Notably, several N-terminal truncations of Ntr1p that contained the Lif1p interaction domain and the entire C-terminus exhibited marked toxicity in the two-hybrid assay, some of them only under co-expression of Lif1p (data not shown).

We then applied GST- and Ni^{2+}-NTA-based fractionation techniques to corroborate the interaction between Ntr1p and Lif1p. Indeed, co-expression of Lif1p with GST-tagged (GST-Ntr1p) or 6-histidine-tagged Ntr1p (His-Ntr1p) in bacteria and in *S. cerevisiae*, respectively, allowed specific and efficient copurification of Lif1p with the tagged Ntr1p, and this after stringent washing with 637 mM NaCl, 0.2% NP40 and 20% glycerol (Figure 1D and E).

Ntr1p is a conserved G-patch protein

Homology searches identified Ntr1p orthologs in species across all eukaryotic kingdoms. A putative human ortholog (presently denominated as TFIP11 for tuftelin-interacting protein) shares an overall 22% identity and 40% similarity with the yeast Ntr1p (Figure S1). This homology stretches over the entire length of the protein and shows a degree of conservation that is also found in other yeast and human orthologs, including the NHEJ factors DNA ligase IV/Dnl4p or XRCC4/Lif1p (3,4,37). All orthologs are characterized by the presence of a more highly conserved N-terminal G-patch domain (Figure S1). For Ntr1p, it was shown that the G-patch is necessary for the interaction with Prp43, an RNA helicase associated with the spliceosome disassembly complex (17). Several G-patch-containing proteins have functions in DNA and RNA metabolism. One family member, PinX1, was recently shown to have dual functions in telomere maintenance (22,28,29) and in ribosomal and small nucleolar RNA maturation (30). Others, such as the *A. thaliana* DRT111 and *T. gondii* TgDRE were shown to have functions in DNA repair by complementing UV and mitomycin hypersensitivity of *E. coli ruvC* and *recG* mutant strains (21,23,24). *Drosophila melanogaster* SPF45 could partially complement MMS sensitivity of *E. coli recG* mutant strains, and mutant *spf45* mutant animals displayed an MMS-sensitive mutant phenotype (25).

Ntr1p is an essential protein

To examine the role of Ntr1p in NHEJ in yeast, we disrupted the *NTR1* gene by replacement of the entire YLR424W ORF with a marker gene cassette in a diploid wild-type background (4). Subsequent sporulation of the heterozygous *NTR1*/*ntr1*Δ to haploid progeny revealed a lethal phenotype of the *NTR1* disruption. Spores carrying the *ntr1*Δ allele were able to germinate but the resulting cells then arrested growth after two cell divisions with a large budded morphology (data not shown). This stands in clear contrast to the rather mild phenotype of a NHEJ defect in yeast and may be explained by the essential functions of Ntr1p in spliceosome disassembly (17–19).

Numerous attempts of generating conditional and separation of function mutants of NTR1 by directed and random mutagenesis, N-degron-tagging and metabolic depletion approaches failed, the lethal phenotype always dominated putative non-essential DSBR defects in all experiments. As regards human NTR1/TFIP11 (from now on referred to as NTR1 only), northern blot analysis of total cellular RNA from human fibroblasts confirmed that it is an active and ubiquitously expressed gene in fetal and adult tissues, producing a transcript of 2.9 kb, which is consistent with the largest cDNA sequence reported (DKFZp434B194) (Figure S2A).

Yeast Ntr1p and Dnl4p form mutually exclusive complexes with Lif1p and Nej1p

Given the proximity of the Dnl4p and Ntr1p interaction sites in the core domain of Lif1p, we examined the effect of Ntr1p on the formation of the DNA ligase complex, i.e. Dnl4p/Lif1p/Nej1p, of NHEJ using a three-hybrid approach. Nej1p, a cell-type-specific regulator of NHEJ was shown to interact with the N-terminus of Lif1p (15). In these experiments, the co-expression of Ntr1p significantly reduced the two-hybrid interaction between Lif1p and Dnl4p (Figure 2), while it had no effect on the interactions between p53 and SV40-LTA (data not shown) or Nej1p and Lif1p (Figure 2). Hence, in this assay Ntr1p interfered specifically with the formation of the Lif1p/Dnl4p complex. Furthermore, Nej1p binds the N-terminal region of Lif1p between amino acids 2 and 69 (15), but it does not interact directly with Dnl4p or Ntr1p in a two-hybrid experiment. However, co-expression of Lif1p mediates close proximity of Nej1p and Ntr1p (or Dnl4p, data not shown), thus allowing survival under selective conditions in a three-hybrid setup, and this is independent of whether Nej1p or Ntr1p are fused to the Gal-AD or the Gal-DB domain (Figure 2). Thus, Lif1p is able to act as a bridging factor for both proteins, indicating that, under three-hybrid conditions, Lif1p and Nej1p form two alternative ternary complexes, one that contains Dnl4p and another that contains Ntr1p.

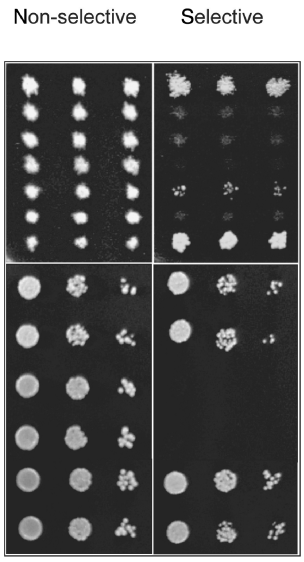

Three-hybrid setup		
Gal 4-BD	MET	Gal 4-AD
$Lif1p_N$	–	$Dnl4p_C$
$Lif1p_N$	Ntr1p	$Dnl4p_C$
$Lif1p_N$	Ntr1p	$Dnl4p_C$
$Lif1p_N$	–	AD-control
BD-control	–	$Dnl4p_C$
$Lif1p_N$	Ntr1p	AD-control
p53	–	SV40LTA
Nej1p	–	Lif1p
Nej1p	Ntr1p	Lif1p
Nej1p	–	Ntr1p
Ntr1p	–	Nej1p
Nej1p	Lif1p	Ntr1p
Ntr1p	Lif1p	Nej1p

Figure 2. Interference of Ntr1p with the formation of NHEJ-relevant protein complexes in yeast three-hybrid analyses. Full-length Nej1p, Ntr1p, Lif1p, or domains of Dnl4p ($Dnl4p_C$, amino acids 632–945), Lif1p ($Lif1p_N$, amino acids 1–260) were expressed as Gal4-BD or Gal4-AD fusions. Where indicated (MET), Ntr1p or Lif1p were expressed under the control of a methionine-repressible promotor. p53 and SV40LTA serve as positive controls for protein interactions. BD and AD are vector controls pBridge and pACT2, respectively. One representative colony out of four analyzed is plated as a serial dilution on appropriate selection media (non-selective, -Leu-Trp; selective, -Leu-Trp-His-Met) and grown for 4 days.

Overexpression of Ntr1p affects DNA DSBR efficiency in yeast

The negative effect of Ntr1p on the formation and/or stability of Dnl4p/Lif1p complexes (Figure 2) prompted us to examine a possible negative regulatory role of Ntr1p in NHEJ. First, we assessed the NHEJ efficiency of cells expressing endogenous levels or an excess Ntr1p in a plasmid re-ligation assay. This assay measures the relative efficiency of homology-independent joining of double-stranded DNA ends of a linearized plasmid upon transformation of yeast cells (4). We found that overexpression of different variants of NTR1 (full-length untagged and EGFP-tagged protein, Lif1p-interaction competent truncations) in wild-type cells and in the background of an EGFP-Ntr1p complemented *ntr1*Δ deletion strain consistently reduced plasmid ligation efficiency by 2–3-fold (Figures 3, S3 and data not shown). Suppression of NHEJ was apparent with both EcoRI and PstI cut plasmid, i.e. on substrates with 5′ and 3′ single-stranded overhangs, respectively (Figure 3A). Yet, the precision of the end-joining events was not affected as determined by PCR amplification and re-digestion of the junctions (data not shown). Co-expression of Lif1p restored plasmid rejoining efficiency to near wild-type levels (Figure S3). In a *dnl4*Δ deficient strain, however, overexpression of Ntr1p did not further reduce plasmid re-ligation efficiency. Thus, overexpression of Ntr1p reduces mildly but reproducibly and significantly Dnl4p-dependent plasmid re-circularization.

To address the role of Ntr1p in the repair of chromosomal DNA breaks, we tested the resistance of DSBR-proficient and -deficient yeast cells expressing endogenous levels or an excess of Ntr1p to DSBs generated by the endonucleases HO or EcoRI (34). Expression of HO in *S. cerevisiae* induces cleavage of the chromosomal DNA once at the *MAT* locus. The resulting DSB is repaired by *RAD52*-dependent HR, a process engaging an intact donor sequence from either of two silent mating-type loci (*HML* or *HMR*) located on the same chromosome (38). Unlike HO, EcoRI will often generate breaks at homologous positions in sister chromatids that require repair by NHEJ rather than by HR. We thus established strains carrying plasmid constructs for the expression of either of these nucleases under the control of the *GAL1* promoter, and of *NTR1* under the control of the constitutive *ADH1* promoter. Note that the *NTR1* construct used here produced an N-terminal GAL4-DNA-BD-fusion of Ntr1p, the functionality of which had been validated first by complementation of

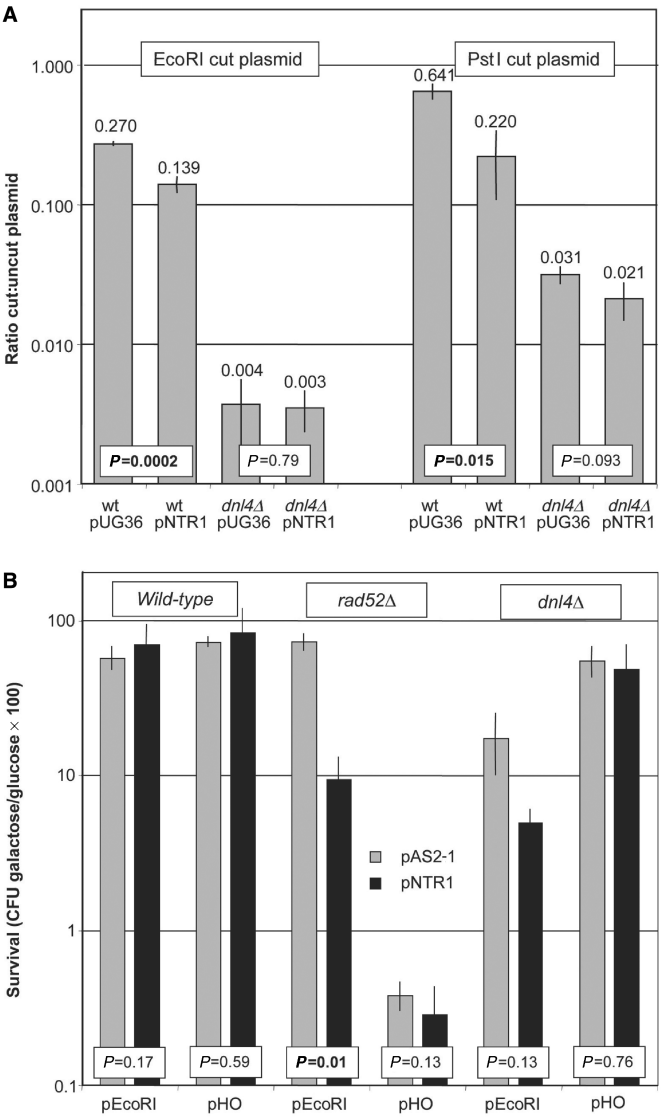

Figure 3. Ntr1p overabundance affects NHEJ of linearized plasmid DNA transformed into yeast, or of chromosomal DNA double-strand breaks in different genetic backgrounds. (**A**) Wild-type (wt) or NHEJ-deficient *dnl4*Δ yeast strains constitutively producing full-length EGFP-tagged-Ntr1p from plasmid pUG36 (vector control) were transformed with equal amounts of digested or undigested plasmid pBTM116, which is a substrate for NHEJ (4). Results are presented as relative transformation efficiencies (ratios of cut:uncut plasmid). EcoRI cut indicates 5′-overhangs, PstI cut indicates 3′-overhangs. Error bars represent one standard deviation, statistical significance (*P*-values) by a two-tailed students *t*-test is indicated. (**B**) Wild-type (wt), HR-deficient *rad52*Δ, or NHEJ-deficient *dnl4*Δ strains constitutively producing full-length Ntr1p from plasmid pAS2–1. Chromosomal breaks were induced by additional expression of EcoRI or HO (GAL1-inducible) upon transformation of the respective expression vectors (35). Results are presented as percentage of survival of cells carrying an NTR1-expressing vector or the respective control vector (pAS2-1) when grown on galactose containing medium. Error bars represent one standard deviation, *P*-values of a two-tailed students *t*-test are indicated.

the lethality of an *ntr1*Δ strain. Parental vector controls were included to assess Ntr1p-specificity of the effects following nuclease induction. Cells carrying these constructs were cultured in the presence of glucose and then dropped in serial dilutions onto media containing either glucose or raffinose/galactose.

Consistent with a predominance of the HR pathway in the repair of HO-induced DSBs, we found *rad52*Δ cells, but not *dnl4*Δ cells, to be highly sensitive to HO expression (survival: wild-type, 73%; *rad52*Δ, 0.38%). *Vice versa*, *dnl4*Δ cells were more sensitive to EcoRI-induced DSBs (survival: wild-type, 58%; *dnl4*Δ, 17%) than *rad52*Δ cells (Figure 3B). These results confirm that cells proficient in HR do rarely employ NHEJ to repair HO-induced DSBs at the MAT locus, and that breaks generated by EcoRI are dealt with predominantly by NHEJ. Ntr1p expression had little effect on the wild-type cells in this assay, but it clearly sensitized the *rad52*Δ (8-fold) and somewhat less the *dnl4*Δ (3.5-fold) mutant strains to DNA strand breaks generated by EcoRI. The suppression of the viability in the *rad52*Δ background is statistically significant, implicating that an excess of Ntr1p channels the repair of EcoRI-induced DSBs into the HR pathway, which, in this strain, is non-functional. Although a similar trend was notable in the *dnl4*Δ mutant, this effect is not statistically significant, suggesting that Ntr1p does not interfere with DSBR in an NHEJ-deficient, HR-proficient background. Consistently, Ntr1p overexpression had little effect on cellular survival upon inductions of HO breaks, which are predominantly repaired by the HR pathway. Thus, Ntr1p affects plasmid ligation efficiency and the productive repair of chromosomal EcoRI breaks by NHEJ.

Human NTR1 is a structural and functional homolog of yeast Ntr1p

Although the evolutionary conservation of the Ntr1p seems clear, much of it appears to be accounted for by the presence of the G-patch. The interaction of Ntr1p with Lif1p, however, requires less conserved sequences downstream of the G-patch (Figure S1). We wondered whether this interaction is conserved in humans and thus examined if human NTR1 forms a complex with XRCC4, the human ortholog of yeast Lif1p. Following deletion of N- and C-terminal sequences of NTR1, which was necessary to reduce autoactivation in two-hybrid assays, we were able to show a specific interaction between XRCC4 and NTR1 (Figure 4A). Like for the yeast counterparts, we could confirm this interaction in a GST-copurification experiment with GST-tagged NTR1 and XRCC4 co-expressed in *E. coli* (Figure 4B). Using this assay, we also mapped the XRCC4 interaction region within NTR1 to amino acids 289 – 343 (Figures 4B, S1), which coincides with the Lif1p interaction domain of yeast Ntr1p (Figure S1). In addition, glutathione sepharose beads coated with bacterially expressed GST-NTR1 (192–580) were able to recover endogenous human XRCC4 protein from HeLa cell extracts (Figure 4C). Further evidence for structural homology between the yeast and human NTR1 proteins came from experiments with antisera raised against the two proteins. Both antisera showed cross-reactivity with the respective orthologous NTR1 proteins, despite the fact that the antibody against the human

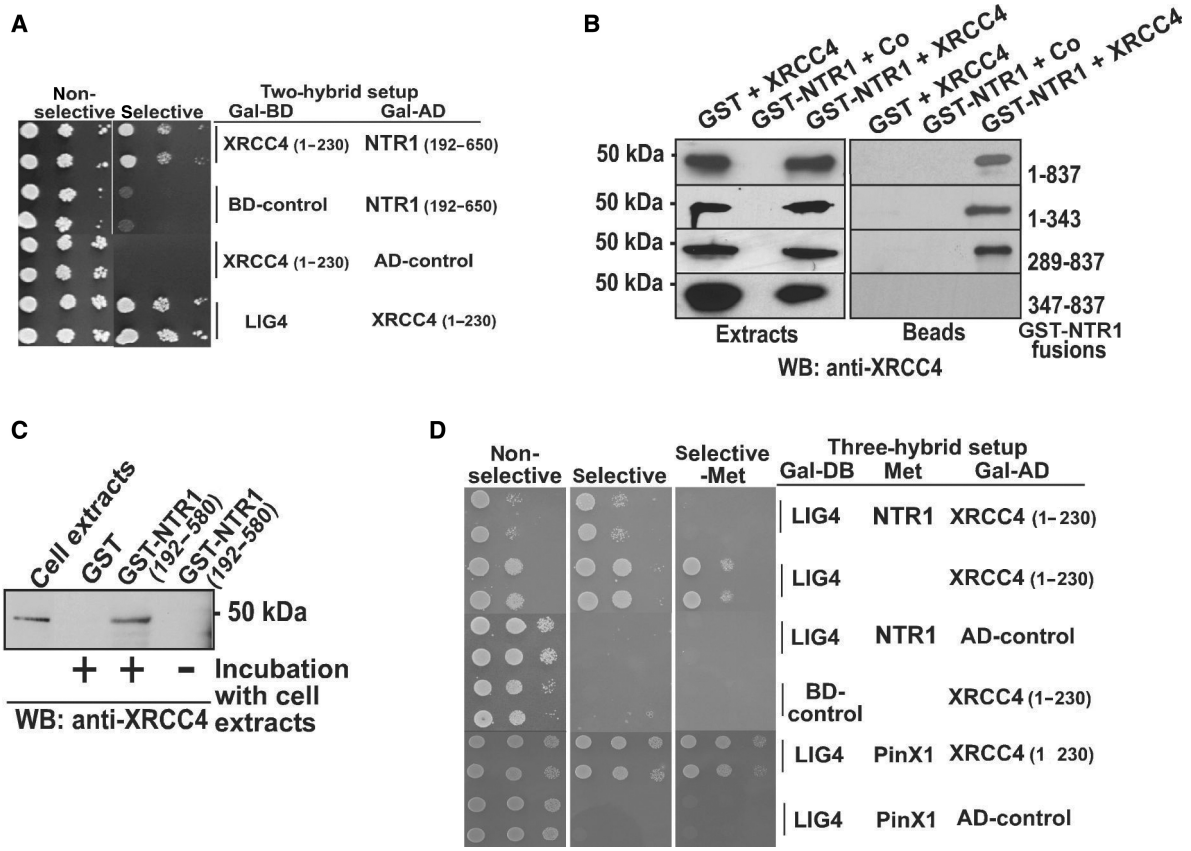

Figure 4. Human NTR1 interacts with XRCC4. (**A**) Two-hybrid interaction of huNTR1 and XRCC4. Fragments containing the indicated amino acids of XRCC4 (1–230), NTR1 (192–650) and full-length LIG4 were fused to the Gal4 DNA-binding (Gal-DB) and activation domains (Gal-AD) as indicated. Serial dilutions of two randomly picked clones were plated on appropriate selection media (as in Figure 1B). (**B**) Copurification of XRCC4 from bacteria expressing recombinant XRCC4 and various fragments of GST-tagged huNTR1. Western blot analysis of bacterial extracts and glutathione sepharose-bound proteins using anti-XRCC4 antibody (experimental conditions as in Figure 1D). The upper panel shows expression of recombinant XRCC4 in 20 μg of bacterial extracts in different combinations with a GST-expressing vector or GST-fused NTR1. The lower panel shows XRCC4 copurification after pull down of GST-fused full-length and truncated forms of NTR1 (amino acids as indicated). (**C**) Purification of XRCC4 from HeLa cell extracts with GST-NTR1 (192–580)-coated glutathione sepharose beads. GST-NTR1 or GST-containing beads were incubated HeLa cell extracts overnight and stringently washed. Western blot analysis of eluted proteins was performed with anti-XRCC4. (**D**) Overexpression of NTR1 disrupts interaction between LIG4 and XRCC4 in three-hybrid analyses. LIG4 and XRCC4 (1–230) were fused to the Gal4-BD and -AD, respectively. NTR1 and PinX1 (used as control) were expressed under the control of a methionine-repressible promotor where indicated. Serial dilutions of two randomly picked clones. Experimental conditions as in Figure 2.

NTR1 was raised against a fragment (289–837) that lacked the conserved G-patch (Figure S2B).

Functionally, three-hybrid experiments with human LIG4, NTR1 and XRCC4 showed that, like its yeast counterpart, human NTR1 interferes with two-hybrid interaction between LIG4 and XRCC4, suggesting that NTR1 competes with LIG4 for the binding site in XRCC4 (Figure 4D). However, while we were successful in co-immunoprecipitating endogenous DNA ligase IV (or Dnl4p) with XRCC4 (or Lif1p), we have thus far not been able to do the same for the endogenous NTR1 proteins (data not shown). The interaction between NTR1 and XRCC4 (or Lif1p) may be short-lived and/or occurs only under specific physiological conditions, e.g. in particular phases of the cell cycle and/or in response to certain forms of genotoxic stress.

Despite the structural and functional conservation between the yeast and the human NTR1 proteins, however, expression of human NTR1 in yeast failed to rescue the lethality of an *ntr1*Δ mutation (data not shown).

Human and yeast NTR1 interact with PinX1, another G-patch protein

To get further clues regarding the function of NTR1, we performed two-hybrid screening of a HeLa cDNA library with a fragment of human NTR1 (1–580). This identified PinX1 as an additional interaction partner. Mapping of the PinX1 interaction domain of NTR1 located the contact site between amino acids 192 and 580 (Figure 5A). This is C-terminal to the conserved G-patch and overlaps with the region required for interaction with XRCC4 (289–343). In addition, co-expression of NTR1 with GST-tagged PinX1 (GST-PinX1) bacteria allowed specific and efficient copurification of NTR1 with the tagged PinX1 (Figure 5B), and glutathione sepharose beads coated with bacterially expressed GST-NTR1 (192–580) were able to recover

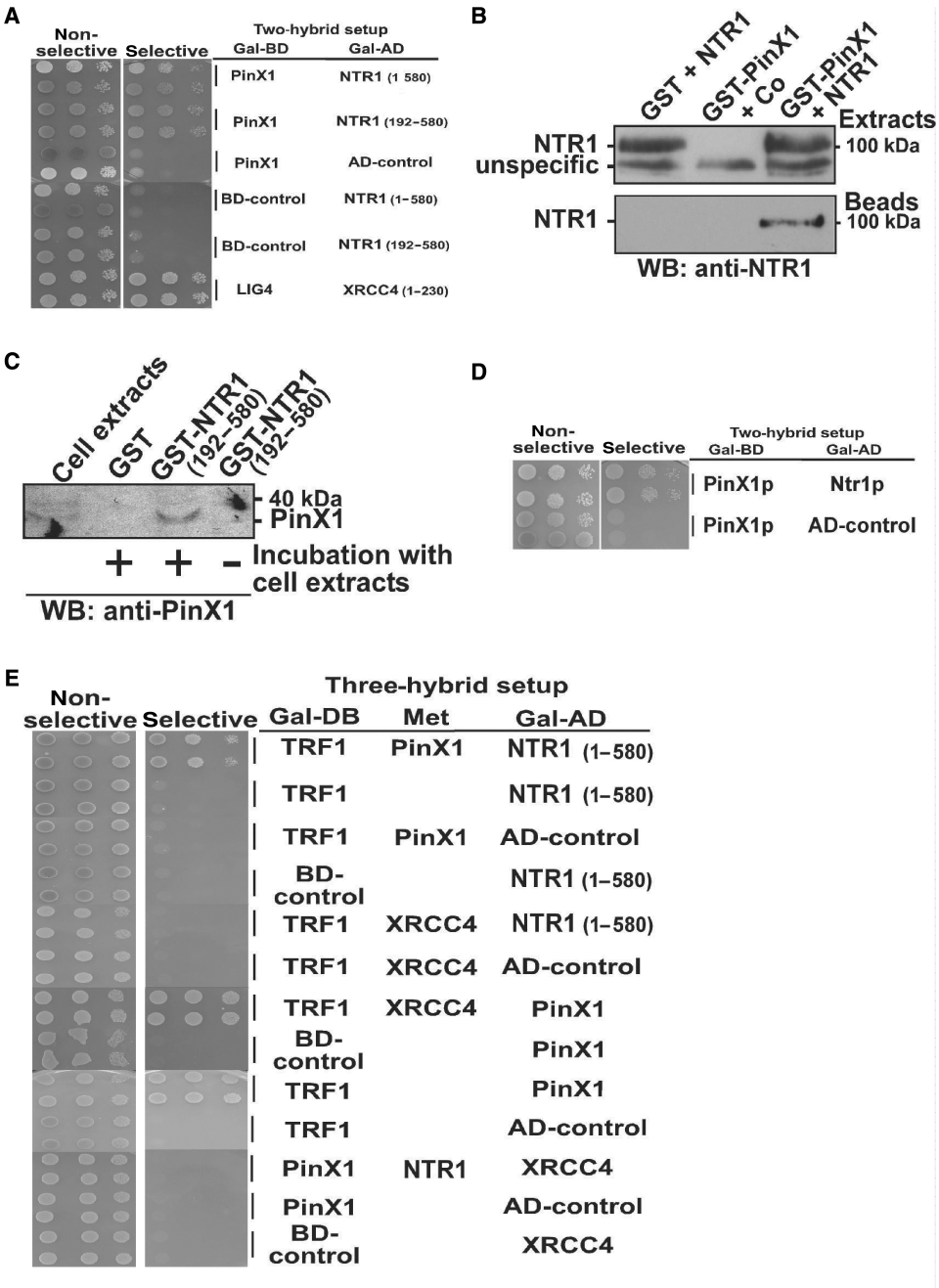

Figure 5. Yeast and human NTR1 interact with the respective orthologs of PinX1. (**A**) Two-hybrid interaction of human NTR1 and PinX1. Two-hybrid analyses were performed with the indicated Gal-BD and -AD fusions of PinX1 and NTR1. Numbers in brackets indicate amino acids. Experimental conditions as in Figure 1B. The interaction of LIG4 and XRCC4 (1–230) was used as a positive control. (**B**) Copurification of human NTR1 from bacteria expressing recombinant NTR1 and GST-fused PinX1. Experimental conditions as in Figure 1D. western blot (WB) analysis of bacterial extracts and glutathione sepharose-bound proteins using anti-NTR1 antibody. Upper panel: expression of recombinant NTR1 in 20 µg of bacterial extracts in the presence of a GST-expressing vector (GST) and a vector expressing a GST-fused form of PinX1 (GST-PinX1). Lower panel: corresponding NTR1 copurification after pull down of GST-tagged proteins and several washes at high salt stringency. (**C**) Purification of PinX1 from HeLa cell extracts with GST-NTR1 (192–580). Experimental conditions as in Figure 4C. Western blot analysis was performed with anti-PinX1. (**D**) Two-hybrid interactions of yeast Ntr1p and PinX1p. Experimental conditions as in Figure 1B. (**E**) Overexpression of PinX1 mediates proximity between NTR1 and TRF1 in three-hybrid analyses. Serial dilutions of two randomly picked clones. Experimental conditions as in Figure 2. TRF1 and NTR1 (1–580) were fused to the Gal4-BD and -AD, respectively. PinX1, XRCC4 or NTR1 were expressed under the control of a methionine-repressible promotor whereever indicated.

endogenous human PinX1 protein from HeLa cell extracts (Figure 5C). Again, this interaction appears to be conserved between yeast and human, as PinX1p figures in the list of the many interaction partners of Ntr1p previously identified in genome wide two-hybrid screens for protein-protein interactions (39) and could be reproduced in an additional two-hybrid analysis of the yeast proteins (Figure 5D).

Human PinX1 was first identified as an interaction partner of the telomere-binding protein Pin2/TRF1 and subsequently shown to regulate telomerase activity (22,29). The yeast PinX1p has been associated with rRNA and nucleolar RNA maturation (30) as well as to interact physically with telomerase to regulate its catalytic activity (28). Hence, the link to PinX1 suggested a function of NTR1 at telomeres. We therefore asked whether human PinX1 might act as a bridging factor between NTR1 and TRF1. Indeed, co-expression of PinX1 mediated close proximity of NTR1 and TRF1, allowing cells to grow under selective conditions in the three-hybrid assay (Figure 5E). Thus, TRF1 and NTR1 bind PinX1 simultaneously, which may provide a structural link of NTR1 to telomere metabolism.

Human and yeast NTR1 co-localize with telomere-associated proteins

To corroborate an association of NTR1 with telomeres, we used confocal microscopy and live cell imaging to localize the protein in cells. Expression of a functional EGFP-Ntr1p under the control of the inducible MET25 promoter in NTR1-proficient and -deficient (*ntr1*Δ) yeast cells revealed a nuclear localization of the protein with a dot-like pattern (Figure 6A). These dots varied in numbers and intensity depending on the expression level and the cell ploidy (data not shown). We thus performed co-localization studies under repressed conditions and in haploid cells, where the EGFP-Ntr1p protein level approximates that of the endogenous protein and NHEJ is active (data not shown). We found significant co-localization of the EGFP-Ntr1p dots with endogenous Rap1p, a transcriptional regulator that binds to telomeric sequences and contributes to telomere maintenance and the establishment of the telomere position effect on gene expression (40). Here, $63 \pm 2\%$ (165/262 observations, three independent experiments) of double-positive cells showed complete or partial (>30% of signal) overlap of all EGFP-Ntr1 and Rap1p signals, $14 \pm 2\%$ of cells showed both, co-localizing and separate Ntr1p and Rap1p foci, whereas $24 \pm 1\%$ of cells showed no co-localization of the two proteins (Figure 6A). Thus, the fraction of cells showing co-localization of EGFP-Ntr1p with Rap1p was significantly higher than that without co-localization ($P = 0.0001$, *t*-test). Nevertheless, prompted by the incompleteness of the co-localization with Rap1p and the localization properties of PinX1, which is found not only at telomeres but also in the nucleolus (22), we tested whether Ntr1p might behave similarly. Hence, we examined co-localization of Ntr1p with Nop1p, a nucleolar protein involved in rRNA processing (41). Indeed, we found EGFP-Ntr1p foci to overlap with the signal of a CFP-tagged Nop1p in 74% (118/159 observations, two independent experiments) of the cells, suggesting a possible association of Ntr1p with the nucleolus (Figure 6A). Interestingly, telomeric and nucleolar localization has been described for a number of telomere-associating proteins, including the reverse transcriptase subunit of the telomerase itself (42).

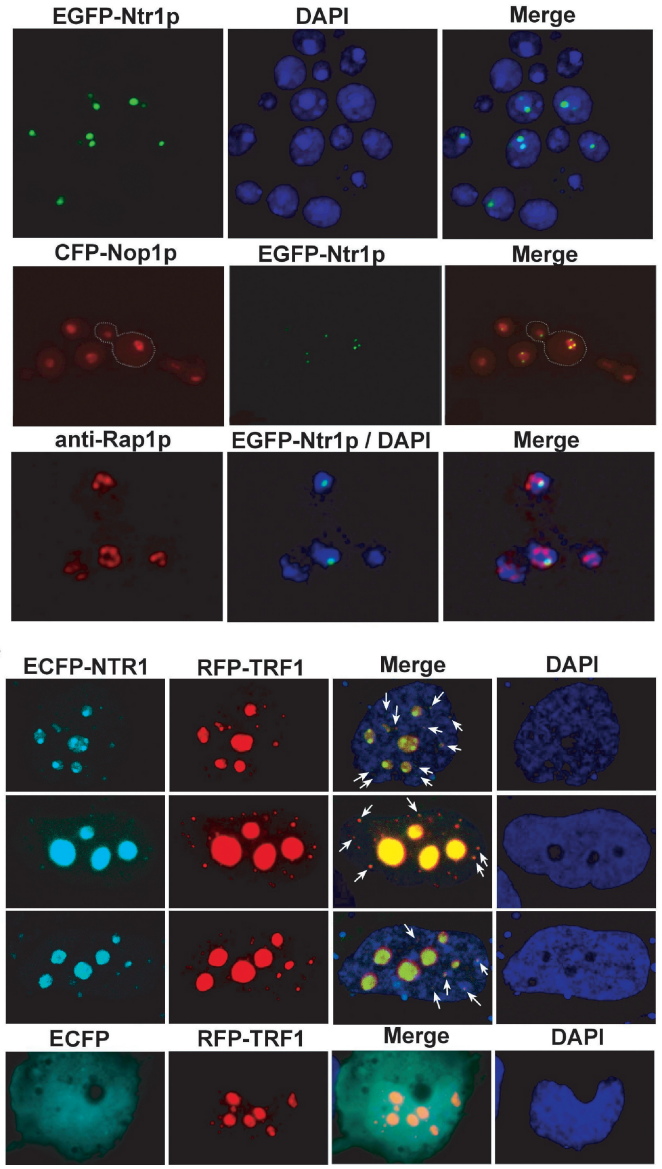

Figure 6. Yeast and human NTR1 co-localize with nucleolus- and telomere-associated proteins. (**A**) Intracellular localization of Ntr1p and co-localization with other proteins. Upper panel: EGFP-Ntr1p (green) localizes to the nucleus (DAPI, light blue) and forms foci. Middle panel: live cell images of CFP-Nop1p (red, false color) and EGFP-Ntr1p (green). Co-localizing signals are shown in yellow in the merge panel. Lower panel: confocal images of EGFP-Ntr1p (green) in fixed cells immunostained for Rap1p (red). DAPI staining of DNA is shown in blue. Co-localization between the two proteins is shown in yellow on the merge panel. (**B**) Intracellular localization of human NTR1 and TRF1. WI26 VA4 cells were co-transfected with expression constructs of ECFP-NTR1 (amino acids 289–580) and RFP-TRF1 (upper three panels). eCFP was used as a control (lower panel). Co-localization in confocal images is shown in yellow on the merge panel and telomeric co-localization is indicated by arrows.

Overexpression of full-length NTR1 in human cell lines was toxic and resulted in aggregate formation and cell lysis. To analyze intracellular localization of human NTR1, we therefore expressed a non-toxic ECFP-NTR1 fragment that contained the interaction region with XRCC4 and PinX1. Upon co-transfection of

ECFP-NTR1 and RFP-TRF1 expressing constructs, we found a nucleolar co-localization in all double-transfected cells. The double-transfected cells showed 40% full and 44% partial co-localization of extranucleolar ECFP-NTR1 foci with RFP-TRF1, indicating an association of NTR1 with telomeres (Figure 6B). A similar telomeric and nucleolar co-localization pattern was previously described for PinX1 and TRF1 (22).

Together, these data support a link between NTR1 function and telomere metabolism as suggested by the three-hybrid interaction observed between NTR1, PinX1 and TRF1.

DISCUSSION

This work establishes a specific physical interaction of the yeast Lif1p and Ntr1p proteins. Ntr1p is G-patch-motif-containing protein that has recently been described to function in spliceosome disassembly. It interacts with Lif1p through its Dnl4p-binding site and, in doing so, forms a complex with Lif1p-Nej1p that lacks the catalytic DNA ligase function. This would implicate a role of Ntr1p in the regulation of NHEJ by sequestering the DNA ligase cofactor Lif1p in an inactive complex. Consistently, overproduction of Ntr1p in yeast cells affects the efficiency of joining of linearized plasmids and alters the way cells process chromosomal DSBs by NHEJ. Ntr1p itself as well as its interaction with the DNA ligase IV cofactor has been conserved in evolution; we show that the human ortholog NTR1 interacts with XRCC4 in a way that excludes the LIG4 in the complex. An additional conserved interaction of the yeast and human NTR1 proteins with PinX1, a G-patch protein implicated in nucleolar RNA maturation and regulation of telomerase activity, and their localization to telomeres and the nucleolus suggests an additional function of the splicing factor in location-dependent regulation of NHEJ.

Consistent with its physical interactions (39), recently published work strongly suggests that the essential function of Ntr1p is the processing/maturation of RNA (17–19). Still, as telomeric terminal rearrangements in yeast and human cells are know to be generated by NHEJ and, thus, to depend on functional DNA ligase IV (43,44), we wanted to exclude that uncontrolled fusion of telomeres contributes to the lethal phenotype of the *ntr1*Δ mutant, i.e. that the loss of Ntr1p leads to a de-repression of fatal ligation of free telomere ends. We therefore tested whether the lethality of the *ntr1*Δ mutation can be rescued by an additional *dnl4*Δ or *lif1*Δ defect. This was not the case, indicating that aberrant Dnl4p-mediated ligation of double-stranded DNA ends is not a dominant killing event in the *ntr1*Δ strains. Various attempts to generate NTR1 variants that separate the essential splicing function from the DNA repair function failed. In retrospect, however, this may not be too surprising, considering that the sites for Lif1p and Ntr2p interactions map to the same region of Ntr1p (17). Thus, the role of NTR1 in NHEJ is difficult to address in an unambiguous genetic approach and therefore remains somewhat enigmatic. While there is no evidence for a Dnl4p-independent function of Lif1p (or XRCC4), our plasmid ligation and nuclease survival experiments implicate that Ntr1p, when present in excess, affects the cellular DSBR capacity. The effects, however, though reproducible and statistically significant, are complex and difficult to interpret. In the plasmid ligation assay, overexpression of *NTR1* inhibits NHEJ in a Dnl4p-dependent manner. Yet, compared to a full NHEJ deficiency, this effect is only marginal. In the chromosomal DSBR assay, NTR1 overexpression sensitizes *rad52*Δ cells to EcoRI-induced DSBs to the level of a *dnl4*Δ single mutant, but it remains to be clarified why this effect requires *RAD52* to be inactive. One explanation is that excess Ntr1p and the loss of Dnl4p affect NHEJ at different intermediate stages of the process, the former allowing more efficient rescue of the repair event by the HR pathway and the latter leading to more frequent unproductive (lethal) processing of the EcoRI breaks. An important caveat associated with the interpretation of these results is that the assays used may not adequately mimic the relevant physiological environment for Ntr1p action.

Indeed, the subnuclear localization of Ntr1p as well as its interaction with PinX1 suggests that it acts locally rather than globally in the genome. EGFP-tagged Ntr1p expressed at about endogenous levels from a repressed MET25 promoter localizes to one to two, rarely three, distinct foci in the nucleus. Statistical analyses of these co-localization experiments suggest that, one of these spots seems to non-randomly associate with the nucleolar region (45), while the other(s) may reflect variable associations with telomeres. Interestingly, nucleolar and telomeric localization was also proposed for yeast and human PinX1, which we show here to interact with the respective NTR1 proteins. Besides its role in rRNA and nucleolar RNA maturation (30), yeast PinX1p was recently reported to regulate telomerase by sequestering its catalytic subunit in an inactive complex, presumably in the nucleolus (28). A similar regulatory mechanism could apply to the inhibition of NHEJ by Ntr1p. Ntr1p may sequester Lif1p and thereby prevent the formation or in fact mediate the disassembly of active DNA ligase complexes. Since this will occur only at sites where Ntr1p is enriched, presumably in the nucleolus or at the telomeres, the consequence will be a local inhibition of the ligation step of NHEJ. Testable predictions of such a scenario would be that Ntr1p localization is independent of Lif1p, while Lif1p should partially co-localize with Ntr1p in the nucleus. The focal Ntr1p localization pattern is indeed unaffected in a *lif1*Δ strain fulfilling the first prediction (data not shown). The Lif1p-Ntr1p co-localization, however, has not yet been resolved conclusively. The difficulty here is the diffuse nature of the nuclear localization of Lif1p, which may cover temporary or localized associations of the protein with alternative complexes. However, the localization of the spliceosome disassembly factor Ntr1p to telomeres and nucleoli and its interaction with Lif1p implicate unexpected functions of this protein in telomere metabolism and possibly DNA repair. We do not know whether or not there is a common denominator between spliceosome disassembly and the functions implicated here. It is worth

noting, however, that Ntr1p-depleted cells accumulate lariat-introns as RNA-splicing intermediates, a structure that remotely reminds us of the telomeric loops.

It is unclear to date exactly how cells discriminate between chromosomal DSBs that need to be repaired and the double-stranded DNA ends at telomeres that must not be ligated. This discrimination, however, is likely to occur at the ligation step because upstream key factors of NHEJ, e.g. the Ku heterodimer and the MRE11/RAD50/NBS1, associate with both types of DNA ends. This is where the NTR1 proteins could come into play. Their physical and functional properties as described in this work make them likely candidates for the regulation of NHEJ at the intersection of DNA DSBR and telomere end protection, although the underlying mechanistic details remain to be elucidated.

ACKNOWLEDGEMENTS

We thank Dr Francis Fabre for yeast strains, Dr Susan Gasser for reagents and technical support, and Dr Lukas Landmann and Dr Iakowos Karakesisoglou for competent assistance in confocal microscopy. Preliminary experiments were performed by G.H. and P.S. at the Clare Hall Laboratories, South Mimms, UK and we thank Dr Tomas Lindahl for his interest and support. G.H. was supported by grant He 2675/2–3, 'Sonderforschungsbereich' SFB 589 from the 'Deutsche Forschungsgemeinschaft (DFG)' and by the Köln Fortune Program/Faculty of Medicine, University of Cologne. J.H. was supported by the Köln Fortune Program/Faculty of Medicine, University of Cologne and K.S.-H. by a short-term EMBO Fellowship. S.K. and P.S. were supported by the 'Bonizzi-Theler Stiftung', Zürich. Funding to pay the Open Access publication charge was provided by the DFG.

Conflict of interest statement. None declared.

REFERENCES

1. Ferreira,M.G. and Cooper,J.P. (2004) Two modes of DNA double-strand break repair are reciprocally regulated through the fission yeast cell cycle. *Genes Dev.*, **18**, 2249–2254.
2. Guirouilh-Barbat,J., Huck,S., Bertrand,P., Pirzio,L., Desmaze,C., Sabatier,L. and Lopez,B.S. (2004) Impact of the KU80 pathway on NHEJ-induced genome rearrangements in mammalian cells. *Mol. Cell*, **14**, 611–623.
3. Herrmann,G., Lindahl,T. and Schär,P. (1998) *Saccharomyces cerevisiae* LIF1: a function involved in DNA double-strand break repair related to mammalian XRCC4. *EMBO J.*, **17**, 4188–4198.
4. Schär,P., Herrmann,G., Daly,G. and Lindahl,T. (1997) A newly identified DNA ligase of *Saccharomyces cerevisiae* involved in *RAD52*-independent repair of DNA double-strand breaks. *Genes Dev.*, **11**, 1912–1924.
5. Teo,S.H. and Jackson,S.P. (1997) Identification of *Saccharomyces cerevisiae* DNA ligase IV: involvement in DNA double-strand break repair. *EMBO J.*, **16**, 4788–4795.
6. Wilson,T.E., Grawunder,U. and Lieber,M.R. (1997) Yeast DNA ligase IV mediates non-homologous DNA end joining. *Nature*, **388**, 495–498.
7. Teo,S.H. and Jackson,S.P. (2000) Lif1p targets the DNA ligase Lig4p to sites of DNA double-strand breaks. *Curr. Biol.*, **10**, 165–168.
8. Calsou,P., Delteil,C., Frit,P., Drouet,J. and Salles,B. (2003) Coordinated assembly of Ku and p460 subunits of the DNA-dependent protein kinase on DNA ends is necessary for XRCC4-ligase IV recruitment. *J. Mol. Biol.*, **326**, 93–103.
9. Collis,S.J., DeWeese,T.L., Jeggo,P.A. and Parker,A.R. (2005) The life and death of DNA-PK. *Oncogene*, **24**, 949–961.
10. Dudasova,Z., Dudas,A. and Chovanec,M. (2004) Non-homologous end-joining factors of Saccharomyces cerevisiae. *FEMS Microbiol. Rev.*, **28**, 581–601.
11. Williams,B. and Lustig,A.J. (2003) The paradoxical relationship between NHEJ and telomeric fusion. *Mol. Cell*, **11**, 1125–1126.
12. Riha,K., Heackock,M.L. and Shippen,D.E. (2006) The role of the nonhomologous end-joining DNA double-strand break repair pathway in telomere biology. *Annu. Rev. Genet.*, **40**, 237–277.
13. Frank-Vaillant,M. and Marcand,S. (2001) NHEJ regulation by mating type is exercised through a novel protein, Lif2p, essential to the ligase IV pathway. *Genes Dev.*, **15**, 3005–3012.
14. Kegel,A., Sjostrand,J.O. and Astrom,S.U. (2001) Nej1p, a cell type-specific regulator of nonhomologous end joining in yeast. *Curr. Biol.*, **11**, 1611–1617.
15. Ooi,S.L., Shoemaker,D.D. and Boeke,J.D. (2001) A DNA microarray-based genetic screen for nonhomologous end-joining mutants in Saccharomyces cerevisiae. *Science*, **294**, 2552–2556.
16. Valencia,M., Bentele,M., Vaze,M.B., Herrmann,G., Kraus,E., Lee,S.E., Schär,P. and Haber,J.E. (2001) NEJ1 controls non-homologous end joining in Saccharomyces cerevisiae. *Nature*, **414**, 666–669.
17. Tsai,R.T., Fu,R.H., Yeh,F.L., Tseng,C.K., Lin,Y.C., Huang,Y.H. and Cheng,S.C. (2005) Spliceosome disassembly catalyzed by Prp43 and its associated components Ntr1 and Ntr2. *Genes Dev.*, **19**, 2991–3003.
18. Boon,K.L., Auchynnikava,T., Edwalds-Gilbert,G., Barrass,J.D., Droop,A.P., Dez,C. and Beggs,J.D. (2006) Yeast ntr1/spp382 mediates prp43 function in postspliceosomes. *Mol. Cell. Biol.*, **26**, 6016–6023.
19. Pandit,S., Lynn,B. and Rymond,B.C. (2006) Inhibition of a spliceosome turnover pathway suppresses splicing defects. *Proc. Natl. Acad. Sci. USA*, **103**, 13700–13705.
20. Aravind,L. and Koonin,E.V. (1999) G-patch: a new conserved domain in eukaryotic RNA-processing proteins and type D retroviral polyproteins. *Trends Biochem. Sci.*, **24**, 342–344.
21. Pang,Q., Hays,J.B. and Rajagopal,I. (1993) Two cDNAs from the plant Arabidopsis thaliana that partially restore recombination proficiency and DNA-damage resistance to E. coli mutants lacking recombination-intermediate-resolution activities. *Nucleic Acids Res.*, **21**, 1647–1653.
22. Zhou,X.Z. and Lu,K.P. (2001) The Pin2/TRF1-interacting protein PinX1 is a potent telomerase inhibitor. *Cell*, **107**, 347–359.
23. Dendouga,N., Callebaut,I. and Tomavo,S. (2002) A novel DNA repair enzyme containing RNA recognition, G-patch and specific splicing factor 45-like motifs in the protozoan parasite Toxoplasma gondii. *Eur. J. Biochem.*, **269**, 3393–3401.
24. Frenal,K., Callebaut,I., Wecker,K., Prochnicka-Chalufour,A., Dendouga,N., Zinn-Justin,S., Delepierre,M., Tomavo,S. and Wolff,N. (2006) Structural and functional characterization of the TgDRE multidomain protein, a DNA repair enzyme from Toxoplasma gondii. *Biochemistry*, **45**, 4867–4874.
25. Chaouki,A.S. and Salz,H.K. (2006) *Drosophila* SPF45: a bifunctional protein with roles in both splicing and DNA repair. *PLoS Genet*, **2**, e178.
26. Zhou,Z., Licklider,L.J., Gygi,S.P. and Reed,R. (2002) Comprehensive proteomic analysis of the human spliceosome. *Nature*, **419**, 182–185.
27. Wen,X., Lei,Y.P., Zhou,Y.L., Okamoto,C.T., Snead,M.L. and Paine,M.L. (2005) Structural organization and cellular localization of tuftelin-interacting protein 11 (TFIP11). *Cell. Mol. Life Sci.*, **62**, 1038–1046.
28. Lin,J. and Blackburn,E.H. (2004) Nucleolar protein PinX1p regulates telomerase by sequestering its protein catalytic subunit in an inactive complex lacking telomerase RNA. *Genes Dev.*, **18**, 387–396.
29. Banik,S.S. and Counter,C.M. (2004) Characterization of interactions between PinX1 and human telomerase subunits hTERT and hTR. *J. Biol. Chem.*, **279**, 51745–51748.

30. Guglielmi,B. and Werner,M. (2002) The yeast homolog of human PinX1 is involved in rRNA and small nucleolar RNA maturation, not in telomere elongation inhibition. *J. Biol. Chem.*, **277**, 35712–35719.
31. Critchlow,S.E., Bowater,R.P. and Jackson,S.P. (1997) Mammalian DNA double-strand break repair protein XRCC4 interacts with DNA ligase IV. *Curr. Biol.*, **7**, 588–598.
32. Tirode,F., Malaguti,C., Romero,F., Attar,R., Camonis,J. and Egly,J.M. (1997) A conditionally expressed third partner stabilizes or prevents the formation of a transcriptional activator in a three-hybrid system. *J. Biol. Chem.*, **272**, 22995–22999.
33. Transy,C. and Legrain,P. (1995) The two-hybrid: an in vivo protein-protein interaction assay. *Mol. Biol. Rep.*, **21**, 119–127.
34. Schär,P., Fasi,M. and Jessberger,R. (2004) SMC1 coordinates DNA double-strand break repair pathways. *Nucleic Acids Res.*, **32**, 3921–3929.
35. Barnes,G. and Rio,D. (1997) DNA double strand break sensitivity, DNA replication, and cell cycle arrest phenotypes of Ku-deficient *Saccharomyces cerevisiae*. *Proc. Natl. Acad. Sci. USA*, **94**, 867–872.
36. Gotta,M., Laroche,T. and Gasser,S.M. (1999) Analysis of nuclear organization in Saccharomyces cerevisiae. *Methods Enzymol.*, **304**, 663–672.
37. Tugendreich,S., Bassett,D.E.Jr., McKusick,V.A., Boguski,M.S. and Hieter,P. (1994) Genes conserved in yeast and humans. *Hum. Mol. Genet. Spec. No.*, **3**, 1509–1517.
38. Haber,J.E. (1992) Mating-type gene switching in *Saccharomyces cerevisiae*. *Trends Genet.*, **8**, 446–452.
39. Hazbun,T.R., Malmstrom,L., Anderson,S., Graczyk,B.J., Fox,B., Riffle,M., Sundin,B.A., Aranda,J.D., McDonald,W.H. *et al.* (2003) Assigning function to yeast proteins by integration of technologies. *Mol. Cell*, **12**, 1353–1365.
40. Gotta,M., Laroche,T., Formenton,A., Maillet,L., Scherthan,H. and Gasser,S.M. (1996) The clustering of telomeres and colocalization with Rap1, Sir3, and Sir4 proteins in wild-type Saccharomyces cerevisiae. *J. Cell Biol.*, **134**, 1349–1363.
41. Tollervey,D., Lehtonen,H., Carmo-Fonseca,M. and Hurt,E.C. (1991) The small nucleolar protein NOP1 (fibrillarin) is required for pre-rRNA processing in yeast. *EMBO J.*, **10**, 573–583.
42. Teixeira,M.T., Forstemann,K., Gasser,S.M. and Lingner,J. (2002) Intracellular trafficking of yeast telomerase components. *EMBO Rep.*, **3**, 652–659.
43. Liti,G. and Louis,E.J. (2003) NEJ1 prevents NHEJ-dependent telomere fusions in yeast without telomerase. *Mol. Cell*, **11**, 1373–1378.
44. Smogorzewska,A., Karlseder,J., Holtgreve-Grez,H., Jauch,A. and de Lange,T. (2002) DNA ligase IV-dependent NHEJ of deprotected mammalian telomeres in G1 and G2. *Curr. Biol.*, **12**, 1635–1644.
45. Bystricky,K., Laroche,T., van Houwe,G., Blaszczyk,M. and Gasser,S.M. (2005) Chromosome looping in yeast: telomere pairing and coordinated movement reflect anchoring efficiency and territorial organization. *J. Cell Biol.*, **168**, 375–387.

3.2. Supplement to Ntr1 project

In this section, I will present results of additional experiments performed in attempt to better understand the role of Ntr1 in DSB repair. These represent a supplement to the publication form section 3.1. and haven't been published yet. In each sub-section below, I will first describe the results obtained and then shortly discuss them in respect with current literature and future perspectives. Details of experimental procedures used in this section are described in section 3.2.5.

3.2.1 Impact of Ntr1 expression on the accuracy of the NHEJ reaction

It has been reported that the repair of DSBs by NHEJ can sometimes be inaccurate, leading to introduction of small insertions or deletions at the junction in the repaired DNA (Wilson et al 1997, Boulton and Jackson 1998). In NHEJ deficient cells, the repair of a DSB substrate in the absence of available sequence homology involves extensive end-processing and depends on HR (Schär et al 1997, Teo and Jackson 1997) Since Ntr1 overexpression reduces overall NHEJ capacities in the cell (see 3.1.), I tested a possible effect on the accuracy of DNA end-joining.

For that purpose, colonies arising from the NHEJ plasmid repair assay were restreaked to complete medium (YPD) and grown for 2 days at 30^{o}C. From each colony, DNA was extracted and used as a template for colony-PCR. A pair of primers was designed to anneal to the pBTM116 plasmid few hundred basepairs away from the break site on each side (Fig 1). In case that the plasmid was accurately repaired, the PCR reaction should give a product of 1.1 kb. The products of the colony-PCR were loaded to a 0.8% agarose gel and electrophoresed. In this way, larger insertions and deletions could be detected directly (Fig 2).

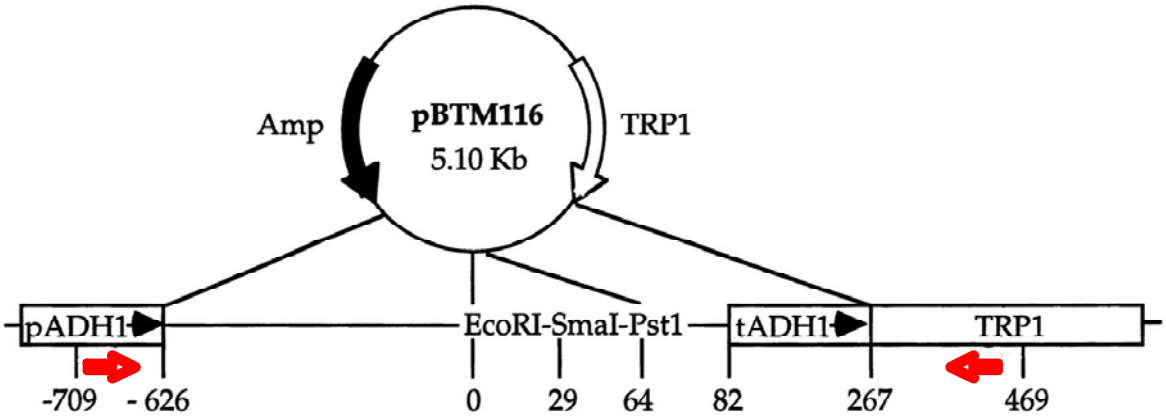

Figure 1. Schematic map of the pBTM116 plasmid. The plasmid carries Amp for selection in E. coli and TRP1 for selection in yeast. Relevant restriction sites (*Eco*RI and *Pst*I) are located in the plasmid region with no homology to the yeast genome. Flanking regions of transcription elements of yeast ADH1 (pADH1, promoter; tADH1, terminator sequence) are shown together with distance in base-pairs from the EcoRI site. Red arrows indicate annealing sites of the PCR primers used for analysis of plasmid repair events.

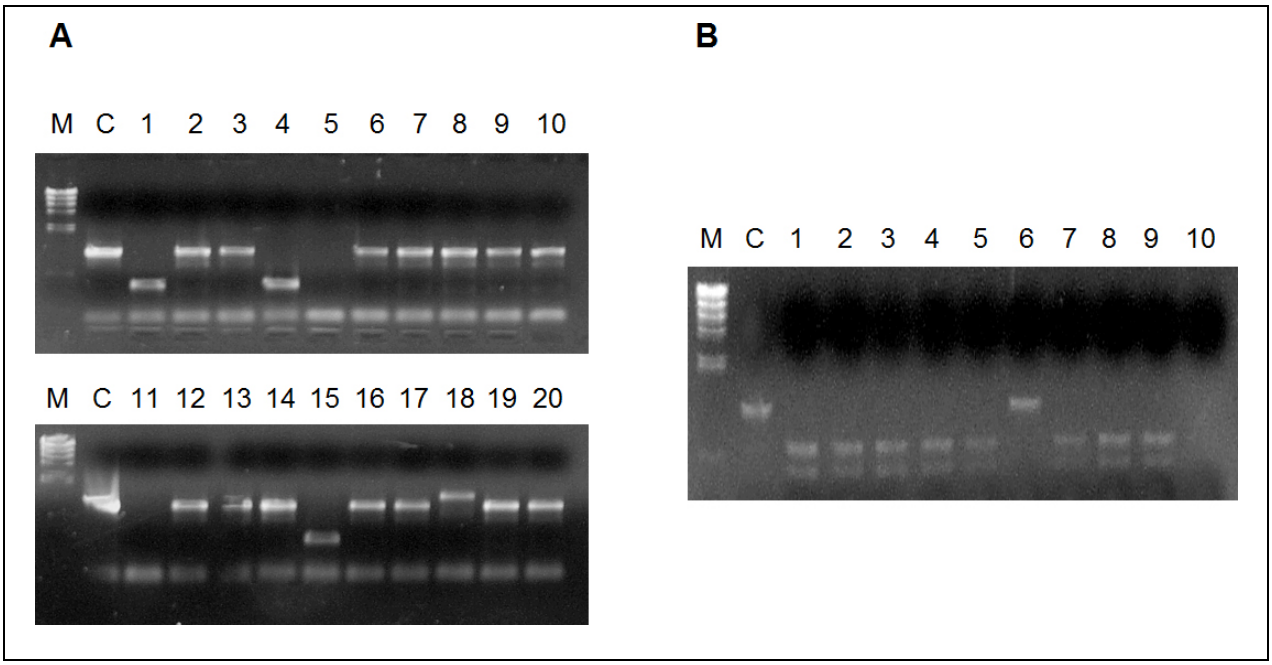

Figure 2. Accuracy of NHEJ repair events. **A**. Representative gel showing migration of colony-PCR products from wt clones (lanes 1-10) and clones with overabundant Ntr1 (lanes 11-20). Lane C, PCR product obtained using pBTM116 plasmid as a template. M, marker; *Hind*III digested λ-phage DNA (NEB). **B**. Representative gel showing migration of colony-PCR products after *Pst*I digestion. Lane C, uncut control. Lanes 1-10: DNA samples from clones overexpressing Ntr1. M, marker, as in A.

However, NHEJ often produces very small insertions or deletions (1-5 bp) (Moore and Haber 1996) and those differences are impossible to detect using solely the size difference comparison. In order to address the question of small size changes during repair, PCR products from the colony PCR were purified by Quiagen PCR purification Kit and digested with the same restriction enzyme used

for initial DSB generation in the pBTM116 plasmid (*Eco*RI or *Pst*I). Fully accurate repair reactions will give rise to digestible PCR products, creating 2 DNA fragments of about 700bp and 400bp length, respectively. If there was an insertion or a deletion within the restriction site, the PCR product was indigestible. After the digestion, 1/6 of a total reaction volume was loaded on the 0.8% agarose gel and analyzed by electrophoresis. Comparison was made between wild-type cells (FF18734) overexpressing Ntr1 from a plasmid and cells carrying a control plasmid (without additional Ntr1).

Table 1. Accuracy of plasmid repair by NHEJ in wild-type cells and cells overexpressing Ntr1.

Strain	Colonies analyzed	PCR products	Same size	Cut	Uncut (same size)	Deletions	Insertions
FF18734 + pUG36	20	10	10	9	1(1)	-	-
	20	20	16	16	4(0)	3	1
	20	18	18	18	0(0)	-	-
	20	11	11	11	0(0)	-	-
Total	80	59	55	54	1	3	1
FF18734 + pNTR1	20	18	14	14	4(0)	3	1
	20	15	14	14	1(0)	1	-
	20	17	16	15	2(1)	1	-
	20	20	19	19	1(0)	1	-
Total	80	70	63	62	1	6	1

Footnote: For both wild-type and wild-type overexpressing Ntr1, 4x20 independent colonies were picked for analysis. PCR products, number of PCR reactions with a product; Same size, number of PCR products having same migration as 1.1 kb control; Cut, number of digested PCR products; Uncut, number of non-digestable PCR products, undigested PCR products of expected size in parenthesis; Deletions, PCR products migrating faster than 1.1 kb control; Insertions, PCR products migrating slower than 1.1 kb control.

In total, 80 colonies from each strain were analyzed. The overabundance of Ntr1 didn't significantly influence the accuracy of plasmid NHEJ repair.

In both samples there was a similar occurrence of insertions and small alterations leading to indigestable PCR products. There is a slight increase in number of larger deletions in cells overexpressing Ntr1. The largest observed

difference comes from inability to obtain a PCR product in colony-PCR. A number of reasons could lead to the lack of a PCR product: suboptimal conditions in a PCR reaction, integration of the pBTM116 plasmid into the genomic DNA during repair, degradation of pBTM116 during repair reaction. Resection of the plasmid and its integration in the genome was indeed shown to occur in NHEJ deficient cells (Schär et al 1997). However, there was no significant difference (Fisher's exact test, p=0.16) in the total number of correctly ligated plasmids in Ntr1 wild-type and overexpressing cells, so this result was not taken for further analysis.

3.2.2. Dominant negative effect of Ntr1 expression on the formation of Dnl4-Lif1 complex

The two-hybrid experiments showed that Ntr1 and Dnl4 both have the potential to bind to the same region in the Lif1 (see 3.1.). The three-hybrid analysis showed that Ntr1 and Dnl4 are not able to bind Lif1 simultaneously, so the possible negative effect of Ntr1 overexpression on the formation of Lif1-Dnl4 complex was examined. For this purpose, the strain PRSY003.1 was used. This strain has a deletion of *DNL4*, so all the Lif1 present in the cells is available for interaction with Ntr1. PRSY003.1 was transformed with either empty plasmid (pACT2, Invitrogen) or with a plasmid carrying the *NTR1* gene under a control of a strong constitutive promoter ADH1 (pGEH066, provided by Gernot Herrmann). Cells transformed with pGEH066 have high levels of Ntr1 and the entire Lif1 pool should be saturated by interaction with Ntr1. After 2 days of growth on the medium lacking leucine (selecting for the presence of the plasmid), cells were additionally transformed with a pYES2 plasmid (Invitrogen) carrying the *DNL4* gene under the control of the GAL1 promoter. Cells were grown for further 2 days at 30^{o}C on medium lacking both uracil and leucine, selecting for the presence of both plasmids. We would expect that in the cells with physiological levels of Ntr1, Lif1 and Dnl4 would be able to form a complex, providing NHEJ repair proficiency, whereas in the cells with overabundant Ntr1, Ntr1 would negatively interfere with Lif1-Dnl4 complex formation, leading to the reduction of NHEJ efficiency. Thus, NHEJ proficiency was tested by standard NHEJ plasmid-

rejoining assay using pBTM116 plasmid digested with either *Pst*I or *Eco*RI restriction enzymes.

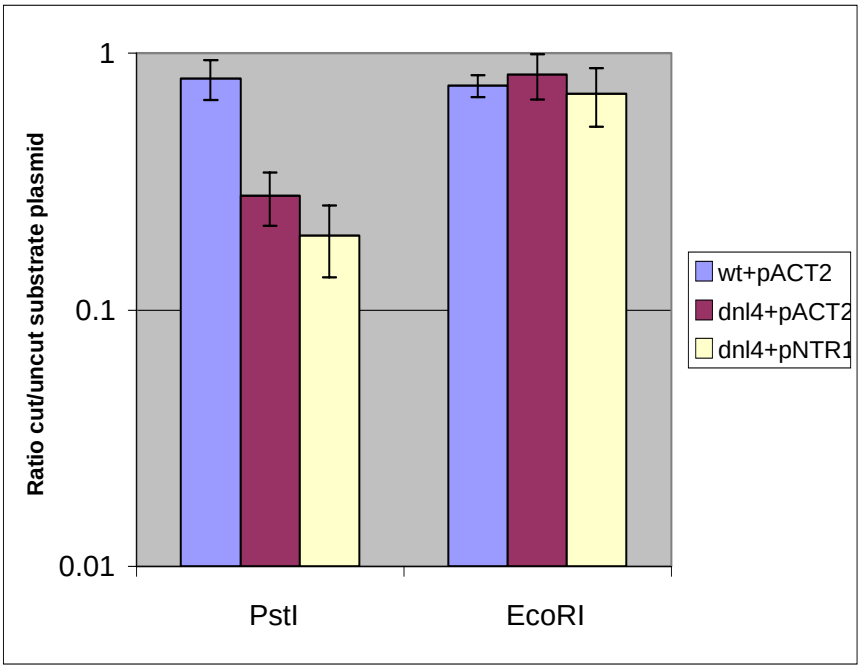

Figure 3. Effect of Ntr1 overexpression on formation of Lif1-Dnl4 complex as scored by NHEJ proficiency. Wild-type (wt) or NHEJ deficient (*dnl4*) yeast strains containing vector control (pACT2) or expressing Ntr1 from pGEH066 plasmid were transformed with equal amounts of digested or undigested plasmid pBTM116, which is a NHEJ substrate. Results present relative ratios of transformation efficiencies between cut and uncut substrate. Columns are means from three independent experiments; error bars are standard deviations.

In both cases, irrespective of the DSB end-structure (*Pst*I or *EcoR*I), repair was efficient (Figure 3). Overexpression of Ntr1 didn't influence the efficiency of repair, when compared to cells with physiological levels of Ntr1.

Following the three-hybrid results, showing that Dnl4 and Ntr1 form mutually exclusive complexes with Lif1, we expected Ntr1 to interfere with formation of Dnl4-Lif1 complex and, thus, to affect complementation of NHEJ upon expression of *DNL4*. This was not seen in the experimental setup chosen, and number of reasons can be considered. Dnl4 could have a higher affinity to Lif1 then Ntr1, and therefore displace Ntr1 from pre-formed complexes with Lif1. Similarly an overaboundance of Dnl4, could affect the stoichiometrical balance between the interacting components in favor of Dnl4-Lif1 complexes. Finally, the observed results might reflect a localization effect. Due to distinct localization of Ntr1 to few nuclear foci, which colocalize with telomeres and nucleoli (see 3.1.), Ntr1 might affect formation of Dnl4-Lif1 complexes only at those subnuclear sites. This would be in accordance with the rather mild effect of Ntr1 expression on NHEJ plasmid repair assays (see 3.1.). Since transformed linearized plasmids in

this assay are not likely to be targeted to sites of Ntr1 localization, their re-circularization by NHEJ would not be subject to inhibition by Ntr1. Hence neither global protein interaction studies nor the plasmid repair assay seems to be adequate to assess the role of Ntr1 in NHEJ. Full elucidation of this problem would, however, need additional experiments.

3.2.3. Subcellular localization of Ntr1

3.2.3.1. Localization of Ntr1 in presence and absence of Lif1

Since Ntr1 interacts with Lif1, the subcellular localization of Ntr1 could be dependent on Lif1. To check this hypothesis, a strain (MAV26) was used that has a full deletion of *LIF1*. The corresponding isogenic wild-type strain (JKM179) and MAV26 were transformed with a plasmid carrying EGFP-Ntr1 under the control of the repressible MET25 promoter. For the fluorescence microscopy, cells were grown in liquid medium containing 1mM methionine, to keep the levels of EGFP-Ntr1 close to the physiological levels. After overnight growth, cells were washed, stained with DAPI, and examined under the fluorescent microscope.

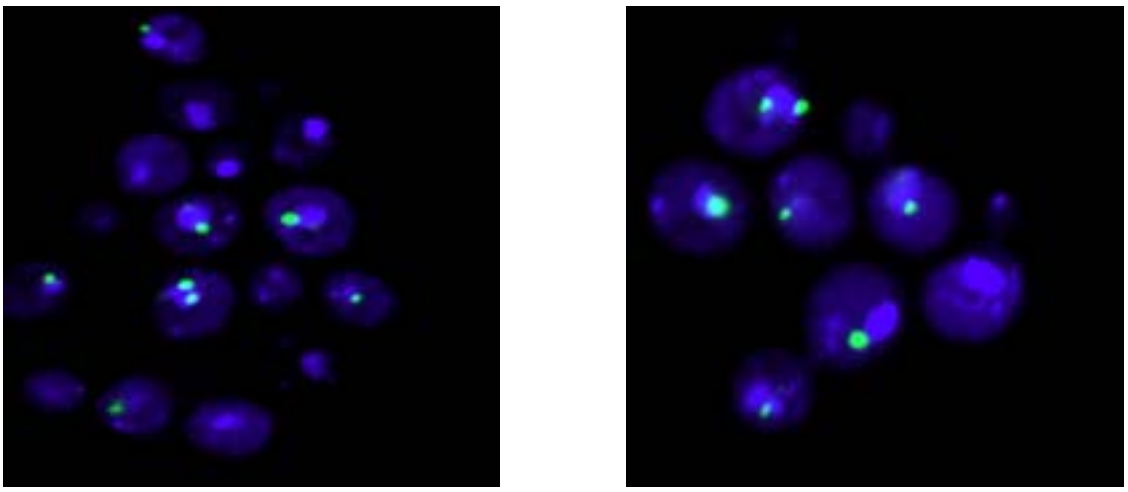

Figure 4. Localization of Ntr1 in wild-type and *lif1* mutant cells. EGFP-Ntr1 localizes to the nucleus (light blue, DAPI) and forms foci at the nuclear periphery in wt cells (left panel). This localization pattern is not affected in *lif1* mutant background (right panel).

As shown in Figure 4, in both wild-type and *lif1* cells, Ntr1 localizes to 1-2 foci at the periphery of cell nucleus. Therefore, it can be concluded that localization of Ntr1 is independent of Lif1.

Ntr1 and Lif1 interact in yeast two-hybrid and GST pull-down assays. At the same time, Ntr1 shows a particular focal localization in the nucleus. One could thus expect that localization of Ntr1 and Lif1 is interdependent. Microscopy experiments show, that Ntr1 localizes to nuclear foci independently of Lif1. Of course, the reverse is also possible; that Ntr1 influences the localization of Lif1. Direct testing of this hypothesis is difficult because Ntr1 disruption causes cell death, and different approaches (directed and random mutagenesis, N-degron tagging and metabolic depletion) to generate conditional mutants failed (data not shown). However, Lif1 shows a diffuse nuclear staining (Valencia et al 2001), which would argue against this hypothesis. It is possible though, that the diffuse localization masks the detection of focal staining and cells need to be pre-treated with detergent for visualization of foci. The reduction of background staining by detergent pre-extraction might increase sensitivity and enable foci detection. A similar treatment was in fact successfully used in detection of Mre11-Rad51 colocalization (Mirzoeva and Petrini 2001). This should be tested for the putative Ntr1-dependent Lif1 localization.

3.2.3.2. Localization of Ntr1 upon induction of DNA damage

Under normal growth conditions Ntr1 is localized in the nucleus, forming 1-3 foci at the nuclear periphery (see 3.1.). Ntr1 foci colocalize with those of telomeric protein Rap1 and, partially, nucleolar protein Nop1. To investigate if this localization pattern changes upon induction of DNA damage, 3 different approaches were used.

Ntr1 localization was examined upon induction of single DSB in the genomic DNA. For this purpose JKM179 and MAV26 cells were used. Both strains express HO-endonuclease under the control of the inducible GAL 1,10 promoter. Upon growth in galactose containing medium, HO-endonuclease will thus be expressed and will induce a single DSB at the MAT locus on chromosome III. Both strains were transformed with EGFP-Ntr1 containing plasmid and grown overnight in selective medium containing glucose. After that, cells were washed and transferred to galactose containing medium. Localization of EGFP-Ntr1 was checked every 30 min for 4 hours. No difference in localization pattern was observed at any time point (data not shown).

To induce multiple DSBs in the genomic DNA, two different DNA damaging agents were used. Cells were either irradiated with X-rays (1000Gy) or incubated in a selective medium in the presence of 0.012% MMS. Wt (FF18734) cells transformed with EGFP-Ntr1 carrying plasmid were observed immediately after treatment and after 1 hr recovery. In all cases studied, there was no change in the Ntr1 localization pattern (data not shown).

Using three different experimental setups, we observed that Ntr1 localization doesn't change upon induction of DSBs. Although this is negative evidence, it is in agreement with a function of Ntr1 as a local regulator of DSB repair (see 3.1.) at telomeres, and/or within the nucleolus. If Ntr1 was needed to regulate DSB repair at specific genomic locations, then we would expect it to stay stably associated with such sites, irrespective of DNA damage being induced at other locations in the genome. Our results would argue in favor, but of course not prove such scenario.

3.2.4. Chromatin immunoprecipitation of Ntr1 to yeast telomeres

Ntr1 localizes to nuclear foci that are situated at the nuclear periphery. These foci partially overlap with Rap1 foci (see 3.1.), indicating a possible localization of Ntr1 to telomeres. Chromatin immunoprecipitation (ChIP) was chosen to test this hypothesis. In order to perform ChIP, the endogenous *NTR1* gene was first tagged with a sequence encoding either a C-terminal 13-Myc-tag, or a 3-HA-tag, in a wild-type (FF18734) and a *lif1* (PRSY031) mutant background. The tagging was achieved as described earlier (Longtine et al 1998). Protein expression was verified by Western-blotting using an anti-myc antibody (9E10, SantaCruz) or an anti-HA antibody (Roche) for detection (Figure 5, data not shown). Tagged Ntr1 was expressed in all clones, so they were suitable for ChIP analysis. In the ChIP, either an anti-myc or an anti- HA antibody was used for immunoprecipitation of crosslinked proteins. As negative control, I used a wild-type strain with no tags, and as a positive controls for protein enrichment at telomeres a strain carrying Sir4-13Myc (GA1216, gift from Susan Gasser) and a strain carrying Yku80-3HA (GA2469, gift from Susan Gasser). After immunoprecipitation, putative enrichment was detected by quantitative PCR (qPCR) using 2 different telomeric probes, one (Probe 1) hybridizing to Y' elements of yeast telomeres (present at most of subtelomeric regions) and another (Probe 2) specific for the right telomere of chromosome VI. The output was normalized to product amplified with an *SMC2* probe (housekeeping single copy gene, far away from telomeres).

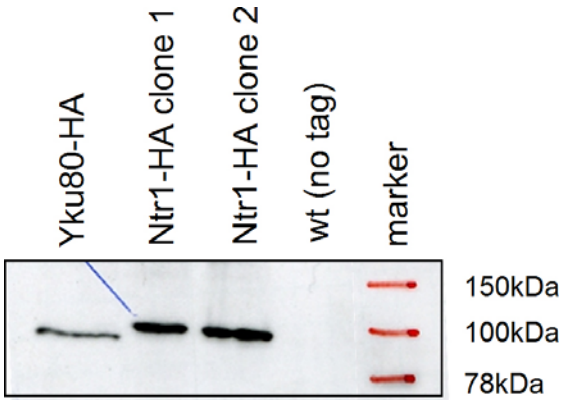

Figure 5. Expression of Ntr1-HA in wt cells. Total protein extract were prepared from strains expressing no tagged proteins (wt), Ntr1-HA or Yku80-HA and analyzed by Western blotting using anti-HA antibody (Roche). Lanes: 1- Yku80-HA, positive control; 2,3- Ntr1-HA clones 1 and 2, respectively; 4- wt (no tag), negative control. M, marker (Precision Plus All Blue protein marker, BioRad).

As shown in Figure 6, ChIP experiment was performed successfully and it was possible to detect Sir4p-13Myc and Yku80-HA specifically at the telomeres, while the negative control (with no tagged proteins) didn't show any enrichment, as expected. Both, Ntr1-13Myc and Ntr1-HA didn't show a significant enrichment at the telomeres, irrespective of the probe used for the enrichment detection.

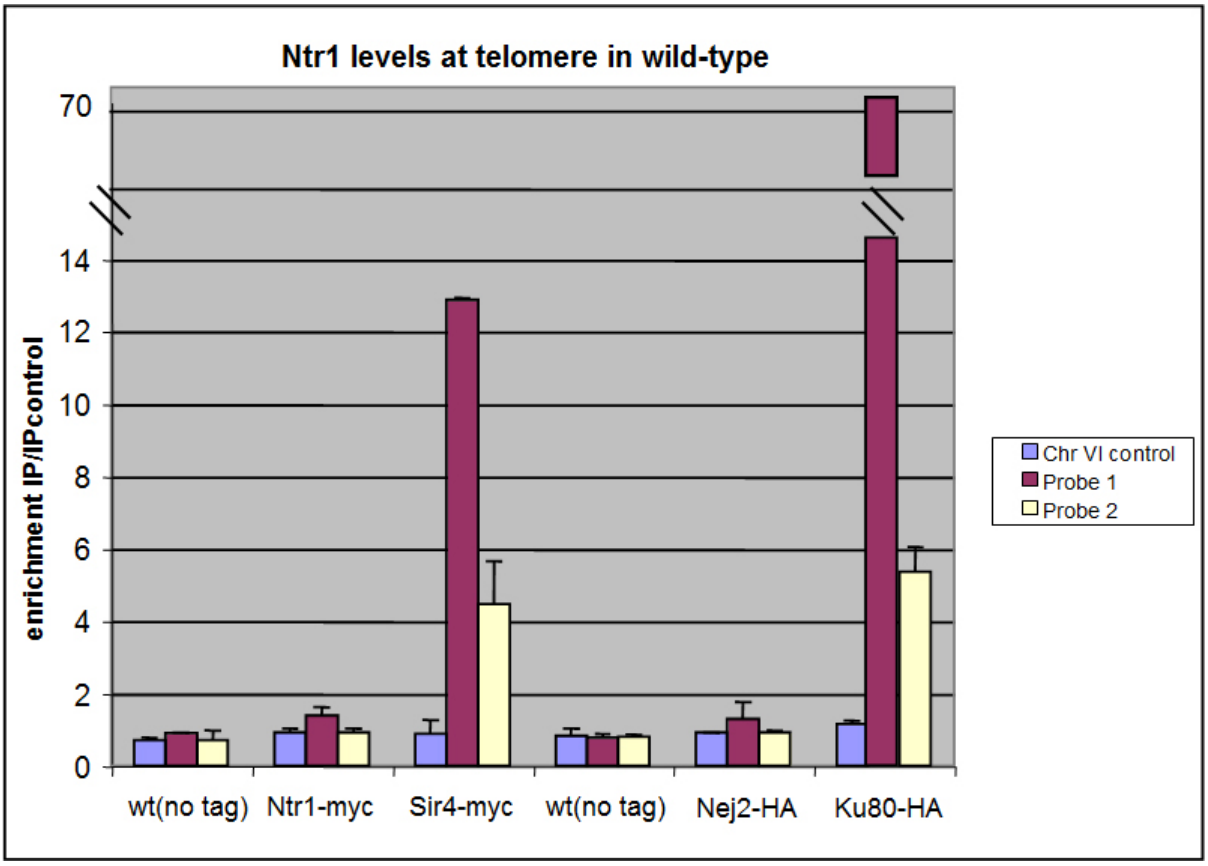

Figure 6. Summary of ChIP experiments. Enrichment of individual ChIP signals compared to ChIP control (BSA) and normalized to *SMC2*. Columns represent means of two independent experiments; error bars are standard deviations

The lack of Ntr1 enrichment at telomeres was unexpected, given its apparent colocalization with Rap1. However, this doesn't *a priori* exclude the possibility that Ntr1 associates with telomeres. Ntr1 binding to telomeres could be only transient and/or mediated through other protein(s) (i.e. PinX1). In both cases, an enrichment of Ntr1 on telomeres would hardly be detectable by ChIP. It is also possible that Ntr1 indeed doesn't localize close enough to the sequences

tested by ChIP. Binding near telomeres (e.g. at repair and/or mRNA splicing centers), would also give positive colocalization with Rap1, but negative evidence in telomere ChIP. Since all these possibilities can not be ruled out easily, we consider the negative ChIP results as non conclusive.

3.2.5. Materials and methods

Yeast strains

Table 2. Yeast strains

Strain name	Genotype	(constructed by)
FF18734	*leu2 trp1 ura3 his7-1 lys1-1 MATα*	F.Fabre
JKM179	*Δho Δhml::ADE1 Δhmr::ADE1 ade1-110 leu2,3-112 lys5 trp::hisG ura3-52ade3::GAL10:HO MATα*	J. Haber
MAV26	*Δho Δhml::ADE1 Δhmr::ADE1 ade1-110 leu2,3-112 lys5 trp::hisG ura3-52ade3::GAL10:HO lif1::KAN MATα*	J. Haber
PRSY003.1	*leu2 trp1 ura3 his7-1 lys1-1 dnl4::kanMX4 MATα*	P.Schär
GA2469	*Sir4-13Myc::TRP1 hml::ADE1 hmr::ADE1 ade3::GAL10:HO ade1 leu2,3-112 lys5 trp1::hisG ura3-52 MATα*	S. Gasser
GA1216	*Esc1-13Myc::kanMX Ku80-3HA::TRP1 ade2-1 trp1-1 his3-11 115can1-100 ura3-1 leu2,3-112 TelVII::URA3*	S. Gasser

NHEJ plasmid rejoining assay

pBTM116 plasmid DNA was digested to completion with either *Eco*RI or *Pst*I restriction enzymes (New England Biolabs).Restriction enzymes were inactivated by incubation at 65°C for 20 min, and plasmid DNA was ethanol precipitated. Samples of undigested plasmid were subjected to the same procedure except that restriction enzymes were omitted. Equal amounts (160 ng) of undigested and digested plasmid DNA were used for parallel transformation of competent yeast cells (described in the Yeast Protocols Handbook from Clontech Laboratories, Inc. (Protocol # PT3024-1, Version # PR13103)). Serial dilutions were plated on medium lacking tryptophan and TRP1 transformants were counted after 3 days of incubation at 30°C. NHEJ efficiency is calculated as

relative ratio between number of colonies transformed with cut plasmid to that transformed with uncut plasmid.

Colony PCR

Individual colonies originating from NHEJ plasmid rejoining assay were re-streaked on complete-medium plates (YPD) and grown at 30°C for 2 days. Each colony was resuspended in 100µl H_2O and 0.3g of glass beads were added (acid washed glass beads, Sigma). All samples were vortexed for 1 minute followed by short spin-down. 10µl of extracts were used as template for PCR reactions.
PCR reactions were performed using a following pair of primers: TRP1-ORF-PR (5'-ATGTTAGCTGGTGGACTGACG-3'); ADH-PROM-2 (5'-GCTATACCAAGCATACAATC-3'). PCR was performed according to a standard protocol used in the Schär laboratory. The reaction mix was prepared by mixing a master-mix 1 and a master-mix 2, followed by the addition of the template DNA and the polymerase. Master-mix 1 contained 0.2mM dNTP's and 50pM of both the sense primer and antisense primer, up to a volume of 15 µl per reaction. Master-mix 2 contained PCR-buffer+$MgSO_4$ and H_2O up to an appropriate volume to produce a total volume of 50µl per reaction. Finally, 2.5U of Taq DNA polymerase (NewEnglandBiolabs) were added just before starting the reaction. All preparation steps were performed on ice. PCR program is described in Table 3.

Table 3 PCR program

Cycles	Temperature, Time	Process
1x	94°C, 2min	melting
30x	94°C, 15sec	melting
	51°C, 30sec	annealing
	72°C, 90sec	extension
1x	72°C, 7min	extension

Restriction digest of colony-PCR products

PCR products from colony-PCR were purified using PCR Purification Kit (Qiagen) according to the instructions provided by manufacturer. Purified DNA was eluted in 50 µl elution buffer. 1/10 of the volume was used for the digestion. DNA was diluted in the appropriate 1X buffer, to constitute a total reaction volume of 30µl. To each digestion mix 20U of restriction enzyme was added (either *Eco*RI or *Pst*I) and the reactions were incubated for 1hr at 37^{o}C. After digestion, 1/6 of digestion mix was loaded to 0.8% agarose gel and electrophoresed.

Microscopy

Prior to microscopy, cells were washed 2x in H_2O and resuspended in the appropriate amount of mounting medium (50% glycerol, 1XDAPI). Microscopy was carried out on a LEICA microscope with 'PL Fluortar' objectives (times 40 oil/times 100 oil). Images were captured with a digital camera 'LEICADC200' and processed with Adobe Photoshop.

Chromatin immunoprecipitation (ChIP)

ChIP was performed as described (http://www.epigenome-noe.net/researchtools/protocol.php?protid=27). An aliquot of each extract was not immunoprecipitated and was used as Input. The following antibodies were used: Mab anti-Myc (9E10), Mab anti-HA (Roche). Input and immunoprecipitated DNA were purified and analyzed by rt–PCR, using the Perkin-Elmer ABI Prism 7700 Sequence Detector System. For each ChIP, real-time (rt) PCR was performed two times. Absolute fold enrichment was calculated as follows. The signal from the telomere or genomic site was normalized to that from the SMC2 locus in ChIP and input DNA samples. The normalized ChIP signals were normalized to input DNA signals. ChIP results are presented as the mean of two experiments +/- standard deviation of mean.

Protein extraction and Western blotting

Total protein extracts were prepared using TCA-method, as described in Ulrich et al 1994. Protein samples were separated by sodium dodecylsulfate polyacrylamide gel electrophoresis (SDS-PAGE), using the Biorad mini gel system. The samples were mixed with 1V of SDS 2x sample buffer (Table 7) and heated to 37°C for 5min and centrifuged at 16100g (Eppendorf 5415D centrifuge, 13200rpm) for 5min at room temperature, before loading. The SDS-gels were made using 4x lower and upper Tris buffers (Table 4). Final polyacrylamide concentration of the SDS separation gel was 10% (Table 5). The stacking gel contained 5% of polyacrylamide (Table 6). Gels were run at constant 35mA per gel. After running, the gels were used for Western blot analysis.

Table 4. Buffers for the polyacrylamide (PAA) gels.

Buffer	**Composition**
4x Lower buffer (LB)	1.5M Tris pH 8.8, 0.4% SDS
4x Upper buffer (UB)	0.5M Tris pH 6.8, 0.4% SDS

Table 5. Composition of the SDS separation gel (quantities for 2 gels).

final % PAA	**40% PAA [ml]**	**4x LB [ml]**	**10% APS [µl]**	**TEMED [µl]**	**H_2O [ml]**
10	2.5	2.5	100	10	4.9

Table 6. Composition of the stacking gel (quantities for 2 gels).

final % PAA	**40% PAA [µl]**	**4x UB [ml]**	**10% APS [µl]**	**TEMED [µl]**	**H_2O [ml]**
5	630	1.25	50	5	3.1

APS and Temed were added immediately before pouring the gels. After filling the gel system with the separation gel solution, 1ml isopropanol was added on top to flatten the gel surface and prevent evaporation. After polymerization, the isopropanol was removed and rinsed out with water. Afterwards, the stacking gel

was added on top and the combs were inserted.

Table 7. Buffers for running and staining of SDS-PAGE.

Buffer	Composition
SDS 2x sample buffer	120mM Tris-HCl pH 6.8, 4% SDS, 20% glycerol, 200mM DTT (fresh), bromophenol blue
SDS running buffer pH 8.3	25mM Tris, 192mM glycine, 0.1% SDS

After separation of proteins by SDS-PAGE, the proteins had to be transferred from the polyacrylamide gel onto a nitrocellulose membrane for hybridization with specific antibodies. The nitrocellulose membrane (Schleicher & Schuell) and the Whatman filter papers were equilibrated in transfer buffer (25mM Tris pH 8.0, 192mM glycine, 20% methanol). All transfers were carried out in Mini-Protean chambers from Biorad. The equipment was assembled according to the manufacturer's instructions. The transfer was performed at 4°C, either over night at 30V or for 2h at 100V. After the transfer, the nitrocellulose membrane was rinsed in water, and then stained with Ponceau solution (Sigma) to estimate the efficiency of the protein transfer. After washing off the Ponceau with water, the membrane was blocked with TBST (100mM Tris pH 8.0, 150mM NaCl, 0.5% Tween20) containing 5% w/v non-fat milk powder (Migros) for 1h at 20°C. After the incubation with a primary anti-HA antibody (Roche) and a secondary antibody (anti-rat HRP, Sigma), the membrane was washed 3x briefly and 3x for 10-15min in TBST containing 0.5% Tween20 (Sigma). Incubation with antibodies and washing was performed at 20°C. Primary and secondary antibodies were diluted in TBST containing 0.5% Tween20 and 5% milk powder. The signal was detected by ECL Western blotting detection reagent (ECL Western Blotting Detection System, GE Healthcare) according to the manufacturer's instructions. Afterwards, the membrane was exposed to Hyperfilm (GE Healthcare) in Kodak film cassettes.

3.3. Manuscript in preparation

DNA Double-Strand Breaks at the Ribosomal Replication Fork Barrier are Fixed by Both Homologous Recombination and Non-Homologous End-Joining

Sanja Kais, Martin D. Burkhalter, José M. Sogo' and Primo Schär

manuscript in preparation

DNA Double-Strand Breaks at the Ribosomal Replication Fork Barrier are Fixed by Both Homologous Recombination and Non-Homologous End-Joining

Sanja Kais[1], Martin D. Burkhalter[2, 3], José M. Sogo[2,*] and Primo Schär[1,*]

[1]Center for Biomedicine, Department of Clinical Biological Research, University of Basel, CH-4058 Basel, Switzerland and [2]Institute of Cell Biology, Department of Biology, ETH Hönggerberg, CH-8093 Zürich, Switzerland
[3]present address: Lineberger Comprehensive Cancer Center, University of North Carolina at Chapel Hill, NC 27599, USA

Running head: Generation and repair of DSBs in the rDNA locus of *S. cerevisiae*

Key words: DNA replication, replication fork barrier, DNA double strand-break repair, ribosomal DNA.

*Corresponding authors (jose.sogo@cell.biol.ethz.ch and primo.schaer@unibas.ch)

Abstract

To study the contribution of NHEJ and HR to replication fork stability, the generation and repair of DSBs occurring at a natural fork-pausing site (RFB) in the yeast ribosomal DNA was monitored. DSB levels in cells deficient for factors influencing replication fork stability (*sgs1* and *top3*) and/or DSB repair (*rad52* and *dnl4*) was examined by means of 2D DNA gel electrophoresis and electron microscopy. We detected increased levels of DSBs in *sgs1* and *top3* mutant cells when compared with wild-type strain. Unexpectedly, the highest levels of DSBs were observed in a *dnl4* mutant background, establishing for the first time an involvement of this DNA ligase and thus, presumably NHEJ, in the repair of S-phase DSBs. By contrast, *rad52* mutant cells had wild-type levels of DSBs and Rad52 defect suppressed the effects observed in *sgs1* and *dnl4* mutant cells. This suggests a role of HR in the generation of DSBs occurring at the RFB.

Introduction

Replication forks are fragile structures. When a replication fork reaches a damaged DNA template, an unusual secondary structure, or a protein-DNA complex it will arrest and eventually collapse if the block cannot be removed. If replication forks collapse, the replisome dissociates, which destabilizes the fork structure in a way that it may break. Yet, there are natural replication fork pausing sites in the genome, usually DNA-protein structures that stop or slow down the fork progression. Examples are Tus-Ter in *E.coli*, RFB in the rDNA locus of *S. cerevisiae* and mammalian cells, RFB in rDNA and RTS1 in mating-type locus in *S. pombe* (reviewed in Mirkin and Mirkin, 2007).

Replication fork barriers (RFB) have been identified in genomes of many organisms. Among them, the RFB in the ribosomal DNA array (rDNA) of *S. cerevisiae* is best characterized. The rDNA locus of S. cerevisiae is a clustered array of 100-200 copies of rDNA repeat units. Each unit consists of a 35S and a 5S rRNA gene separated by two non-transcribed spacer regions (NTS1 and NTS2). An origin of replication (rARS) is located in the NTS2 (Fig 1A). The rARS element acts as bidirectional origin of DNA replication, provided the upstream 35S rRNA gene is actively transcribed (Brewer and Fangman, 1988; Muller et al., 2000). The RFB sequence contains one major (RFB1) and two minor (RFB2/3) replication fork barriers (Brewer and Fangman, 1988; Linskens and Huberman, 1988; Gruber et al., 2000) that represent strong pausing sites for replication forks in the presence of functional Fob1 (Kobayashi and Horiuchi, 1996) Thus, when DNA replication initiates at rARS, the fork invading the 5'-end of the 35S gene will progress freely, whereas the other, moving in the opposite direction, will pause at the RFB. This fork will remain at this position until it fuses with one that approaches from an upstream origin, implying that termination of replication in the rDNA also takes place near the RFB.

The rDNA locus is also a heavily transcribed region, even during S-phase of the cell cycle. The 35S and 5S rRNA genes are transcribed by RNA polymerases I

and III, respectively. Since the RFB sequence is near the 35S rRNA transcription termination site, it is assumed that the RFB serves to prevent deleterious collisions between replication and transcription machineries that move in opposite directions (Brewer et al 1992).

Replication forks pausing at the ribosomal RFB may eventually disintegrate and give rise to DNA single- and double-strand breaks (DSBs) (Weitao et al., 2003; Burkhalter and Sogo, 2004). These are thought to trigger *RAD52*-dependent break-induced replication (BIR) so that an intact replication fork can be reestablished (Kraus et al., 2001). Occasionally, this homologous recombination (HR) process can lead to the “pop-out” of rDNA (repeat) units and, thus, produce extra-chromosomal ribosomal circles (ERC) that accumulate in aging yeast cells (Sinclair and Guarente, 1997).

Consistently, genetic defects that affect replication fork progression, such as those impairing the DNA helicases Sgs1 and Rrm3, elevate the rate of recombination genome wide and, within the rDNA, ERC formation (Watt et al., 1996; Ivessa et al., 2000; Ivessa et al., 2003). Sgs1 forms a complex with Top3, a type Ia topoisomerase (Wallis et al., 1989), which was proposed to suppress sister chromatid exchange by promoting non-crossover resolution of double Holliday junctions (reviewed in Heyer et al., 2003) or, alternatively, by stabilizing DNA polymerases at stalled forks, preventing fork collapse (Cobb et al., 2003; Bjergbaek et al., 2005). Together with data showing recombinogenic activity of an RFB located outside of the rDNA in fission yeast (Lambert et al., 2005), these observations firmly establish a causal link between replication fork stalling, DSB formation, and initiation of HR.

Replication fork stability is usually studied under DNA damaging conditions (Branzei et al 2006, Liberi et al 2005), or in a situation where fork progression is blocked by nucleotide depletion, following HU treatment (Cobb et al 2003, Sogo et al 2002). These are usually circumstances when DNA damage signaling is highly active in cells, which will affect the way cells handle stalled forks. As the amounts of spontaneously occurring endogenous DNA damage rarely reach

levels that activate DNA damage response, it is important to also understand how cells stabilize forks under such, so called unperturbed, conditions. Stability of replication forks in unperturbed conditions was not studied extensively. The molecular transactions associated with natural replication fork-stalling and resolution are, thus, still a subject of speculation.

Here we used a combination of genetic, biochemical and biophysical methods to identify molecular pathways that control the integrity of naturally stalled replication forks at the ribosomal RFB. We examined RFB activity, DSB formation and the structure of stalled forks in yeast cells mutated in genes controlling the stability of replication forks (*SGS1*, *TOP3),* or the repair of DSBs *(DNL4*, *RAD52)*. Surprisingly, *rad52* mutant cells had DSB levels comparable to wild-type. Increased levels of DSBs were apparent in *sgs1*, *top3* and, particularly, in *dnl4* mutant strains and the effect was suppressed in *sgs1 rad52*, *top3 rad52* and *dnl4 rad52* double mutants. Electron microscopy revealed an increased occurrence of regions of single-stranded DNA (ssDNA) at the RFB in *sgs1*, *top3*, and *dnl4* mutant cells. We postulate that these structural intermediates accompany the generation of distinct types of DSBs that require either HR or NHEJ for repair.

Results

It has been shown previously that replication forks stalled at the RFB have a potential to break (Burghalter and Sogo 2004, Weitao et al 2003). To identify factors controlling fork stability at the RFB, and address the mechanism underlying DSB formation and repair, we carried out a candidate gene approach. We focused on the roles of Sgs1, Top3, Rad52 and Dnl4 and generated a series of single and double isogenic mutant strains to monitor the occurrence of DSBs under those genetic conditions.

DSB formation at replication forks stalled at the ribosomal RFB

Burghalter and Sogo (2004) showed that in a W303 background DSBs are generated at the RFB during S-phase. We wanted to investigate generation and repair of such DSBs in series of isogenic mutant strains originating from FF18733, the genetic background used for DNA repair studies in our laboratory. Due to the variability in synchronization ability of different mutant strains, we chose to analyze the genomic DNA from logarithmically growing cultures rather than from synchronized cells. Therefore, prior to analyzing a whole set of mutants, we needed to confirm that DSBs can be detected in logarithmically growing FF18733 cultures. Thus, cells from wild-type (FF18733) and *fob1* mutant cultures were embedded in agarose plugs and DNA was extracted within plugs, to maximally preserve structure of replication intermediates (RIs). DNA within agarose plugs was then digested with *Bgl*II. *Bgl*II cuts twice in the rDNA unit and generates two fragments of 4568bp and 4578bp size (Figure 1A). The restriction fragments were separated by monodimensional agarose gel electrophoresis, transferred to membranes and detected by Southern blotting using two different probes (Figure 1A). The autoradiogram obtained with Probe 1 shows an intense signal at the top corresponding to the expected 4.6kb *Bgl*II restriction fragment (Figure 1B). Two distinct bands migrating faster than the 2.3kb *Hind*III-*Bgl*II marker were detected. They differ in intensity and are not detectable in a *fob1*

mutant. This corresponds well with the previous findings of Burghalter and Sogo (2004) (see also Figure 1C) and indicates that these fragments represent molecules arising from DSBs generated at RFB1 or RFB2/3. We were able to detect three additional bands, but they were not Fob1p dependent, and were thus not further characterized. Hence, DSBs occuring in the newly replicated strands can also be detected in the FF18733 genetic background. The membrane form Figure 1C was then stripped and hybridized with Probe 2 (Figure 1D). Apart from the expected 4.6kb *Bgl*II restriction fragment, a diffuse signal of about the size of the 2.2kb *Hind*III-*Bgl*II marker band could be detected. The signal was Fob1 dependent, (absent from *fob1* mutant) suggesting that DSBs of a less determined length also occur in the ARS distal region of the RFB. As this is the region where termination of replication is believed to occur (Brewer and Fangman 1988), we concluded that termination molecules, i.e. RIs consisting of two converging forks at the RFB, also contribute to the generation of DSBs at the rDNA locus.

DSB detection by neutral-neutral 2D electrophoresis

To be able to compare the amounts of DSBs generated in different mutant backgrounds, we had to develop means of quantifying the levels of DSBs in respect to the amount of RIs in a given genetic background. In this context, molecules stalled at the RFB and termination region (Ter) were considered RIs relevant for DSB formation. The RFB and Ter signals have so far been successfully resolved and detected by neutral-neutral 2D agarose electrophoresis (Pohlhaus and Kreuzer 2006), so we wanted to assess if DSBs can also be detected on the same 2D gel.

As illustrated in Figure 2A, the linear 4.6kb *Bgl*II fragments migrate in the monomer spot (M). Different RIs containing a single replication fork migrate in the Y-arc emanating from the M-spot. A spot at the inflection point of Y-arc represents Y-shaped molecules stalled at the RFB. Where the Y-arc joins again the linear arc, molecules of twice the size of the monomer migrate in the 2n spot.

The arc above the RFB-spot contains RIs with two converging but still separated forks, whereas terminating molecules containing two converging forks at the RFB migrate in the Ter spot.

We performed 2D gel electrophoresis for wild-type (FF18733) and *fob1* genomic DNA isolated in agarose plugs and digested by *Bgl*II. Care was taken that molecules smaller than monomer were included in the analysis. Southern blotting with Probe 1 detected all expected signals in the wild-type (Figure 2B). In the *fob1* mutant, discrete RFB and Ter spots were not detectable. This was expected since *fob1* mutants fail to establish an RFB and, hence, lack fork stalling and termination at the RFB (Mohanty and Bastia 2004, Kobayashi 2003). In addition to previously described signals, Probe 1 detected four spots of positions corresponding to sizes smaller than 4.6kb in wild-type. In the *fob1* mutant only three spots were detectable. This pattern of spots resembles that of the fragments observed in 1D gels (Figure 2B, compare with Figure 1B). The wild-type specific spot migrates faster than a *Hind*III-*Bgl*II marker fragment (Supplementary Figure 1). From its migration relative to other features and the dependency on Fob1, we concluded that this spot represents DNA fragments generated through DSBs occurring at the RFB. Probe2 hybridization detected four spots in wild-type and three in *fob1*. The wild-type specific spot is diffuse (Figure 2B, lower panel), as was the case with the DSB band in 1D gel (Figure 1D), and runs about the size of *Hind*III-*Bgl*II marker fragment (Supplementary Figure 1). These results show that DSBs can also be detected by 2D gel electrophoresis. In this way, all relevant signals can be monitored and quantified on the same membrane, which makes a comparison between different mutants feasible.

Variability of DSB levels in different mutant backgrounds

To investigate possible differences in DSB levels and/or fork stalling between different mutants, we proceeded to analyze replication structures from different mutants by 2D gel electrophoresis. As shown in Figure 3, all mutants show the

typical features of replication forks as visible in 2D gels (compare with Figure 2A). As expected, the *fob1* mutant lacks RFB and Ter signals, while wild-type and all other mutants show all expected features, although the relative intensities of the different signals vary. Moreover, *sgs1* and *sgs1 top3* mutants show an additional spot (Figure 3, arrows) running below the Ter spot, close to the 2n spot. The nature of the DNA structure represented in this spot has not been characterized before. At a similar position, in the *dnl4* mutant, we observed 2 spots of lesser intensity (Figure 3, ladder symbol), the nature of which is also elusive.

To be able to compare the amounts of DSBs occurring in different mutants, we quantified relevant signals, including, the Ter spot, the RFB spot, the DSB spot, the 2n spot and the total RI signal (replication intermediates) (Figure 4A). The RI signal represents all molecules running higher than the Monomer spot (including Ter and RFB spots, but excluding 2n spot), and serves as a mean of normalization (to account for the variable proportion of S-phase cells between different mutant strains and experiments). All quantitations are based on at least three independent experiments for all strains.

To assess the amount of DSBs generated in an individual S-phase, we related the signal intensity of the DSB spot to the RI signal. In wild-type cells 7.8% (+/- 1.5%) of RIs had a DSB while in *fob1* mutant cells this was the case for only 0.5% (+/- 0.08%) of RIs (Supplementary Figure 2A). Considering an average number of repeat unit of 150, with every fifth of them being actively replicated (Muller et al. 2000), the 8% broken RIs in the wild-type would translate to 1-2 DSBs per cell and S-phase. Other signals i.e.the RFB, Ter and 2n spots can be analyzed in the same manner and compared among all mutant backgrounds (Supplementary Figure 2B).

DSBs as observed and described before (Burghalter and Sogo 2004, Weitao et al 2003), were shown to be Fob1- and S-phase dependent. However, it remains unclear whether the induction of DSBs requires fork stalling at RFB, or whether DSBs can also arise during DNA replication through a process involving Fob1,

but independent of fork stalling. This is relevant with regard to quantification of DSBs relative to the appropriate precursor structures. If fork stalling is prerequisite of DSB formation, RFB and Ter molecules would be relevant precursor structures.

Following the hypothesis that fork stalling precedes DSB formation, the DSB signals were normalized to the total of RFB, Ter and DSB signals (Figure 4B, upper left panel). In this way, *sgs1*, *top3*, and *dnl4* mutants show increased levels of DSBs when compared to wild-type. Surprisingly, in the background of a Rad52 defect, the increase in DSB levels in *sgs1* and *dnl4* is suppressed, suggesting that Rad52 is responsible for the generation of those breaks. The high level of DSBs in *dnl4* mutant indicates that a substantial amount of DSBs is repaired through a Dnl4-dependent process, most likely the non-homologous end-joining (NHEJ) pathway (Schär et al 1997). Other relevant signals including RFB, Ter and 2n, were also normalized in the same way (Figure 4B). Both RFB and Ter signals don't show as striking differences between strain backgrounds as the DSBs do. Obvious is that, in general, RFB and Ter signals appear to be inversely correlated to that of DSBs i.e. the higher the DSB signal, the lower RFB and Ter signals and *vice versa*. This indicates that DSBs arise from processing of molecules that used to contribute to RFB and Ter signals. Interestingly, the 2n signal shows the same strain-specific changes as the DSB signal. So far, the 2n signal was described in the literature as almost fully replicated linear molecules, approximately 2X the size of monomer, that hold two newly replicated strands together by means of base-pairing through a few nucleotides (Ivessa et al 2002).

Structural integrity of replication forks stalled at the RFB

In addition to 2D gel electrophoresis, the anatomy of RIs can be studied also by electron microscopy (EM). EM analysis enables direct visualization of structure of RIs observed by 2D gel electrophoresis. In order to visualize different replication and recombination intermediates and examine the structural integrity of the forks stalled at the ribosomal RFB in different genetic backgrounds, we synchronized

wild-type, *sgs1*, *top3*, and *dnl4* mutant cells with α-factor and isolated psoralen-crosslinked genomic DNA. Following enrichment for rDNA by centrifugation in CsCl/Actinomycin D gradient (Dammann et al., 1993; Lucchini and Sogo, 1994) and digestion with *Pvu*I, a BND-cellulose step was used to isolate RIs. Resulting molecules were then analyzed by EM (Figure 5) under non-denaturing conditions (Sogo et al., 2002). More than 100 replicating rDNA molecules were examined for each strain. These RIs contained the stalled fork at the RFB either as part of an Y-shaped structure (Figure 5B) or, less frequently, a terminating molecule i.e. a double Y-shaped RI with one fork stalled at the RFB (Figure 5D).

Two classes of molecules with stalled forks at the RFB were distinguishable by the absence (Figure 5A) or the presence (Figure 5B) of ssDNA at the forks. RIs with stretches of ssDNA were identified in rDNA from all strains examined. Normally, the ssDNA was present in one arm of the stalled fork only. The length of the ssDNA regions ranged from 127 to 165 nucleotides (Table 1), showing only insignificant differences between the strains analyzed. A significant difference between wild-type and mutant strains emerged for the occurrence of these ssDNA regions. Whereas 27% of the molecules from wild-type cells showed ssDNA stretches, the fraction was increased 2 to 3 fold in all mutants examined (Table 1, $p \leq 0.0001$ for all mutants, contingency tables, Fisher's exact test).

Discussion

We have established a new method for quantitative assessment of DSB occurrence (i.e. formation and/or repair) at the ribosomal RFB in logarithmically growing yeast cells. We then applied this method to evaluate variation of DSB levels in different genetic backgrounds. Finally, we investigated the structural integrity of RFs stalled at the RFB by EM. Our 2D gel analysis revealed significant effects of genetic background on RFB associated DSBs. Strikingly, in wild-type up to 8% of all RIs are broken, which translates into 1-2 DSBs in the rDNA array per cell cycle. Compared to the wild-type cells, we detected increased levels of DSBs in *sgs1*, *top3* and *dnl4* but, surprisingly, not in *rad52*, *sgs1 rad52* or *dnl4 rad52* mutant cells. The DSB levels correlated inversely with the RFB and the Ter signals, but directly with the intensity of the 2n spot and, as observed by EM, the occurrence of ssDNA regions at the stalled forks. Fragments corresponding to DSBs at the RFB were detected with Southern probes against sequences on either side of the RFB, suggesting that breaks do occur on both sides. Finally, we also found strain-background-dependent structural features in 2D gels that have not been described previously and may represent intermediates of fork resolution.

To establish the method for assessment of DSB occurrence, logarithmically growing cells of FF18733 background were first tested for the existence of S-phase dependent DSBs by 1D and 2D DNA electrophoresis. In line with previously published results (Burkhalter and Sogo 2004), we detected two major bands corresponding to DNA fragments arising from DSBs generated at RFB1 and RFB2/3 in Southern blots of 1D gels. We were also able to detect DSBs using a probe (Probe 2) (Figure 1A), which hybridizes to the ARS-distal side of the RFB. This probe showed a more diffuse signal, indicating that DSBs on the ARS-distal side of RFB show a wider distribution in size. Interestingly, this is the region where termination of replication is believed to occur (Brewer and

Fangman 1988, Linskens and Huberman 1988). As replication is terminated at random positions within a small region, rather than at distinct positions in the DNA, the diffuse signal of DSBs might highlight breaks induced in terminating molecules, thus creating a population of differently sized broken DNA molecules. In any case, signal by Probe 2 clearly indicates that DSBs are also created in a ARS-distal region of the RFB, either in non-replicated part of the molecule, or more likely, in replication terminating molecules consisting of two converging forks. Converging forks were indeed identified by EM (Figure 5D).

To be able to compare DSB formation and fork progression among mutants, we optimized the detection and quantitation methods. By including molecules of molecular sizes smaller than the monomer in the 2D gel analysis, we obtained a distinct pattern of spots on the linear arc in the profile (Figure 2). This was reminiscent of the fragment pattern observed by 1D gels (Figure 1 B, C). Taking into consideration the relative size of the fragments and their Fob1 dependence, we concluded that two of the signals visible on 2D gels corresponded to those that are S-phase- and Fob1-dependent in 1D gels, and, thus, reflect the products of DSBs at the RFB. Additional Fob1-independent signals were not reproducible between experiments. Therefore, we concluded that these spots most probably arise through experimental handling of samples, possibly by star-activity of the restriction enzyme and are thus not related to replication associated breaks.

Apart from the usual features of the 2D gel profile, we observed additional signal in the strains mutated in *SGS1* or *SGS1* and *TOP3* (Figure 3, arrows). Given its position on the 2D gel and its dependence on genetic background, we propose that this spot represents a branched molecule, resulting from recombination initiated at forks converging at the RFB during replication termination. This structure occurs in the absence of Sgs1 but it is not present in *sgs1 rad52* double defective cells. This suggests that the formation of this particular molecular structure requires a Rad52-dependent process and accumulates in the absence of Sgs1. Although further experiments would be needed to resolve the exact

structure and nature of the spot, we speculate that it contains a structure similar to a double reversed fork in terminating molecules. In the absence of Sgs1, termination of replication would be compromised and the attempt to resolve the situation by HR could lead to the formation of such structures. However, lack of the spot in *sgs1 dnl4* mutant cannot easily be accounted for by this model.

In a previous study, the signals in the 2D profile were normalized to the monomer spot (Burkhalter and Sogo 2004). This feature is the most prominent in the profile and present in all genetic backgrounds and under all experimental conditions, facilitating simple comparisons. However, normalization to the monomer is not as straightforward as it was shown. There are two possible precursors of molecules contributing to this signal: linear molecules that haven't been replicated yet, as well as fully replicated and separated linear molecules. Since DSB formation is dependent on replication, normalization to the monomer doesn't give an accurate and consistent result. Furthermore, the monomer signal does not account for differences in fork progression and/or cell cycle distribution (cells in S-phase) between individual mutant backgrounds we compared. Therefore, we chose to normalize all signals (DSB, RFB, Ter, 2n) to the relevant replication intermediates. The question is, what is relevant?

Published data (Burghalter and Sogo 2004, Weitao et al 2003) show that DSB formation is replication- and Fob1- dependent. It is, however, not clear whether replication fork stalling is a prerequisite for DSB formation or whether the presence of Fob1 only is sufficient. So, there are two possibilities for normalization. If we assume that replication fork stalling is necessary for DSB formation, all individual signals should be related to the total of stalled molecules (RFB+Ter+DSB) (Figure 4B). The DSB signal itself is included in the total because we assume it to be a direct product of stalled fork. Alternatively, we could normalize individual signals to the total of all replication intermediates (Supplementary Figure 2A, B), if we assume that Fob1p presence, but not fork stalling, is required for DSB formation. We favor the first possibility because of

evidence from published data suggesting that fork stalling is a recombinogenic event.

RFB sites are often associated with an increased frequency of recombination, suggesting that paused forks stimulate recombination directly through the rapid disassembly of the replisome and the collapse of the fork structures (Defossez *et al*, 1999; Admire *et al*, 2006; Kobayashi *et al*, 1998; Lambert *et al*, 2005). Consistently, fork destabilization by mutating RecQ helicases or topoisomerases, gives rise to elevated levels of spontaneous mitotic recombination and so do replication fork blocking DNA lesions, suggesting destabilization itself, without involvement of Fob1 gives rise to breaks that induce recombination. On the other hand, Fob1-dependent DSBs generation without fork stalling would suggest that Fob1 is responsible for generation of DSBs. Although, *in silico* simulations of Fob1 structure propose putative nuclease activity for Fob1 (Dlakic 2002) such an enzymatic activity has not been reported. Therefore, we favor the first hypothesis and we performed quantitation of 2D gel profiles accordingly.

The quantitation of 2D gels revealed that, the relative intensities of RFB, Ter, 2n and monomer spots as well as Y-arc, X-spike and RI signals varied between different strains (Figure 4B). In the *fob1* mutant, no RFB and Ter signals were observed (Figure 3) which is consistent with binding of Fob1 being responsible for establishment of the fork barrier at the RFB sequence (Kobayashi and Hirouchi, 1996). In the absence of a barrier, forks do not stall, explaining the lack of RFB and Ter signals. DSB signals were increased in *sgs1* and *top3* mutant backgrounds. This was expected, because both Sgs1 and Top3 have been implicated in maintenance of fork stability (Cobb et al 2003, Bjergbaek et al 2005, Liberi et al 2005). Unexpected was that a *dnl4* mutant shows high levels of DSBs, while *rad52* does not. This is surprising because yeast cells are believed to preferentially employ HR in the repair of DSBs (Paques and Haber 1999, Aylon and Kupiec 2004) and HR is generally associated with the restart of collapsed replication forks (Haber and Heyer 2001). Interesting was also the

observation that the strain-specific behavior of DSB signals correlates with that of the 2n signals.

The molecules accumulating in the 2n spot were interpreted to be replication intermediates having a structure of almost fully replicated monomers held together by a small stretch of unreplicated base-pairs (Ivessa et al 2002). However, such replication intermediate would be unstable during handling, and, there are no obvious structures or barriers that would stall and stabilize the forks specifically close to *Bgl*II site. We therefore propose an alternative explanation. From the behavior of the 2n spot in different strain backgrounds we would conclude that these structures, like the DSBs, arise from processing of stalled replication forks. Under specific circumstances this will create structures of two fully replicated molecules held together at one end by a Holliday junction (HJ) or a hemi-catenate. We believe such molecules arise by *in vitro* branch-migration of Holliday junctions arising as recombination intermediates at the RFB at replication termination. During the DNA digestion step with *Bgl*II, it is conceivable that spontaneous branch-migration of already existing recombination intermediates would be possible in both directions. Binding of *Bgl*II to the DNA ends would block resolution of branch migration and lead to accumulation of molecules having a HJ at one end. Further processing of samples at lower temperature and altered salt conditions will stabilize such structures enabling their detection by 2D gels. Accumulation of 2n structures is clearly Fob1- and Rad52-dependent (Figure 3), it is absent in *rad52* mutants and suppressed in *sgs1 rad52*, *top3 rad52* and *dnl4 rad52* double mutants. Taken together, these data strongly support that 2n molecules are branched recombination intermediates.

If the the 2D gel profiles are normalized to total RIs (Supplementary Figure 2B), the effects of different mutant backgrounds on DSB and 2n levels are less striking but follow a similar trend.

Finally, we examined the anatomy of stalled forks by EM. All mutant strains examined show stretches of ssDNA at the forks. This corresponds well with

primer extension data, which indicated that 20-30% of nascent DNA strands at the ribosomal RFB are not fully elongated (Gruber et al., 2000). In the light of the EM data presented here, these shorter primer extension products can now be interpreted to represent molecules with ssDNA-regions at RFB stalled forks. The data also suggest that the mutant strains accumulate a significant amount of ssDNA during DNA replication. For instance, the 58% of stalled forks with ssDNA patches in the *dnl4* mutant would translate to about 2.6kb of ssDNA arising in the rDNA during replication. Replication stress, however, was not apparent in these cells (data not shown), suggesting that ssDNA at ribosomal RFBs goes unnoticed by the S-phase DNA damage checkpoint (Shimada et al., 2002). This may apply to RFBs in general. Lambert et al. (2005) reported that replication stress signaling does not contribute to fork stabilization when both, DNA unwinding and synthesis are blocked. In addition, the *top3* mutant showed a small fraction of unusual structures-"entangled" forks (Figure 5C), that could be interpreted as partially reversed forks. Together, these analyses demonstrate that the structural integrity of replication forks stalled at the ribosomal RFB is impaired in *sgs1*, *top3*, and surprisingly also *dnl4* mutants, implicating a role for all these proteins in the establishment of replication fork stability.

Taken into account all data presented in this work, we propose the following model depicted in Figure 6 to explain the observed. It postulates that replication forks stall at RFB in a Fob1-dependent manner. Such forks are not fully replicated and have stretches of ssDNA (Figure 6A). They can collapse and spontaneously break, or be processed by structure-specific endonucleases such as Mus81-Mms4 (Figure 6A) (Bastin-Shanower et al. 2003, Fricke et al. 2005). DNA ends coming from broken forks will be resected, followed by Rad52-dependent BIR, which will restore the nascent strands. In *sgs1* and *top3* mutants, forks stalled at the RFB will be destabilized (Cobb et al. 2003). This will lead to more frequent collapse of forks at the RFB, giving rise to ssDNA by nuclease digestion. At the destabilized forks, Rad52 will promote strand re-annealing and fork reversal (Figure 6A). This will create a HJ, which will consequently be a

substrate for structure-specific nuclease/resolvase. A nuclease/resolvase, presumably Mus81-Mms4 will then induce DSBs, which will, again, be a substrate for Rad52-dependent BIR, which leads to resolution and re-establishment of intact replication forks. Top3 will additionally be needed for resolution of "entangled" structures that might form at the destabilized fork at the beginning of fork reversal. Sgs1 counteracts fork reversal and promotes fork re-establishment without employment of HR. The same rationale can be applied to terminating molecules. However, large proportion of DSBs occurring at the RFB is repaired by Dnl4-dependent repair (Figure 6B). The successful resolution of termination requires Rad52 activity, as reflected in *rad52 dnl4* mutant cells, which don't show increased levels of DSBs.

Our model suggests a role for Mus81 in the induction of DSBs at forks stalled at the RFB. This would predict that *mus81* mutant cells would have greatly reduced levels of DSBs. We are currently testing this hypothesis in yeast cells. However, Hanada et al (2007) showed recently in mouse embryonic stem cells Mus81-dependent DSB induction in forks stalled by replication inhibitors. These results strongly argue in favor of our model. Our model is also in accordance with observations that *sgs1* and *top3* mutants show hyperrecombination phenotypes (Watt et al, 1996; Wallis et al, 1989). In the absence of either of Sgs1 or Top3, there would be no factors to counteract HR active at stalled forks, hence recombination would be promoted leading to formation of reversed forks. However, reversed forks have only been observed under stressed conditions (Table 1; Sogo et al, 2002). The reason for that might be that Mus81-Mms4 acts on those reversed forks inducing breaks and promoting efficient resolution. Reversed forks are, therefore, short-lived structures that escape detection by EM. We speculate that reversed forks would be accumulated in *mus81 sgs1* mutant. This mutant, however, is not viable, perhaps because of the accumulation of such structures that cannot be successfully resolved. The synthetic lethality of *mus81 sgs1* mutant can be reversed by additional *rad52* deletion, corroborating that HR is responsible for generation of toxic structures in

the absence of both Sgs1 and Mus81, which is also in accordance with our model. Furthermore, in the case of terminating molecules, the nuclease activity responsible for DSB induction was proposed to be Slx1-Slx4 (Figure 6B, left panel) (Frike and Brill 2003). Interestingly, an *slx1 sgs1* double mutant is also synthetic lethal (Mullen et al 2001), but this phenotype is not reversed by additional deletion of *rad52* (Fabre et al 2002, Bastin-Shanower et al 2003). Since the *dnl4* defect (NHEJ) is suppressed by *rad52* and a substrate to *dnl4* can only be generated by breakage of terminating molecules, we propose that Rad52-dependent fork reversal in terminating molecules generates a substrate for Mus81-dependent cleavage (Figure 6B, right panel). This will then require NHEJ process for repair. The model, however, does not yet offer a straightforward explanation for the suppression of DSB levels in *sgs1 top3* and *sgs1 dnl4* mutant backgrounds. Additional experiments should provide the answers.

We have been able to show an involvement of Sgs1, Top3, Dnl4 and Rad52 in the generation and processing of DSBs created at the RFB in rDNA locus. Rather surprisingly, Dnl4 seems to play a major role in the repair of such DSBs in wild-type. It seems, therefore, that *S. cerevisiae* employs NHEJ DSB repair much more frequently than previously thought. Although, this could reflect a special feature of the highly repetitive rDNA locus, a possible role of NHEJ in replication termination certainly needs careful investigations.

Materials and Methods

Yeast strains

Yeast strains were isogenic derivatives of the FF18733/FF18734 series in an A364 background (Francis Fabre, pers. comm., Schär et al., 1997). Single mutants were created by standard gene replacement method using either *kanMX4*, *URA3* or *TRP1* as selectable markers. Double mutants were created by crossing appropriate single mutants (Supplementary Table 1). The *top3* strain was backcrossed to wild-type several times to isolate suppressor free clones.

DNA isolation, Gel electrophoresis and Southern blotting

DNA preparation in agarose plugs from logarithmically growing cells, was done as described (Weitao et al., 2003) and followed by digestion with *Bgl*II for 24 hours at 37°C. Gels and Southern blotting were done as described by Burkhalter and Sogo (2004). Radioactive membranes were exposed to Phospho-screens for at least 25 hours. Signals were then detected by Typhoon 9400 (GE-Healthcare) and quantified using ImageQuant software (ver. 8); rolling circle model was used for background substraction.

Southern blot probes and radio-labeling

Probes 1 and 2, used for Southern blotting, were produced by PCR amplification using genomic DNA as a template and a pair of appropriate primers. Primers used for PCR amplification were: rDNA-447(5'-ATCCCATAACTAACCTAC-3') and rDNA-1053 (5'-AAAATACTACGAACTACG-3') for Probe1; rDNA-37L (5'-ATTGTCAGGTGGGGAGTTTG-3') and rDNA-43R (5'-GCCACAAGGACGCCTTATTC-3') for Probe2. Both probes have a size of 606bp. Five PCR reactions were pooled together and purified using Qiagen PCR purification kit according to the instructions provided by the manufacturer. Probe-DNA was eluted in 50μl 10mM Tris (pH 8.0) and used for radioactive labeling.

For the radioactive labeling of the probes, the Fermentas HexaLabel DNA Labeling Kit was used according to the instructions provided by the manufacturer, using (α-^{32}P)-dCTP (6000Ci(222TBq)/mmol, PerkinElmer) as a source of radioactivity. The incorporation efficiency was usually 15%. Unincorporated nucleotides were removed using QIAquick Nucleotide Removal Kit (Qiagen).

CsCl-Actinomycin D gradients, BND cellulose enrichment of RI and electron microscopy (EM)

The DNA used for the EM analysis was isolated (Qiagen genomic tips) from synchronized cells. Cells were grown in YPD at 30°C to early logarithmic phase, synchronized in G1 by adding 2 mg/ml α-factor and released into fresh YPD. After 30 minutes of release, cells were inactivated by adding 0.1% sodium-azide. The DNA was psoralen-crosslinked and subjected to CsCl/Actinomycin D-gradients for enrichment of rDNA (Dammann et al., 1993). Samples with enriched rDNA were digested overnight using *Pvu*I and RIs were enriched by binding and elution from BND-cellulose (Muller et al., 2000). After concentration of the samples using centricon columns (Millipore), the EM analysis was performed as described (Sogo et al., 2002). Molecules were photographed and measured to verify that they represent replication forks stalled at the ribosomal RFB.

Acknowledgements

We thank Olivier Fritsch for discussions and critical reading of the manuscript. This work was supported by the Swiss National Science Foundation (to J.M.S.) and the Bonizzi-Theler Stiftung, Zürich (to P.S.).

References

Admire, A., L. Shanks, N. Danzl, M. Wang, U. Weier, W. Stevens, E. Hunt and T. Weinert. 2006. Cycles of chromosome instability are associated with a fragile site and are increased by defects in DNA replication and checkpoint controls in yeast. *Genes Dev* **20:** 159–173.

Aylon, Y., and M. Kupiec. 2004. New insights into the mechanism of homologous recombination in yeast, *Mutat. Res.*, **566**:231–248.

Bastin-Shanower, S.A., W.M. Fricke, J.R. Mullen and S.J. Brill.2003. The mechanism of Mus81-mms4 cleavage site selection distinguishes it from the homologous endonuclease Rad1-Rad10. *Mol. Cell. Biol*., **23**:3487-3496.

Brewer, B.J. and W.L. Fangman. 1988. A replication fork barrier at the 3' end of yeast ribosomal RNA genes. *Cell* **55**: 637-643.

Brewer, B.J., D. Lockshon, and W.L. Fangman. 1992. The arrest of replication forks in the rDNA of yeast occurs independently of transcription. *Cell* **71:** 267–276.

Bjergbaek, L., J.A. Cobb, M. Tsai-Pflugfelder and S.M. Gasser. 2005. Mechanistically distinct roles for Sgs1p in checkpoint activation and replication fork maintenance. *EMBO J.* **24**: 405-417.

Branzei, D., J. Sollier, G. Liberi. X. Zhao, D. Maeda, M. Seki, T. Enomoto, K. Ohta and M. Foiani. 2006. Ubc9- and mms21-mediated sumoylation counteracts recombinogenic events at damaged replication forks. *Cell*.**127**: 509-522.

Burkhalter, M.D. and J.M. Sogo. 2004. rDNA enhancer affects replication initiation and mitotic recombination: Fob1 mediates nucleolytic processing independently of replication. *Mol. Cell* **15**: 409-421.

Cobb, J.A., L. Bjergbaek, K. Shimada, C. Frei and S.M. Gasser. 2003. DNA polymerase stabilization at stalled replication forks requires Mec1 and the RecQ helicase Sgs1. *EMBO J.* **22**: 4325-4336.

Dammann, R., R. Lucchini, T. Koller and J.M. Sogo. 1993. Chromatin structures and transcription of rDNA in yeast Saccharomyces cerevisiae. *Nucleic Acids Res.* **21**: 2331-2338.

Defossez P.A., R. Prusty, M. Kaeberlein, S.J. Lin, P. Ferrigno, P.A. Silver, R.L. Keil and L. Guarente. 1999. Elimination of replication block protein Fob1 extends the life span of yeast mother cells. *Mol Cell* **3:** 447–455.

Dlakic, M. 2002. A model of the replication fork blocking protein Fob1p based on the catalytic core domain of retroviral integrases. *Protein Sci* **11**: 1274-1277.

Fabre, F., A. Chan, W.D. Heyer and S. Gangloff.2002. Alternate patways involving Sgs1/Top3, Mus81/Mms4 and Srs2 prevent formation of toxic recombination intermediates from single-stranded gaps created by DNA replication., *Proc Natl Acad Sci USA*, **99**: 16887-16892.

Fricke W.M. and S.J. Brill. 2003. Slx1-Slx4 is a second structure-specific endonuclease functionally redundant with Sgs1-Top3. *Genes Dev*. **17**:1768-1778.

Gruber, M., R.E. Wellinger and J.M. Sogo. 2000. Architecture of the replication fork stalled at the 3' end of yeast ribosomal genes. *Mol Cell. Biol.* **20**: 5777-5787.
Hickson, I.D. 2003. RecQ helicases: caretakers of the genome. *Nat. Rev. Cancer* **3**: 169-178.

Haber J.E. and W.D. Heyer. 2001. The fuss about Mus81. *Cell* **107**:551–554.

Hanada, K., M. Budzowska, S.L. Davies, E. van Drunen H. Onizawa, H.B. Beverloo, A. Maas, J. Essers, I.D. Hickson and R. Kanaar. 2007. The structure-specific endonuclease Mus81 contributes to replication restart by generating double-strand DNA breaks. *Nat Struct Mol Biol* **14**: 1096-1104.

Heyer WD, Ehmsen KT, Solinger JA, (2003), Holliday junctions in the eukaryotic nucleus: resolution inside?, *TIBS*, **28**, 548-557

Ivessa, A.S., J.Q. Zhou and V.A. Zakian. 2000. The Saccharomyces Pif1p DNA helicase and the highly related Rrm3p have opposite effects on replication fork progression in ribosomal DNA. *Cell* **100**: 479-489.

Ivessa, A.S., J.Q. Zhou, V.P. Schulz, E.K. Monson and V.A. Zakian. 2002. Saccharomyces Rrm3p, a 5' to 3' DNA helicase that promotes replication fork progression through telomeric and subtelomeric DNA. *Genes Dev.***16**: 1383-1396.

Ivessa, A.S., B.A. Lenzmeier, J.B. Bessler, L.K. Goudsouzian, S.L. Schnakenberg and V.A. Zakian. 2003. The *Saccharomyces cerevisiae* helicase Rrm3p facilitates replication past nonhistone protein-DNA complexes. *Mol. Cell* **12**: 1525-1536.

Kobayashi, T. and T. Horiuchi. 1996. A yeast gene product, Fob1 protein, required for both replication fork blocking and recombinational hotspot activities. *Genes Cells* **1**: 465-474.

Kobayashi T., D.J. Heck, M. Nomura and T. Horiuchi. 1998. Expansion and

contraction of ribosomal DNA repeats in *Saccharomyces cerevisiae*: requirement of replication fork blocking (Fob1) protein and the role of RNA polymerase I. *Genes Dev* **12:** 3821–3830.

Kobayashi T. 2003. The replication fork barrier site forms a unique structure with Fob1p and inhibits the replication fork. *Mol Cell Biol*. **23**: 9178-9188.

Kraus, E., W.Y. Leung and J.E. Haber. 2001. Break-induced replication: a review and an example in budding yeast. *Proc Natl Acad Sci U S A* **98**: 8255-8262.

Lambert, S., A. Watson, D.M. Sheedy, B. Martin and A.M. Carr. 2005. Gross chromosomal rearrangements and elevated recombination at an inducible site-specific replication fork barrier. *Cell* **121**: 689-702.

Liberi, G., G. Maffioletti, C. Lucca, I. Chiolo, A. Baryshnikova, C. Cotta-Ramusino, M. Lopes, A. Pellicioli, J.E. Haber and M. Foiani. 2005. Rad51-dependent DNA structures accumulate at damaged replication forks in *sgs1* mutants defective in the yeast ortholog of BLM RecQ helicase. *Genes Dev.* **19**: 339-350.

Linskens, M.H. and J.A. Huberman. 1988. Organization of replication of ribosomal DNA in Saccharomyces cerevisiae. *Mol. Cell. Biol.* **8**: 4927-4935.

Lucchini, R. and J.M. Sogo. 1994. Chromatin structure and transcriptional activity around the replication forks arrested at the 3' end of the yeast rRNA genes. *Mol. Cell. Biol.* **14**: 318-326.

Mirkin E.V. and S.M. Mirkin. 2007. Replication fork stalling at natural impediments. *Microbiol Mol Biol Rev.* **71**: 13-35.

Mohanty, B.K., D. Bastia. 2004. Binding of the replication terminator protein Fob1p to the Ter sites of yeast causes polar fork arrest. *J Biol Chem*. **279**: 1932-1941.

Mullen J.R., V. Kaliraman, S.S. Ibrahim and S.J. Brill. 2001. Requirement for three novel protein complexes in the absence of the Sgs1 DNA helicase in Saccharomyces cerevisiae. *Genetics*. **157**:103-118.

Muller, M., R. Lucchini and J.M. Sogo. 2000. Replication of yeast rDNA initiates downstream of transcriptionally active genes. *Mol. Cell* **5**: 767-777.

Paques F. and J.E. Haber.1999. Multiple pathways of recombination induced by double-strand breaks in Saccharomyces cerevisiae, *Microbiol. Mol. Biol. Rev.* **63**: 349–404.

Pohlhaus, J.R. and K.N. Kreuzer. 2006. Formation and processing of stalled

replication forks-utility of two-dimensional agarose gels. *Methods Enzymol*. **409**: 477-493.

Schär, P., G. Herrmann, G. Daly and T. Lindahl. 1997. A newly identified DNA ligase of Saccharomyces cerevisiae involved in RAD52-independent repair of DNA double-strand breaks. *Genes Dev.* **11**: 1912-1924.

Shimada, K., P. Pasero and S.M. Gasser. 2002. ORC and the intra-S-phase checkpoint: a threshold regulates Rad53p activation in S phase. *Genes Dev.* **16**: 3236-3252.

Sinclair, D.A. and L. Guarente. 1997. Extrachromosomal rDNA circles-a cause of aging in yeast. *Cell* **91**: 1033-1042.

Sogo, J.M., M. Lopes and M. Foiani. 2002. Fork reversal and ssDNA accumulation at stalled replication forks owing to checkpoint defects. *Science* **297**: 599-602.

Wallis, J.W., G. Chrebet, G. Brodsky, M. Rolfe and R. Rothstein. 1989. A hyper-recombination mutation in S. cerevisiae identifies a novel eukaryotic topoisomerase. *Cell* **58**: 409-419.

Watt, P.M., I.D. Hickson, R.H. Borts and E.J. Louis. 1996. SGS1, a homologue of the Bloom's and Werner's syndrome genes, is required for maintenance of genome stability in Saccharomyces cerevisiae. *Genetics* **144**: 935-945

Weitao, T., M. Budd, L.L. Hoopes and J.L. Campbell. 2003. Dna2 helicase/nuclease causes replicative fork stalling and double-strand breaks in the ribosomal DNA of *Saccharomyces cerevisiae*. *J. Biol. Chem*. **278**: 22513-22522.

Figure legends

Figure 1

Double-strand break formation at the RFB in the rDNA locus. **A**. Structural organization of one rDNA repeat unit of *S. cerevisiae*. Relevant restriction sites, fragment sizes and probe-annealing sites are shown. 35S and 5S, rRNA transcription units; RFB, replication fork barrier; ARS, autonomous replicating sequence; NTS1 and NTS2, non-transcribed spacer regions, P1, Probe1; P2, Probe2. **B.** 1D gel-electrophoresis of *Bgl*II or *Bgl*II-*Hind*III (HB) digested DNA. Genomic DNA from logarithmically growing cells (wild-type or *fob1*) was isolated in agarose plugs, digested with *Bgl*II, separated on 1% agarose gel and detected by Southern blotting, using Probe1. 1-5; fragments smaller than monomer. **C**. Same as B except that genomic DNA from S-phase synchronized wild-type W303 cells, as described in Burghaler and Sogo, 2004, was examined. **D**. Membrane form C was subsequently stripped and re-probed with Probe2. Bands corresponding to fragments generated by DSBs at RFB are indicated. 1'-4' fragments smaller than monomer, detected with Probe2. HB- *Hind*III-*Bgl*II fragment of rDNA.

Figure 2

DSB detection using neutral-neutral 2D electrophoresis of DNA isolated in agarose plugs. **A**. Typical schematic profile of *Bgl*II digested rDNA after 2D electrophoresis. Major features and mobility of molecules with different secondary structures are indicated. M, linear monomer unit of rDNA; RFB, spot representing molecules stalled at the RFB in rDNA; Ter, termination spot representing structures arising from fusion of 2 converging replication forks at replication termination **B**. Southern blots of 2D gels of DNA from wild-type and *fob1* cells. DNA from logarithmically growing cultures was isolated in agarose plugs, digested with *Bgl*II and separated by neutral-neutral 2D electrophoresis. rDNA was detected by Southern blotting using Probe1 and Probe2 (after stripping). Spots corresponding to DSBs at the RFB are marked with an asterisk.

Numbering of fragments smaller than monomer (1-5 and 1'-4') same as in Figure 1.

Figure 3

Variation in 2D gel profiles of rDNA replication intermediates in different mutant strains. DNA from logarithmically growing cells of the strains indicated was isolated in agarose plugs, separated by neutral-neutral 2D electrophoresis (as in Figure 2) and hybridized to a P^{32}-labeled Probe 1. Representative examples of Southern blot scans for each mutant are shown. All strains are derivatives of FF18733 (wild-type). The respective relevant mutant gene(s) are indicated on each scan. Previously undescribed spots are marked with arrows (*sgs1* and *sgs1 top3*) or ladder symbol (*dnl4*). DSB spots are marked with asterisks.

Figure 4

Quantification of DSB and RI signals from 2D Southern blots. Phosphoimage screens were exposed to Southern blot membranes, scanned on a Typhoon (GE-Healthcare) and analyzed by ImageQuant software (ver. 8). **A**. Example of a scan from wild-type (FF18733); relevant signals that were measured and used for quantitation are indicated. Ter, termination spot; RFB, replication-fork barrier spot; 2n, 2n spot; DSB, double-strand break spot; RI, replication intermediates; **B.** Relative levels of DSBs, RFB, Ter and 2n signals normalized to the amount of relevant precursors, namely stalled replication forks, and compared to wild-type. Columns represent the mean of 3 independent scans with standard errors.

Figure 5

Anatomy of replication forks stalled at RFB. **A**. Representative electromicrogram of an intact fork stalled at RFB. **B**. Electromicrogram of a fork harboring a stretch of single-stranded DNA (asterisk) in the nascent strand of a fork stalled at RFB. **C**. Representative "entangled" fork from *top3* mutant. **D**. Electromicrogram of a terminating molecule; two forks converging at the RFB, **E**. Schematic drawing of *Pvu*I restriction fragment and the different classes of RIs detected.

Figure 6

Possible model explaining generation and repair of DSBs at the rDNA locus. **A.** Generation of Rad52-dependent and -independent DSBs in wild-type. **B**. Proposed role of NHEJ in repair of rDNA DSBs. Red arrows represent the cutting step by Mus81-Mms4 nuclease and green arrows that of Slx1-Slx4.

Supplementary Figure 1

Comparison of 2D gel migration of *Hind*III-*Bgl*II fragment of rDNA and BglII-digested genomic DNA from logarithmically growing wild-type (FF18733) cells. **A**. Autoradiogram obtained by hybridization to Probe 1. **B**. Same membrane stripped and re-probed with Probe2. HB- *Hind*III-*Bgl*II fragment of rDNA. The X marks the origin of DNA migration.

Supplementary Figure 2

Evaluation of the amount of DSBs in respect to the pool of total RIs. **A**. Comparison of DSB levels between wild-type and *fob1* genetic backgrounds. Columns represent the mean of 3 independent scans; error-bars are standard errors. **B**. Individual signals (DSB, RFB, Ter and 2n) are compared to total RIs. The relative ratios of individual signals are shown for all mutant backgrounds tested.

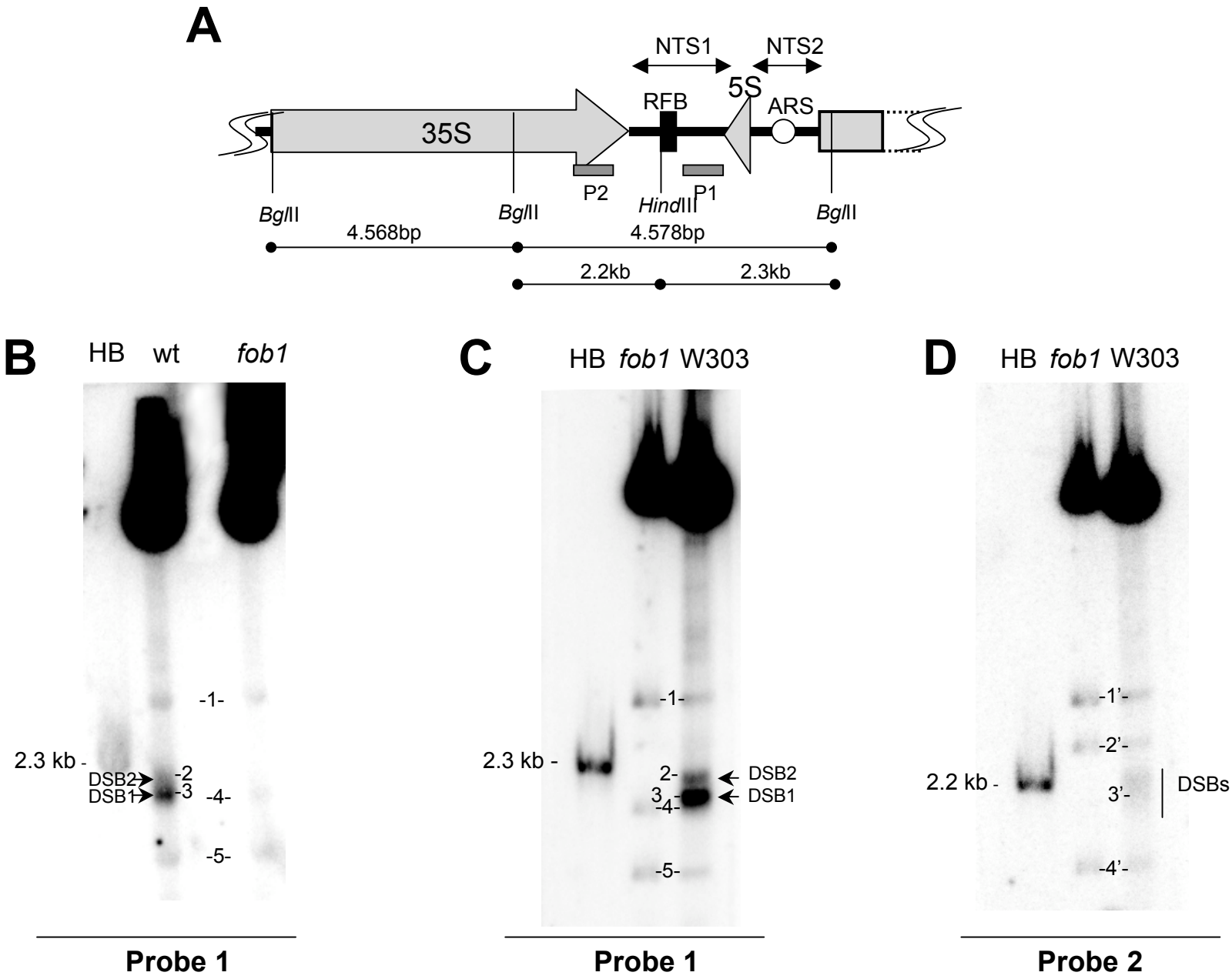
A
NTS1
NTS2
5S
RFB
ARS
35S
P2
P1
BglII
HindIII
BglII
BglII
4.568bp
4.578bp
2.2kb
2.3kb
B
HB wt fob1
2.3 kb
DSB2
DSB1
-1-
-2
-3
-4-
-5-
Probe 1
C
HB fob1 W303
2.3 kb
-1-
2-
3
-4-
-5-
DSB2
DSB1
Probe 1
D
HB fob1 W303
2.2 kb
-1'-
-2'-
3'-
-4'-
DSBs
Probe 2

Kais et al. Figure 2

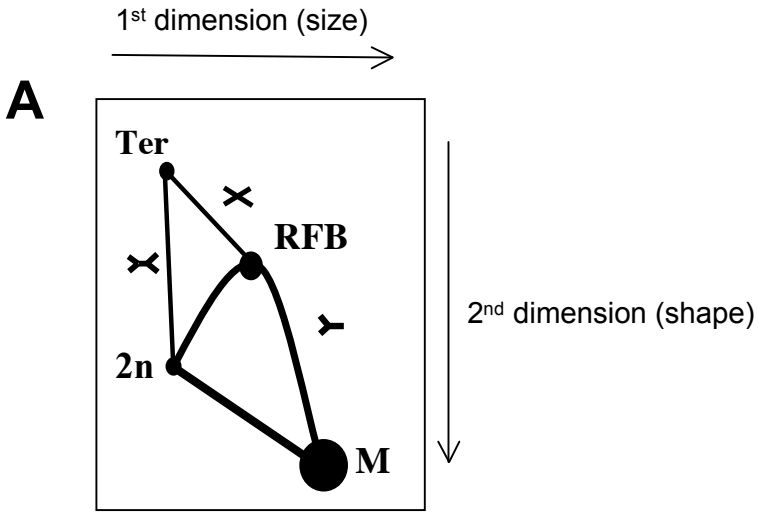

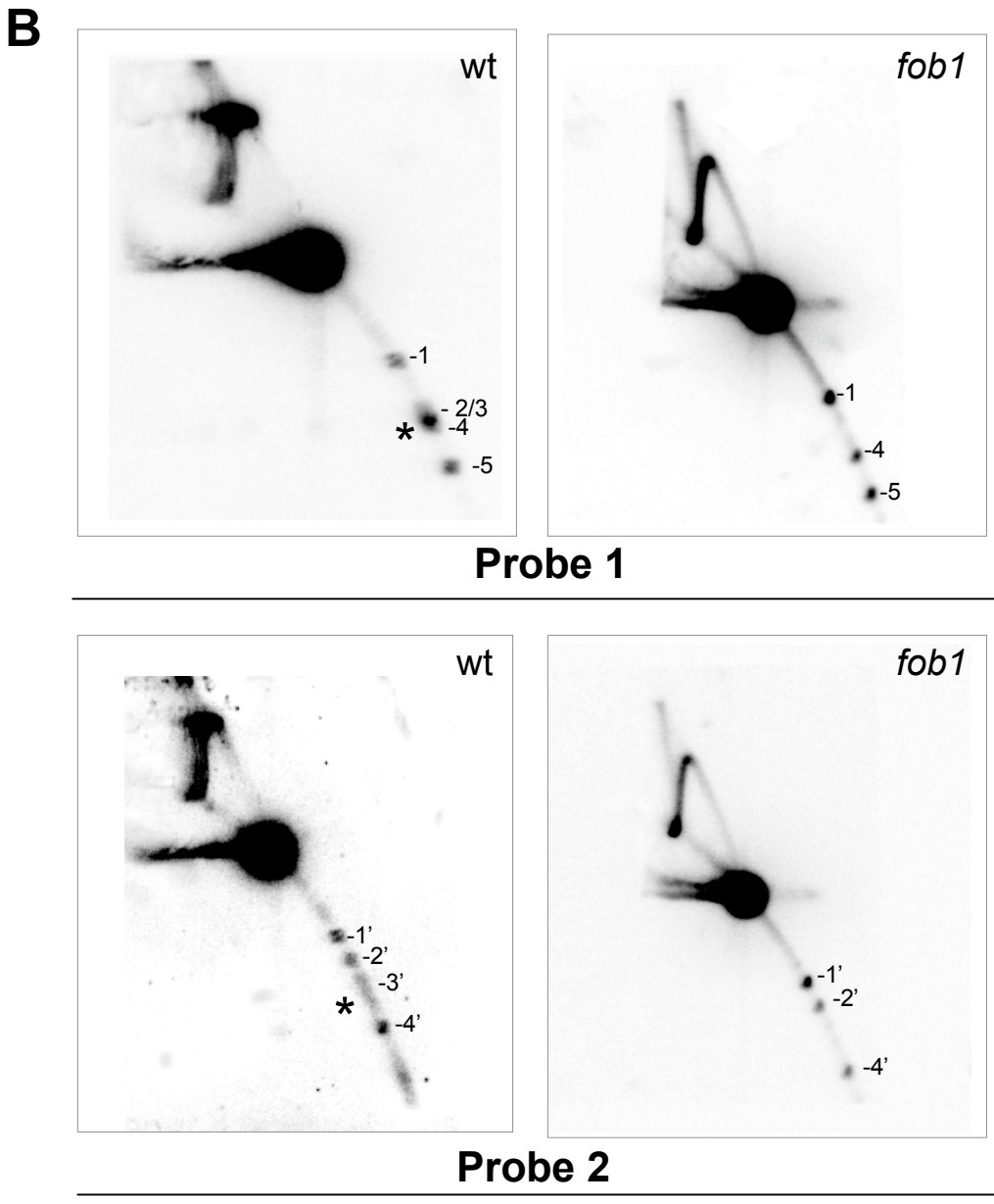

Kais et al. Figure 3

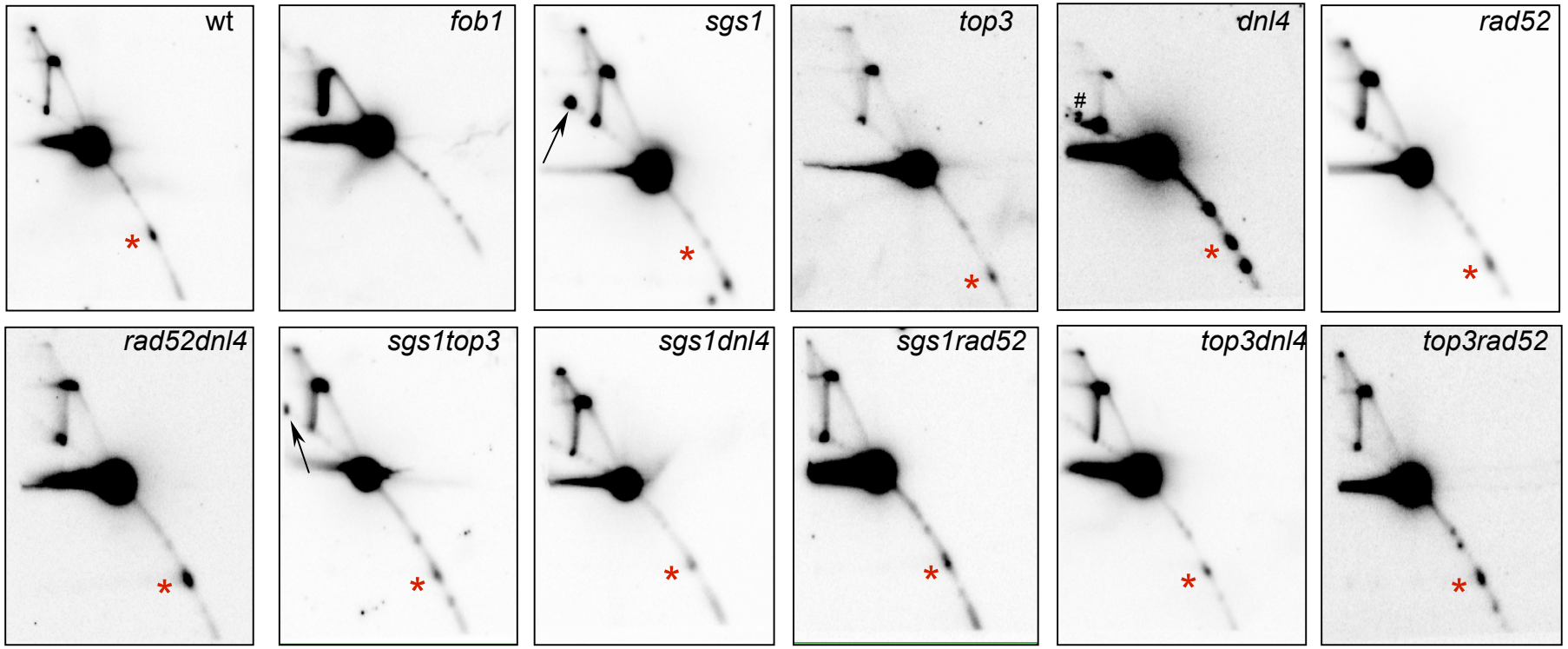

Kais et al. Figure 4

A

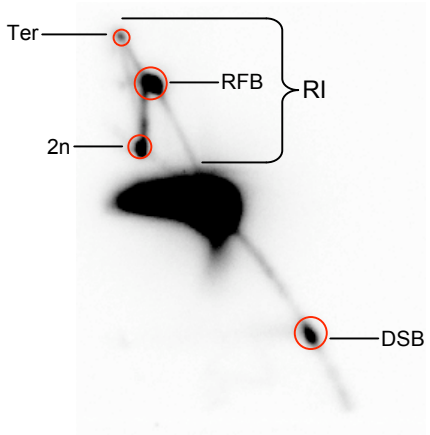

B

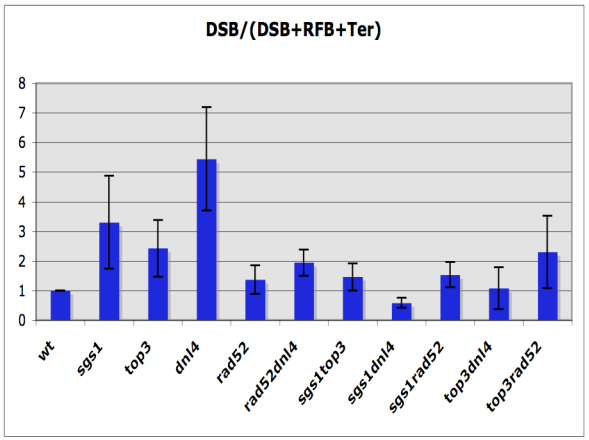

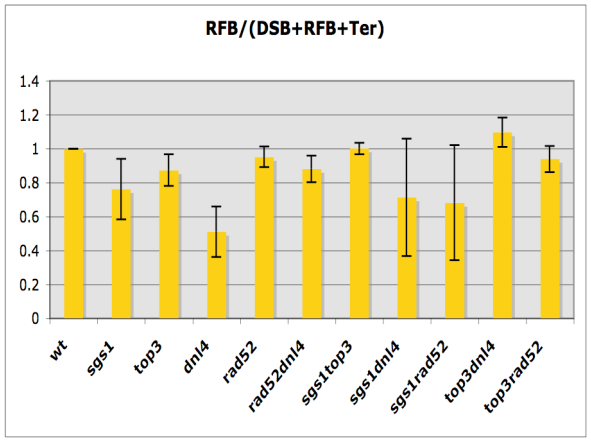

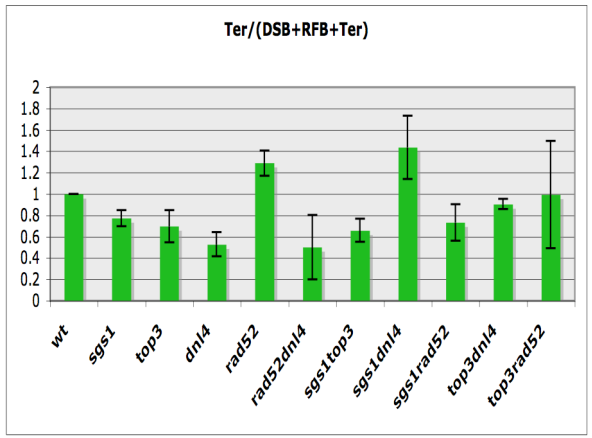

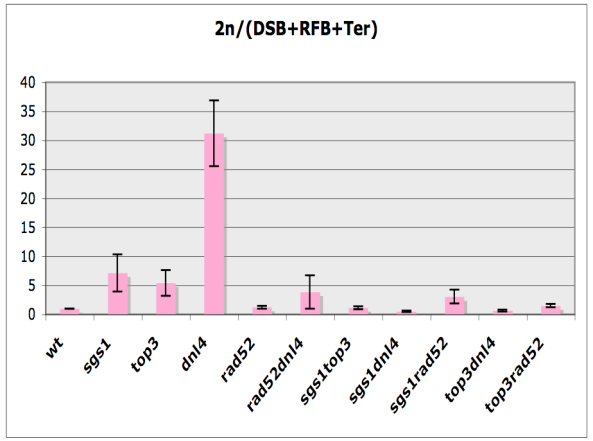

Kais et al. Figure 5

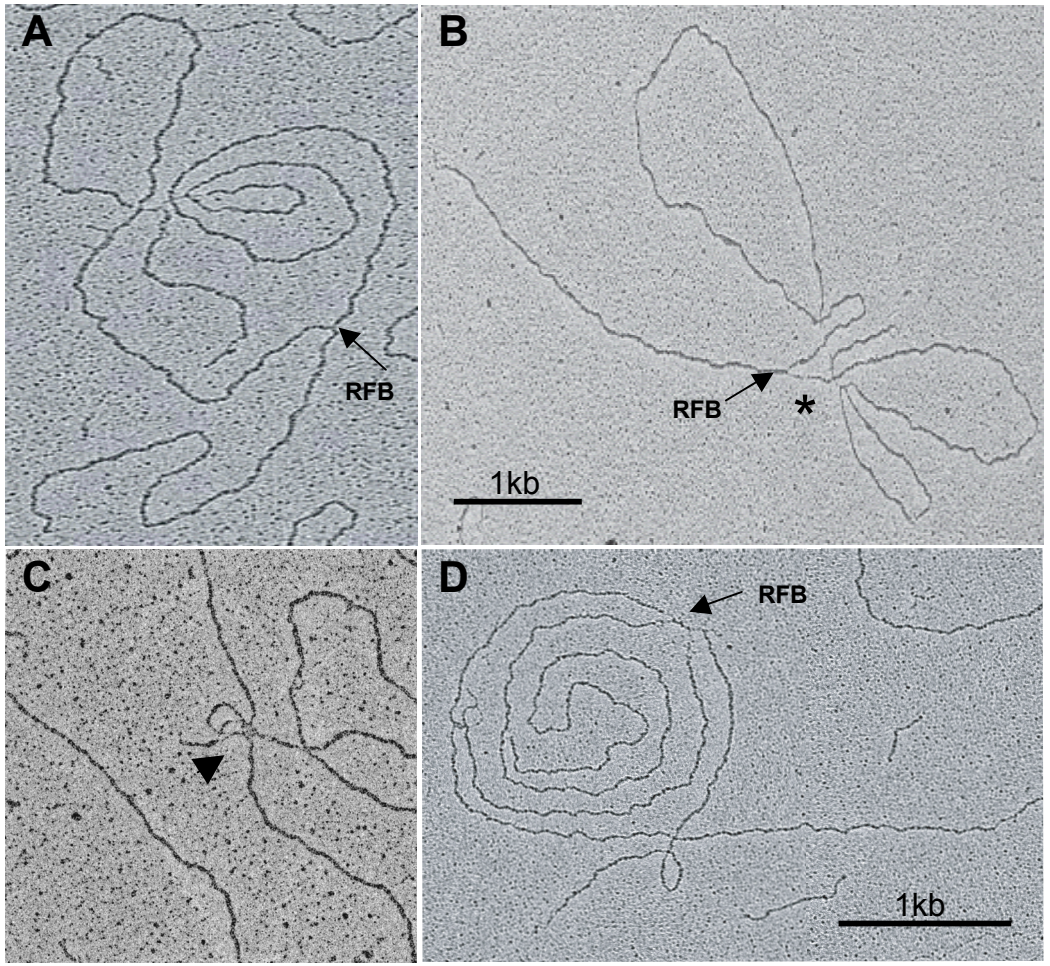

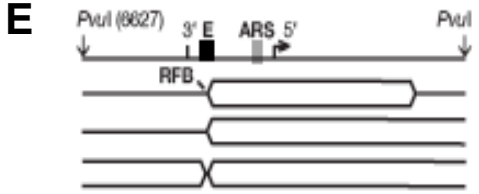

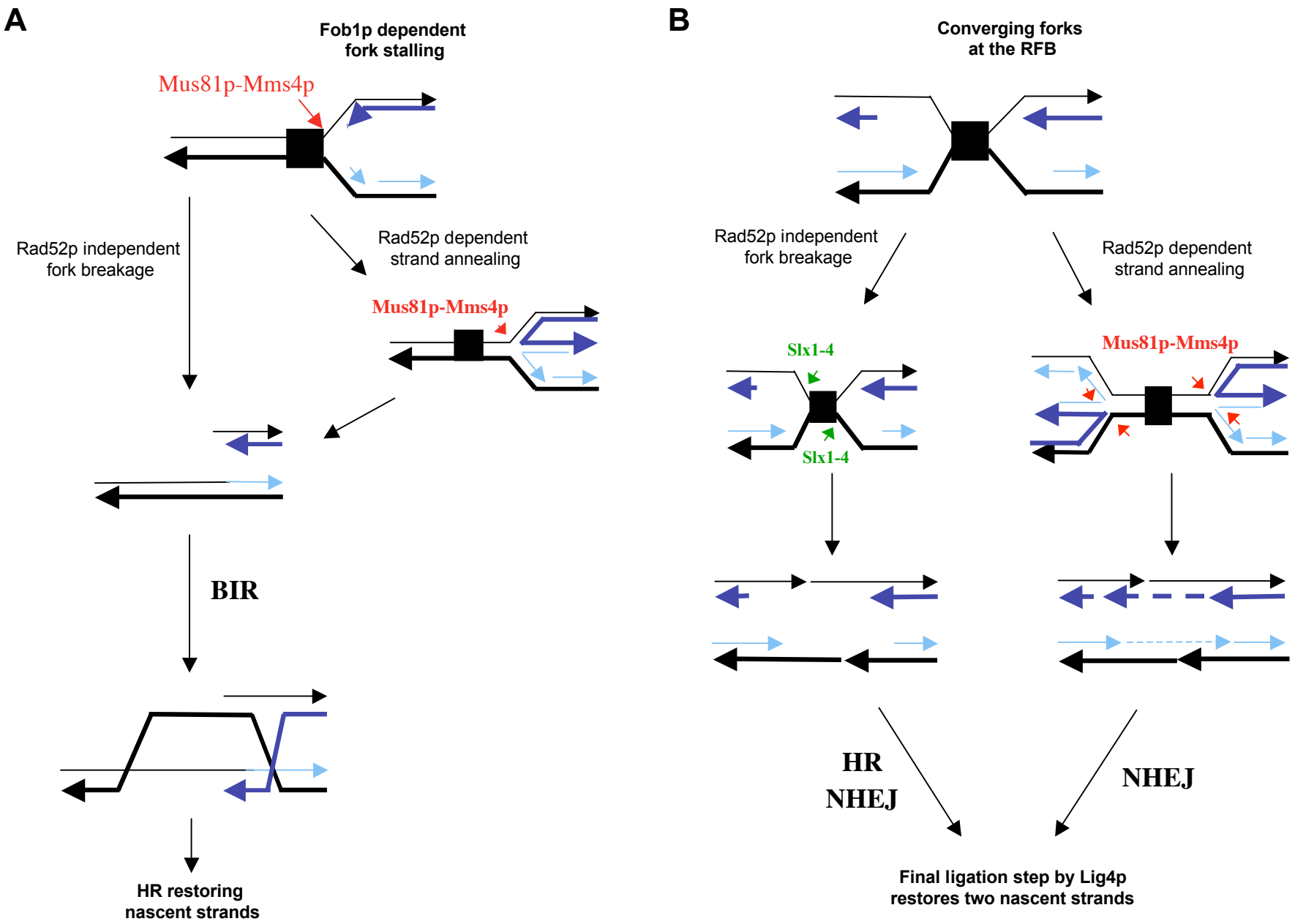
A
Fob1p dependent
fork stalling
Mus81p-Mms4p
Rad52p independent
fork breakage
Rad52p dependent
strand annealing
Mus81p-Mms4p
BIR
HR restoring
nascent strands
B
Converging forks
at the RFB
Rad52p independent
fork breakage
Rad52p dependent
strand annealing
Slx1-4
Slx1-4
Mus81p-Mms4p
HR
NHEJ
NHEJ
Final ligation step by Lig4p
restores two nascent strands

Kais et al. Supplementary Figure 1

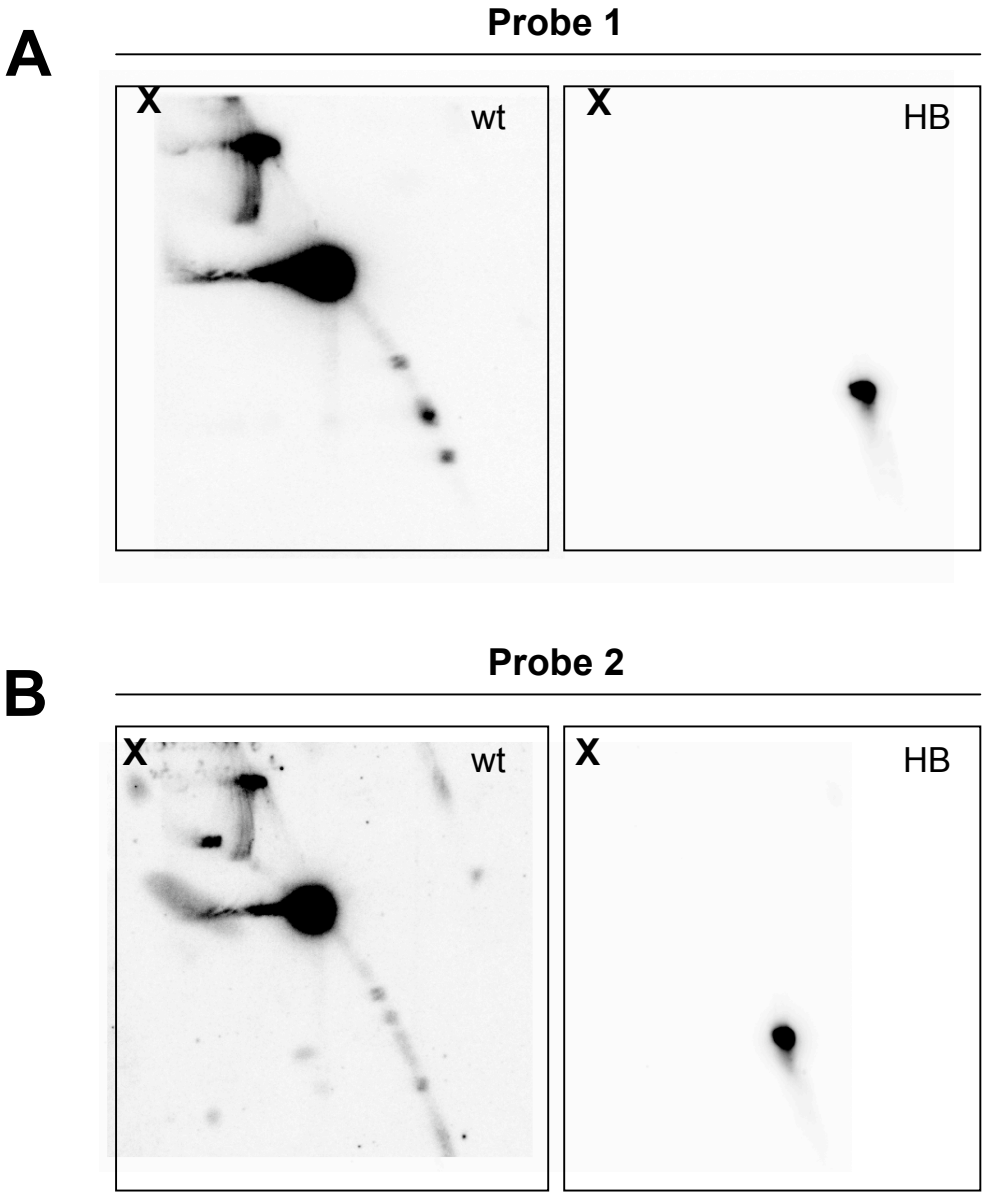

Kais et al. Supplementary Figure 2

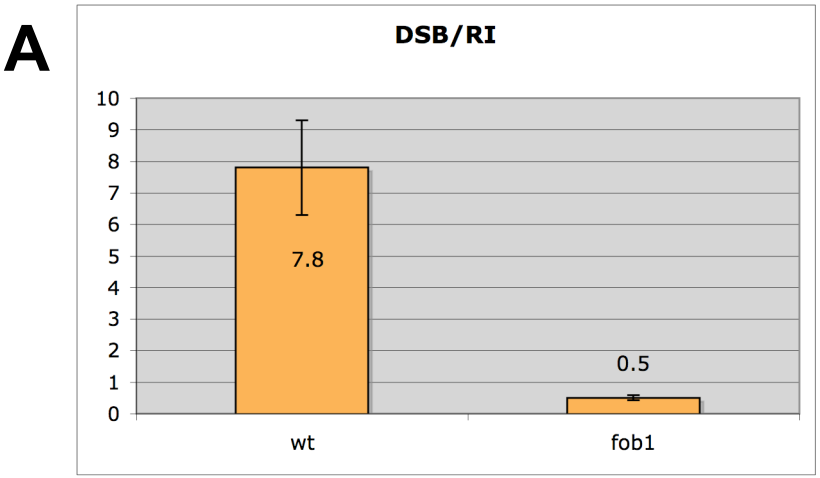

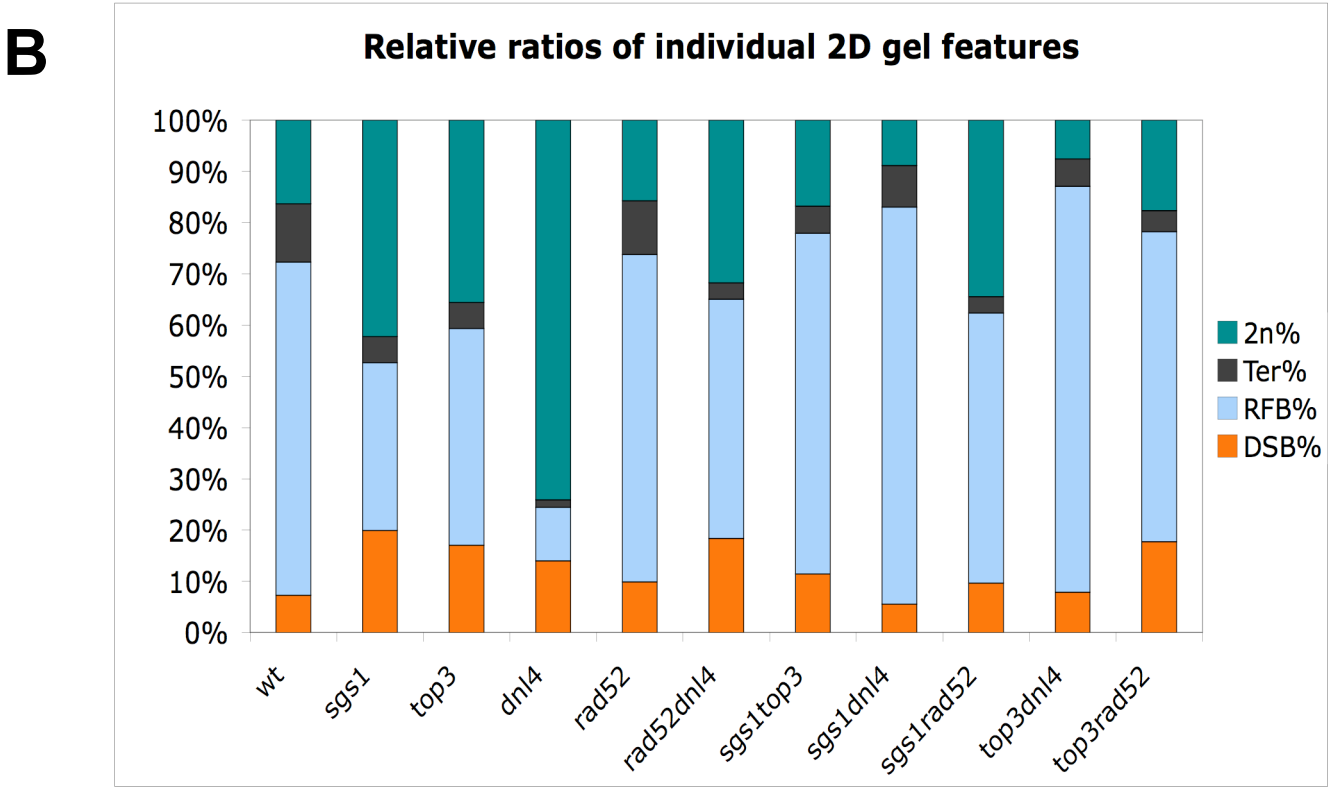

Kais et al Table1.

Size and frequency of ssDNA regions in replication forks stalled at RFB

Mutant phenotype	Molecules Analyzed	Molecules with ss-region	Size of ss-region (nt)	"Entangled" forks
wt	101	27(27%)	127(+/-43)	0
lig4	106	61(58%)	147(+/-58)	0
sgs1	128	73(57%)	165(+/-86)	0
top3	107	57(53%)	154(+/-74)	3(3%)

Supplementary Table 1. Yeast strains.

Mutant	Strain name	Genotype	Created	Source/reference
wt	FF18733	*leu2-3 trp1-289 ura3-52 his7-2 lys1-1 MATa*	-	Francis Fabre
sgs1	GP100	*leu2 ura3 his7-1 lys2-1 sgs1::URA3*	-	G. Pedrazzi, lab collection
dnl4	PRSY004.1	*leu2 trp1 ura3 his7-2 lys2-1 lig4::kanMX4 MATa*	-	P.Schär, lab collection
rad52	FF18742	*leu2 trp1 ura3 his7-2 lys1-1 rad52::URA3 MATa*	-	Francis Fabre
rad52dnl4	PRSY006	*leu2 ura3 his7-? lys2-1 rad52::URA3 lig4::kanMX4 MATa*	-	P.Schär, lab collection
top3	PRSY220.4	*leu2-3 ura3 his7-1 lys1-1 trp1 top3::TRP1 MATa*	Cross PRSY220.2 X FF18734	this study
fob1	PRSY210	*leu2-3 trp1-289 ura3-52 his7-2 lys1-1 fob1::URA3 MATa*	Gene replacement in FF18733	this study
sgs1top3	PRSY221d	*leu2 lys2-1 ura3 his7-1 TRP1 sgs1::URA3 top3::TRP1 MATa*	Cross GP100 X PRSY220.1	this study
sgs1dnl4	PRSY224	*leu2 trp1 ura3 his7-? sgs1::URA3 lig4::kanMX4 MATa*	Cross GP100 X PRSY005	this study
sgs1rad52	PRSY225	*leu2 lys? his7-? ura3 sgs1::URA3 rad52::URA3 MATa*	Cross GP100 X PRSY005	this study
top3dnl4	PRSY213.1	*leu2 lys1-1 ura3 trp1 his7-1 top3::TRP1 lig4::kanMX4 MATa*	Cross PRSY220.4 X PRSY003.1	this study
top3rad52	PRSY211.2	*leu2 lys1-1 his7-? ura3 trp1 top3::TRP1 rad52::URA3 MATa*	Cross PRSY220.4 X FF18742	this study

4. Discussion & Future Perspectives

Genome stability is of primary importance for the survival and proper functioning of all organisms. DNA damage, and particularly DNA double-strand breaks (DSBs), must be efficiently repaired to ensure integrity and functionality of the genome. All cells from bacteria to human cells have a potential to repair DSBs by either homologous recombination (HR) or non-homologous end-joining (NHEJ). In multicellular organisms NHEJ is the preferred pathway, and the opposite is true in bacteria and yeast. This could be intrinsic to their genomic organizations. The genomes of multicellular eukaryotes, unlike yeast, have a substantial fraction of repetitive DNA. Therefore, the homology driven repair could be dangerous in repetitive genomes as it could lead to gross chromosomal rearrangements and translocations.

Obviously, either or both of the DSB repair processes should be regulated in the cells in order to avoid improper repair or futile cycles of nonproductive repair. But the question still remains- how is the decision made as to whether NHEJ or homologous recombination is used to repair a DSB? This work represents an attempt to answer this question and gain more insight into different aspects of NHEJ regulation and/or utilization.

Negative regulation of NHEJ by Ntr1

Since the mechanisms of two DSBR processes are quite different, the regulation could be happening already at the initial steps (immediately after or during damage recognition). There is a report suggesting that NHEJ could precede HR (Frank-Vaillant and Marcand 2002) by fast binding of Ku heterodimers to the break site. However, NHEJ, although inaccurate, is also active in *yku70* cells (Boulton and Jackson 1996) which makes a regulation at later steps more probable. That led to the search for possible regulators in later steps of NHEJ.

In this work, I characterized Ntr1, a Lif1-interating protein, as a negative regulator of NHEJ. My data suggested that overexpression of Ntr1 negatively effects productive repair of chromosomal *Eco*RI breaks by NHEJ.

It has been speculated that HR and NHEJ might compete for same substrates (Allen et al 2003), either actively or passively. Data presented in this work suggest that channeling from one repair pathway to the other is possible, even though the outcomes of the channeling are not always productive. For example, overexpression of Ntr1 in *rad52* cells harboring *Eco*RI induced DSBs suppressed the viability of those cells 8-fold. This indicates that excess of Ntr1p channels the repair of *Eco*RI induced breaks (that are normally repaired by NHEJ) into the nonfunctional HR pathway, which leads to reduction in viability of those cells. Whether there is a competition between pathways, or certain breaks are designated for a particular type of repair and are repaired by redundant pathway only in the absence of the "correct" pathway, still remains elusive.

Furthermore, it is still unclear how cells discriminate between chromosomal DSBs that need to be repaired and chromosomal ends (telomeres) that must not be ligated. This discrimination is likely to occur at the late steps of repair, because upstream factors of NHEJ (namely Ku and MRX complex) associate with both types of ends (Martin et al 1999, Takata et al 2005). This is where Ntr1, presented here, could come into play. Co-localization data presented here, and interaction between Ntr1 and PinX1, indicates a possible connection of Ntr1 to telomeres. It seems that Ntr1 interferes with DNA repair, probably on telomeres and (negatively) regulate NHEJ at the intersection of DSB repair and telomere protection. The details of the mechanism(s) involved still remain to be elucidated.

Repair of naturally occurring S-phase dependent DSBs

During S-phase, in rDNA locus, DSBs are generated at the position of RFB, probably as a result of collapse of stalled replication forks accumulating there (Burghalter and Sogo 2004). In *dnl4* mutants, I observed an increased number of those breaks, indicating that the remaining repair pathway, namely HR, is alone not sufficient for repair and that both pathways contribute to the repair of S-phase DSBs. Whether the two pathways act on different substrates (HR catalyzing BIR at forks stalled at RFB and NHEJ processing DSBs arising in converging forks) or there is

overlap and possible competition between the repair pathways, needs to be addressed in future. However, reduced levels of DSBs in *dnl4 rad52* mutant background, compared to the *dnl4* mutant, suggest interplay of the two DSB repair pathways in the generation and/or repair of DSBs at the RFB.

Based on the availability of homologous sequences in haploid yeast cells, HR should be possible only in late S- and G2/M-phases of cell cycle. Indeed, cells arrested in G1 cannot perform HR, not only because the lack of homologous sequences (i.e. sister chromatids) but also because DSB ends are not resected to give 3'-overhangs which are initial substrates for HR (Aylon et al 2004). Similar evidence came recently also from study in human cells (Sartori et al 2007). It seems clear that end-resection, confined to S- and G2- phase of cell cycle, represents a commitment step in the choice of pathway utilization. This, however, doesn't exclude the possibility of NHEJ acting also in S- and G2/M-phases of cell cycle, before the resection takes place. Data presented here would support such scenario.

The observed involvement of Dnl4 in the repair of S-phase dependent DSBs in rDNA was rather surprising, particularly in the light of the fact that yeast cells prefer HR for the repair of DSBs (Paques and Haber 1999). One could imagine that due to the repetitiveness of the rDNA locus, cells prefer repair by Dnl4-dependent process, as has been proposed for mammalian genomes. Avoidance of HR would, furthermore, ensure a stable copy number of the repeats in the locus (Johzuka and Horiuchi 2002) minimizing "erroneous" recombination between repeats. To resolve this question, an assay should be constructed to monitor the repair within another repetitive sequence, to rule out the rDNA specificities. Another possibility is to introduce RFB at an ectopic site in the genome (as was already done before, Calzada et al 2005) and monitor DSB generation and repair in the context of single-copy locus.

5. References

Allen C, Halbrook J, Nickoloff JA (2003), Interactive competition between homologous recombination and non-homologous end joining. *Mol. Cancer Res.* **1**: 913–920.

Åström SU, Okamura SM, Rine J (1999), Yeast cell-type regulation of DNA repair. *Nature* **397**: 310-317.

Aylon Y, Kupiec M (2004), New insights into the mechanism of homologous recombination in yeast. *Mutat. Res.* **566**: 231–248.

Aylon Y, Liefshitz B, Kupiec M (2004), The CDK regulates repair of double-strand breaks by homologous recombination during the cell cycle. *EMBO J* **23**: 4868-4875.

Banditt M, Koller T, and Sogo JM (1999), Transcriptional activity and chromatin structure of enhancer-deleted rRNA genes in *Saccharomyces cerevisiae*. *Mol. Cell Biol.* **19**: 4953-4960.

Bastin-Shanower SA, Fricke WM, Mullen JR, Brill SJ (2003), The mechanism of Mus81-mms4 cleavage site selection distinguishes it from the homologous endonuclease Rad1-Rad10. *Mol. Cell. Biol.* **23**: 3487-3496.

Boddy MN, Gaillard PH, McDonald WH, Shanahan P, Yates JR III, Russel P, (2001), Mus81-Eme1 are essential components of a Holliday junction resolvase. *Cell* **107**: 537-548.

Boulton SJ, Jacskon SP (1996), *Saccharomyces cerevisiae* Ku70 potentiates illegitimate DNA double-strand break repair and serves as a barrier to error-prone DNA repair pathways. *EMBO J.* **15**: 5093-5103.

Boulton SJ, Jacskon SP (1998), Components of the Ku-dependent non-homologous end joining pathway are involved in telomeric length maintenance and telomeric silencing. *EMBO J.* **17**: 1819-1828.

Brewer BJ, Fangman WL (1988), A replication fork barrier at the 3' end of yeast ribosomal RNA genes. *Cell* **55**: 637-643.

Burkhalter MD, Sogo JM (2004), rDNA enhancer affects replication initiation and mitotic recombination: Fob1 mediates nucleolytic processing independently of replication. *Mol Cell.* **15**: 409-421.

Calzada A, Hodgson B, Kanemaki M, Bueno A, Labib K (2005), Molecular anatomy and regulation of a stable replisome at a paused eukaryotic DNA replication fork. *Genes & Dev.* **19**: 1905–1919.

Chen L, Trujillo K, Ramos W, Sung P, Tomkinson AE (2001), Promotion of Dnl4-catalyzed DNA end-joining by the Rad50/Mre11/Xrs2 and Hdf1/Hdf2 complexes. *Mol Cell.* **5**: 1105-1115.

Clerici M, Mantiero D, Lucchini G, Longhese MP (2005), The *Saccharomyces cerevisiae* Sae2 protein promotes resection and bridging of double strand break ends. *J Biol Chem.* **280**: 38631-38638.

Cobb JA, Bjergbaek L, Shimada K, Frei C, Gasser SM (2003), DNA polymerase stabilization at stalled replication forks requires Mec1 and the RecQ helicase Sgs1. *EMBO J.* **22**: 4325-4336.

Cobb JA, Schleker T, Rojas V, Bjergbaek L, Tercero JA, Gasser SM (2005), Replisome instability, fork collapse, and gross chromosomal rearrangements arise synergistically from Mec1 kinase and RecQ helicase mutations. *Genes Dev.* **15**: 3055-3069.

Cox MM (2002), The nonmutagenic repair of broken replication forks via recombination. *Mutat Res.* **510**: 107-120.

D'Amours D, Jackson SP (2001), The yeast Xrs2 complex functions in S phase checkpoint regulation. *Genes Dev.* **15**: 2238-2249.

D'Amours D, Jackson SP (2002), The Mre11 complex: at the crossroads of DNA repair and checkpoint signaling. *Nat Rev Mol Cell Biol.* **5**: 317-327.

DeFazio LG, Stansel RM, Griffith JD, Chu G (2002), Synapsis of DNA ends by DNA-dependent protein kinase. *EMBO J.* **21**: 3192-3200.

Drouet J, Frit P, Delteil C, de Villartay JP, Salles B, Calsou P (2006), Interplay between Ku, artemis and DNA-PKcs at DNA ends. *J Biol Chem.* **19**: 356-362

Dudas A, Chovanec M (2004), DNA double-strand break repair by homologous recombination. *Mutat. Res.-Rev. Mutat. Res.* **566**: 131–167.

Dynan WS, Yoo S (1998), Interaction of Ku protein and the DNA-dependent protein kinase catalytic subunits with nucleic acids. *Nucleic Acids Res.* **26**: 1551-1559.

Fabre F, Chan A, Heyer WD, Gangloff S (2002), Alternate patways involving Sgs1/Top3, Mus81/Mms4 and Srs2 prevent formation of toxic recombination intermediates from single-stranded gaps created by DNA replication. *Proc Natl Acad Sci USA*, **99**: 16887-16892.

Featherstone C, Jackson SP (1999), Ku, a DNA repair protein with multiple cellular functions? *Mutat. Res. DNA repair* **434**: 3-15.

Ferreira MG, Cooper JP (2001), The fission yeast Taz1 protein protects chromosomes from Ku-dependent end-to-end fusions. *Mol. Cell* **7**: 55–63.

Ferreira MG, Cooper JP (2004), Two modes of DNA double-strand break repair are reciprocally regulated through the fission yeast cell cycle. *Genes Dev.* **18**: 2249–2254.

Fichtinger-Schepman AMJ, van Dijk-Knijnenburg HCM, van der Velde-Visser SD, Berends F, Baan RA (1995), Cisplatin- and carboplatin-DNA adducts: is PT-AG the cytotoxic lesion? *Carcinogen.* **16**: 2447–2453.

Frankenberg-Schwager M, Kirchermeier D, Greif G, Baer K, Becker M, Frankenberg D (2005), Cisplatin-mediated DNA double-strand breaks in replicating but not in quiescent cells of the yeast *Saccharomyces cerevisiae*. *Toxicology* **212**: 175-184.

Frank-Vaillant M, Marcand S (2001), NHEJ regulation by mating type is exercised through a novel protein, Lif2p, essential to theLigase IV pathway. *Gene Develop*. **15**: 3005-3012.

Frank-Vaillant M, Marcand S. (2002), Transient stability of DNA ends allows nonhomologous end joining to precede homologous recombination. *Mol Cell.* **5**: 1189-1199.

Frei, C, Gasser SM (2000), The yeast Sgs1p helicase acts upstream of Rad53p in the DNA replication checkpoint and colocalizes with Rad53p in S-phase-specific foci. *Genes Dev.* **14**, 81-96.

Gangloff S, McDonald JP, Bendixen C, Arthur L, Rothstein R (1994), The yeast type I topoisomerase Top3 interacts with Sgs1, a DNA helicase homolog:a potential eukaryotic reverse gyrase. *Mol Cell Biol.* **14**: 8391-8398.

Game JC, and Mortimer RK (1974), A genetic study of X-ray sensitive mutants in yeast. *Mutat. Res.* **24**: 821–892.

Gellert M, (2002), V(D)J recombination: RAG proteins, repair factors, and regulation. *Annu. Rev. Biochem.* **71**: 101–132.

Gravel S, Larrivee M, Labrecque P, Wellinger RJ (1998), Yeast Ku as a regulator of chromosomal DNA end structure. *Science* **280**: 741-744.

Gruber M, Wellinger RE, Sogo JM (2000), Architecture of the replication fork stalled at the 3' end of yeast ribosomal genes. *Mol Cell Biol.* **20**: 5777-5787.

Grunstein M (1997), Molecular model for telomeric heterochromatin in yeast. *Curr Opin Cell Biol.* **3**: 383-387.

Harrington JJ, Lieber MR (1994), Functional domains within FEN-1 and RAD2 define a family of structure-specific endonucleases: implications for nucleotide excision repair. *Genes Dev.* **8**: 1344-1355.

Herrmann G, Lindahl T, Schar P (1998), *Saccharomyces cerevisiae* LIF1: a function involved in DNA double-strand break repair related to mammalian XRCC4. *EMBO J.* **14**: 4188-4198.

Hopfner KP, Craig L, Moncalian G, Zinkel RA, Usui T, Owen BA, Karcher A, Henderson B, Bodmer JL, McMurray CT, Carney JP, Petrini JH, Tainer JA (2002), The Rad50 zinc-hook is a structure joining Mre11 complexes in DNA recombination and repair. *Nature* **418**: 562-566.

Hyrien O (2000), Mechanisms and consequences of replication fork arrest. *Biochimie* **82**: 5–17.

Interthal H, Heyer WD (2000), MUS81 encodes a novel helix-hairpin-helix protein involved in the response to UV- and methylation-induced DNA damage in *Saccharomyces cerevisiae*. *Mol.Gen.Genet.* **263**: 812-827

Ira G, Pellicioli A, Balijja A, Wang X, Fiorani S, Carotenuto W, Liberi G, Bressan D, Wan L, Hollingsworth NM, Haber JE, Foiani M (2004), DNA end resection, homologous recombination and DNA damage checkpoint activation require CDK1. *Nature* **431**: 1011-1017.

Ivanov EL, Haber JE (1995), RAD1 and RAD10, but not other excision repair genes, are required for double-strand break-induced recombination in *Saccharomyces cerevisiae*. *Mol Cell Biol* **15**: 2245-2251.

Ivessa AS, Lenzmeier BA, Bessler JB, Goudsouzian LK, Schnakenberg SL and Zakian VA (2003), The Saccharomyces cerevisiae helicase Rrm3p facilitates replication past nonhistone protein-DNA complexes. *Mol. Cell* **12**: 1525-1536.

Ivessa AS, Zhou JQ, Zakian VA (2000), The Saccharomyces Pif1p DNA helicase and the highly related Rrm3p have opposite effects on replication fork progression in ribosomal DNA. *Cell* **100**: 479-489.

Ivessa AS, Zhou JQ, Schulz VP, Monson EK, Zakian VA (2002), Saccharomyces Rrm3p, a 5' to 3' DNA helicase that promotes replication fork progression through telomeric and subtelomeric DNA. *Genes Dev.* **16**: 1383-1396.

Johzuka K, Horiuchi T (2002), Replication fork block protein, Fob1, acts as an rDNA region specific recombinator in S. cerevisiae. *Genes Cells.* **2**: 99-113.

Junop MS, Modesti M, Guarne A, Ghirlando R, Gellert M, Yang W (2000), Crystal structure of XRCC4 DNA repair protein and implications for end joining. *EMBO J.* **19**: 5962–5970.

Kaliraman V, Brill SJ (2002), Role of SGS1 and SLX4 in maintaing rDNA structure in Saccharomyces cerevisiae. *Curr. Genet.* **41**: 389-400.

Kaliraman V, Mullen JR, Fricke WM, Bastin-Shanower SA, Brill SJ (2001), Functional overlap between Sgs1-Top3 and the Mms4-Mus81 endonuclease. *Genes Dev.* **15**: 2730-2740.

Karathanasis E,Wilson TE (2002), Enhancement of *Saccharomyces cerevisiae* end-joining efficiency by cell growth stage but not by impairment of recombination. *Genetics* **161**: 1015–1027.

Katou Y, Kanoh M, Bando H, Noguchi H, Tanaka T, Ashikari K, Sugimoto and K Shirahige, (2003), S-phase checkpoint proteins Tof1 and Mrc1 form a stable replication-pausing complex. *Nature* **424**: 1078–1083.

Kegel A, Sjostrand JOO, Astrom SU (2001), Nej1p, a cell type-specific regulator of nonhomologous end-joining mutants in *S.cerevisiae*. *Science* **294**: 2552-2556.

Kobayashi T (2003), The replication fork barrier site forms a unique structure with Fob1p and inhibits the replication fork. *Mol Cell Biol.* **23**: 9178-9188.

Kobayashi T, Heck DJ, Nomura M, and Horiuchi T (1998), Expansion and contraction of ribosomal DNA repeats in *Saccharomyces cerevisiae*: requirement of replication fork blocking (Fob1) protein and the role of RNA polymerase I. *Genes Dev.* **12**: 3821-3830.

Kobayashi T, Hirouchi T (1996), A yeast gene product, Fob1 protein, is required fro both replication fork blocking and recombinational hotspot activities. *Genes Cells* **1**: 465-474.

Kobayashi T, Nomura M, Horiuchi T (2001), Identification of DNA cis elements essential for expansion of ribosomal DNA repeats in *Saccharomyces cerevisiae*. *Mol Cell Biol.* **21**: 136-147.

Kobayashi T, Horiuchi T, Tongaonkar P, Vu L, Nomura M (2004), SIR2 regulates recombination between different rDNA repeats, but not recombination within individual rRNA genes in yeast. *Cell* **117**: 441-453.

Kraus E, Leung WY, Haber JE (2001), Break induced replication:a review and an example in budding yeast. *PNAS* **98**: 8255-8262.

Kysela B, Doherty AJ, Chovanec M, Stiff T, Ameer-Beg SM, Vojnovic B, Girard PM, Jeggo PA (2003), Ku stimulation of DNA ligase IV-dependent

ligation requires inward movement along the DNA molecule. *J Biol Chem.* **278**: 22466-22474.

Laroche T, Martin SG, Gotta M, Gorham HC, Pryde FE, Louis EJ, Gasser SM (1998), Mutation of yeast Ku genes disrupts the subnuclear organization of telomeres. *Curr. Biol* **8**: 653-656.

Laval J (1996), Role of DNA repair enzymes in the cellular resistance to oxidative stress *Pathol. Biol.* **44**: 14–24.

Lee J, Desiderio S (1999), Cyclin A/CDK2 regulates V(D)J recombination by coordinating RAG-2 accumulation and DNA repair. *Immunity* **11**: 771-781.

Lee SE, Pâques F, Sylvan J and Haber JE (1999), Role of yeast SIR genes and mating type in directing DNA double-strand breaks to homologous and non-homologous repair paths *Curr. Biol.* **9**: 767–770.

Leonce S, Kraus-Berthier L, Golsteyn RM, David-Cordonnier MH, Tardy C, Lansiaux A Poindessous V, Larsen AK, Pierre A (2006), Generation of replication-dependent double-strand breaks by the novel N2-G-alkylator S23906-1. *Cancer Res.* **15**: 7203-7210.

Lieber MR, Ma Y, Pannicke U, Schwarz K (2004), The mechanism of vertebrate nonhomologous DNA end joining and its role in V(D)J recombination. Mol. Cell **3**: 817-26.

Liti G, and Louis EJ (2003), NEJ1 prevents NHEJ-dependent telomere fusions in yeast without telomerase. *Mol. Cell* **11**: 1373-1378.

Longtine MS, McKenzie A III, Demarini DJ, Shah NG, Wach A, Brachat A, Philippsen P, Pringle JR (1998), Additional Modules for Versatile and Economical PCR-based Gene Deletion and Modification in *Saccharomyces cerevisiae*. *Yeast* **14**: 953-961.

Lopes M, Cotta-Ramusino C, Pellicioli A, Liberi G, Plevani P, Muzi-Falconi M, Newlon CS, Foiani M (2001), The DNA replication checkpoint response stabilizes stalled replication forks. *Nature* **412**: 557-561.

Lundblad V, Blackburn EH (1993), An alternative pathway for yeast telomere maintenance rescues est1- senescence. *Cell* **73**: 347-360.

Martin SG, Laroche T, Suka N, Grunstein M, Gasser SM (1999), Relocalization of telomeric Ku and SIR proteins in response to DNA strand breaks in yeast. *Cell* **97**: 621-633.

McEachern MJ, Haber JE (2006), Break-induced replication and recombinational telomere elongation in yeast. *Annu. Rev. Biochem.* **75**: 111-135.

McElhinny SA, Snowden CM, McCarville J, Ramsden DA (2000), Ku recruits the XRCC4-ligase IV complex to DNA ends. *Mol Cell Biol.* **20**: 2996-3003.

Meek K, Gupta S, Ramsden DA, Lees-Miller SP (2004), The DNA-dependent protein kinase: the director at the end. *Immunol Rev.* **200**: 132-41. Review.

Merker RJ, Klein HL (2002), hpr1{Delta} affects ribosomal DNA recombination and cell life span in Saccharomyces cerevisiae. *Mol. Cell. Biol.* **22**: 421-429.

Mezard C, Nicolas A (1994), Homologous, homeologous, and illegitimate repair of double-strand breaks during transformation of a wild-type strain and a rad52 mutant strain of *Saccharomyces cerevisiae*. *Mol Cell Biol.* **14**: 1278-1292.

Michel B, Ehrlich SD, Uzest M (1997), DNA double-strand breaks caused by replication arrest. *EMBO J.* **16**: 430–438.

Michel B, Grompone G, Flores MJ, Bidnenko V (2004), Multiple pathways process stalled replication forks. *Proc Natl Acad Sci USA* **101**: 12783–12788.

Milne GT, Jin S, Shannon KB Weaver DT (1996), Mutations in two Ku homologs define a DNA end-joining repair pathway in S.cerevisiae. *Mol. Cell. Biol.* **16**: 4189-4198.

Mimori T, Akizuki M, Yamagata H, Inada S, Yoshida S, Homma M (1981), Characterization of a high molecular weight acidic nuclear protein recognized by autoantibodies in sera from patients with polymyositis-scleroderma overlap *J. Clin. Invest* **68**: 611-620.

Mohanty BK, Bastia D (2004), Binding of the Replication Terminator Protein Fob1p to the Ter Sites of Yeast Causes Polar Fork Arrest. *J. Biol. Chem.* **279**: 1932-1941.

Moore JK, Haber JE (1996), Cell cycle and genetic requirements of two pathways of nonhomologous end-joining repair of double-strand breaks in *Saccharomyces cerevisiae*. *Mol Cell Biol.* **5**: 2164-2173.

Moreau S, Ferguson JR, Symington LS (1999), The nuclease activity of Mre11 is required for meiosis but not for mating type switching, end joining or telomere maintenance. *Mol. Cell. Biol.* **19**: 556-566.

Moreau S, Morgan EA, Symington LS (2001), Overlapping functions of S.cerevisiae Mre11, Exo1 and Rad27 nucleases in DNA metabolism. *Genetics* **159**: 1423-1433.

Mortensen UH (1996), DNA strand annealing is promoted by the yeast Rad52 protein. *Proc Natl Acad Sci USA* **93**: 10729-10734.

Mullen JR, Kaliraman V, Ibrahim SS, Brill SJ (2001), Requirement for three novel protein complexes in the absence of Sgs1 DNA helicase in *Saccharomyces cerevisiae*. *Genetics* **157**: 103-118.

Myung K, Datta A, Chen C, Kolodner RD (2001), SGS1, the S.cerevisiae homolog of BLM and WRN, suppresses genome instability and homeologous recombination. *Nat Genet*. **27**: 113-116.

Nakada D, Matsumoto K, Sugimoto K (2003), ATM-related Tel1 associates with double-strand breaks through an Xrs2-dependent mechanism. *Genes Dev.* **17**: 1957-1962.

New JH, Sugiyama T, Zaitseva E, Kowalczykowski SC (1998), Rad52 protein stimulates DNA strand exchange by Rad51 and replication protein A. *Nature* **391**: 407-410.

Osborn AJ, Elledge, SJ Zou L (2002), Checking on the fork: the DNA-replication stress-response pathway. *Trends Cell Biol.* **12**: 509-516.
Osman F, Whitby MC (2007), Exploring the roles of Mus81-Eme1/Mms4 at perturbed replication forks. *DNA Repair (Amst).* **6**: 1004-1017.

Pages V, Fuchs RP (2003), Uncoupling of leading- and lagging-strand DNA replication during lesion bypass in vivo. *Science* **300**: 1300–1303.

Pâques F, Haber JE (1999), Multiple pathways of recombination induced by double-strand breaks in *Saccharomyces cerevisiae*. *Microbiol Mol Biol Rev.* **63**: 349-404.

Pardo B, Marcand S (2005), Rap1 prevents telomere fusions by nonhomologous end joining. *EMBO J.* **24**: 3117-3127.

Petukhova G, Sung P, Klein H (2000), Promotion of Rad51-dependent D-loop fomation by yeast recombination factor Rdh54/Tid1. *Genes Dev* **14**: 2206-2215.

Prakash, S Prakash L, Burke W, Montelone BA (1980), Effects of the RAD52 Gene on Recombination in *SACCHAROMYCES CEREVISIAE*. *Genetics* **94**: 31-50.

Rattray AJ, McGill CB, Shafer BK, Strathern JN (2001), Fidelity of mitotic double-strand-break repair in *Saccharomyces cerevisiae*: a role for SAE2/COM1. *Genetics*, **158**:109-122.

Riha K, Heacock ML, Shippen DE (2006), The role of the nonhomologous end-joining DNA double-strand break repair pathway in telomere biology. *Annu Rev Genet.* **40**: 237-277.

Roeder GS (1997), Meiotic chromosomes: it takes two to tango. *Genes Dev.* **11:** 2600-2621.

Rooney S, Sekiguchi J, Zhu C, Cheng HL, Manis J, Whitlow S, De Vido J, Foy D, Chaudhuri J, Lombard D, Alt FW (2002), Leaky Scid phenotype associated with defective V(D)J coding end processing in Artemis-deficient mice. *Mol Cell* **10**: 1379-1390.

Rothkamm K, Lobrich M (2002), Misrepair of radiation-induced DNA double-strand breaks and its relevance for tumorigenesis and cancer treatment. *Int J Oncol*. **21**: 433-440.

Rothstein R, Gangloff S (1995), Hyper-recombination and Bloom's syndrome: microbes again provide clues about cancer. *Genome Res*. **5**: 421-426.

Rothstein R, Gangloff S (1999), The shuffling of a mortal coil. *Nat Genet.* **22**:4-6

Rothstein R, Michel B, Gangloff S (2000), Replication fork pausing andrecombination or "gimme a break". *Genes Dev*. **14**: 1–10.

Roy R, Meier B, McAinsh AD, Feldmann HM, Jackson SP (2004), Separation-of-function mutants of yeast Ku80 reveal a Yku80p-Sir4p interaction involved in telomeric silencing. *J Biol Chem*. **279**: 86-94.

Sartori AA, Lukas C, Coates J, Mistrik M, Fu S, Bartek J, Baer R, Lukas J, Jackson SP (2007), Human CtIP promotes DNA end resection. *Nature*. **28**:754-761.

Schar P, Herrmann G, Daly G, Lindahl T (1997), A newly identified DNA ligase of *Saccharomyces cerevisiae* involved in RAD52-independent repair of DNA double-strand breaks. *Genes Dev*. **11**: 1912-1924.

Schiestl RH, Dominska M, Petes TD (1993), Transformation of Saccharomyces cerevisiae with nonhomologous DNA: illegitimate integration of transforming DNA into yeast chromosomes and in vivo ligation of transforming DNA to mitochondrial DNA sequences. *Mol Cell Biol*. **13:** 2697-2705.

Shinohara A (1998), Rad52 forms ring structures and co-operates with RPA in single-strand DNA annealing. *Genes Cells.* **3**: 145-156.

Sibanda BL, Critchlow SE, Begun J, Pei XY, Jackson SP (2001), Crystal structure of an XRCC4-DNA ligase IV complex. *Nat. Struct. Biol.* **8**: 1015–1019.

Sinclair DA, Millis K, Guarente L (1997), Accelerated aging and nucleolar fragmentation in yeast sgs1 mutants. *Science* **277**: 1313-1316.

Smogorzewska A, Karlseder J, Holtgreve-Grez H, Jauch A, de Lange T (2002), DNA ligase IV-dependent NHEJ of deprotected mammalian telomeres in G1 and G2. *Curr.Biol*. **12** 1635–1644.

Strathern JN, Klar AJS, Hicks JB, Abraham JA, Ivy JM, Nasmyth KA, McGill C (1982), Homothallic switching of yeast mating type cassettes is initiated by a double-stranded cut in the MAT locus. *Cell* **31**: 183-192.

Sugawara N, Haber JE (1992), Characterization of double-strand break-induced recombination: homology requirements and single-stranded DNA formation. *Mol Cell Biol.* **12**: 563-575.

Sulek M, Yarrington R, McGibbon G, Boeke JD, Junop M, (2007), A critical role for the C-terminus of Nej1 protein in Lif1p association, DNA binding and non-homologous end-joining. *DNA Repair (Amst)*

Sung P (1997), Yeast Rad55 and Rad57 proteins form a heterodimer that functions with replication protein A to promote DNA strand exchange by Rad51 recombinase. *Genes Dev* **11**: 1111-1121.

Sung P, Robberson DL (1995), DNA strand exchange mediated by a Rad51-ssDNA nucleoprotein filament with polarity opposite to that of RecA.*Cell* **82**: 453-461.

Sutherland BM, Bennett PV, Sidorkina O, Laval J (2000), A comprehensive review on BIR pathways and their relevance to telomere maintenance. *Proc. Natl. Acad. Sci. USA* **97**: 103-112.

Symington LS (2002), Role of RAD52 epistasis group genes in homologous recombination and double-strand break repair. *Microbiol. Mol. Biol. Rev.* **66**: 630–670.

Takai H, Smogorzewska A, de Lange T (2003), DNA damage foci at dysfunctional telomeres. *Curr. Biol*. **13**: 1549–1556.

Takata H, Tanaka Y, Matsuura A (2005), Late S Phase-Specific Recruitment of Mre11 Complex Triggers Hierarchical Assembly of Telomere Replication Proteins. *Mol Cell* **17**: 573-583.

Takeuchi Y, Horiuchi T, Kobayashi T (2003), Transcription-dependent recombination and the role of fork collision in yeast rDNA. *Genes Dev*. **17**: 1497–1506.

Tarsounas M, West SC (2005), Recombination at mammalian telomeres: an alternative mechanism for telomere protection and elongation. *Cell Cycle*. **4**: 672-674.

Teo SH, Jackson SP (1997), Identification of *Saccharomyces cerevisiae* DNA ligase IV: involvement in DNA double-strand break repair. *EMBO J.* **16**: 4788-4795.

Teo SH, Jackson SP (2000), Lif1p targets the DNA ligase Lig4p to sites of DNA double-strand breaks. *Curr Biol*. **10**: 165-168.

Tong AH, Evangelista M, Parsons AB, Xu H, Bader GD, Page N, Robinson M, Raghibizadeh S, Hogue CW, Bussey H, Andrews B, Tyres M, Boone C (2001), Systematic genetic analysis with ordered arrays of yeast deletion mutants. *Science* **294**: 2364-2368.

Trujillo KM, Roh DH, Chen L, Van Komen S, Tomkinson A, Sung P (2003), Yeast xrs2 binds DNA and helps target rad50 and mre11 to DNA ends. *J Biol Chem*. **278**: 48957-48964.

Trujillo KM, Sung P (2001), DNA structure-specific nuclease activities in the Saccharomyces cerevisiae Rad50*Mre11 complex. *J Biol Chem*. **276**: 35458-35464.

Tseng HM, Tomkinson AE (2002), A physical and functional interaction between yeast Pol4 and Dnl4-Lif1 links DNA synthesis and ligation in nonhomologous end joining. *J Biol Chem.* **277**: 45630-45637.

Tseng HM, Tomkinson AE, (2004), Processing and joining of DNA ends coordinated by interactions among Dnl4/Lif1, Pol4, and FEN-1. *J. Biol. Chem*. **279**: 47580–47588.

Tsukamoto J, Kato I, Ikeda H (1996), Effects of mutations of RAD50, RAD51, RAD52, and related genes on illegitimate recombination in *Saccharomyces cerevisiae*. *Genetics* **142**: 383–391.

Tsukamoto Y, Mitsuoka C, Terasawa M, Ogawa H, Ogawa T (2005), Xrs2p regulates Mre11p translocation to the nucleus and plays a role in telomere elongation and meiotic recombination. *Mol Biol Cell.* **16**:597-608.

Valencia M, Bentele M, Vaze MB, Herrmann G, Kraus E, Lee SE, Schar P, Haber JE (2001), NEJ1 controls non-homologous end joining in *Saccharomyces cerevisiae*. *Nature* **6**: 666-669.

Walker JR, Corpina RA, Goldberg J (2001), Structure of the Ku heterodimer bound to DNA and its implications for double-strand break repair. *Nature* **412**: 607-614.

Wang JC (1991), DNA topoisomerases: why so many? *J. Biol. Chem.* **266**: 6659–6662.

Warner JR (1989), Synthesis of ribosomes in *Saccharomyces cerevisiae*. *Microbiol Rev.* **53**: 256-271.

Watt PM, Louis EJ, Borts RH, Hickson ID (1995), Sgs1: a eukaryotic homolog of E. coli RecQ that interacts with topoisomerase II in vivo and is required for faithful chromosome segregation. *Cell*. **81**: 253-260.

Weitao T, Budd M, Hoopes LL, Campbell JL (2003), Dna2 helicase/nuclease causes replicative fork stalling and double-strand breaks in the ribosomal DNA of *Saccharomyces cerevisiae*. *J Biol Chem.* **278**: 22513-22522.

White CI, Haber JE (1990), Internediates of recombination during mating type switching in *S.cerevisiae*. *EMBO J* **9**: 663-673.

Wilson TE, Grawunder U, Lieber MR (1997), Yeast DNA ligase IV mediates non-homologous DNA end-joining. *Nature* **388**: 495-498.

Wu L, Davies SL, Levitt NC, Hickson ID (2001), Potential role for the BLM helicase in recombinational repair via a conserved interaction with RAD51. *J Biol Chem* **276**: 19375-19381.

Wu L, Davies SL, North PS, Goulaouic H, Riou JF, Turley H, Gatter KC, Hickson ID (2000), The Bloom's syndrome gene product interacts with topoisomerase III. *J Biol Chem.* **275**: 9636-9644.

Wu X, Wilson TE, Lieber MR (1999), A role for FEN-1 in nonhomologous DNA end joining: the order of strand annealing and nucleolytic processing events. *Proc Natl Acad Sci USA*. **96**: 1303-1308.

6. Acknowledgements

This thesis wouldn't have been possible without an input from many people.
Thank you all very much!

"<u>The big and important people</u>"
First, I would like to thank my supervisor, Primo Schär, for giving me the opportunity to be a part of his team. Thank you for the never-ending support, encouragement and many fruitful discussions.

I also thank Joe Jiricny for the great (scientific) atmosphere at the IMCR and for making me feel welcome in Switzerland, after I just moved in.

Many thanks to Michael Hengartner for being kind, cooperative and asking easy questions on the exam.

Big thanks goes to all of the collaborators on both of my projects: Gernot Herrmann, Susan Gasser, Heiko Schober, Jose Sogo and Martin Burkhalter for providing materials, help with performing experiments and exchanging ideas.

And of course, thanks to all the members of the Schär group, for sharing the good and the bad of lab-life. Special thanks goes to Olivier, my "yeast-buddy", for interesting discussion and particularly for reading and correcting my manuscripts. And Patric…well for no particular reason, I just promised him an honorary mention in this section

"<u>The small people", who touched my life in many beautiful ways</u>

I honor the place in You where the whole Universe resides,
I honor the place in You of love, of truth and peace,
I honor the place in You where if You are in that place in You and
I am in that place in me, there is only one of us.

Many thanks go to…
… Ueli Bläuer, for being as good of a teacher as he was a student and for making liters and liters of yeast media
….Miljen, for coming, for leaving and teaching me that "why the hell not" is always the right answer. Ej, frajeru, tko bi pomislio da cemo nas dva dojdeka iz pasivnih krajeva dogurat ovako daleko! We made it, babe!
…. Desa and Lidija for being the sisters I never had. Puno mi nedostajete!
…. Dieter Egli, for dragging me up all of those mountains
…. Nives Selak, the warm motherly type, for offering many words of comfort. Macko, sad cu konacno svaki put imat vremena za kavicu
…. Hendrik; Dank Du, heute liebe ich die schönen Sachen im Leben: bachata, einer guten Tasse Tee und die deutsche Sprache
…. Boris Lenhard for long hours in various museums and even longer ones on Skype
…. all of my friends, here, there and everywhere, for sticking around even after too many times being stood up for some "important" experiment
…. "half-literate Salsa kings"® of Basel, for doing what they do best
…. Agnieszka, for keeping me out of the harm's way. Your kindness, love and care have long gone crossed the borders of a frienship. Ja jestem tak szczęśliwya ze cię mam, Chiquita!
Finally, I would like to thank my loving parents, who never stopped insisting I'm smart. Starceki moji, hvala Vam sto ste uvijek bili tu za mene, makar I samo na drugom kraju telefonske zice. Hvala sto ste imali usi za slusanje, rame za plakanje I uvijek pravu dozu zdravog razuma da me stiti od nevolja.

7. Curriculum Vitae

Last name: First name: Date of Birth: Nationality:	KAIS Sanja 30.07.1979 Croatian

Education

June 1997	High-school graduation from XV gimnazija, Zagreb, Croatia
October 1997- October 2002	Studies of Molecular Biology at the Faculty of Science, University of Zagreb, Croatia
November 2001-April 2002	Visiting student at the Institute of Veterinary Biochemistry and Molecular Biology (Laboratory of Prof. I.Stagljar), University of Zurich, Switzerland
October 2002	**Bachelor of Science in Molecular Biology** at the Faculty of Science, University of Zagreb, Croatia; the practical part of the Diploma thesis was performed at the Institute of Veterinary Biochemistry and Molecular Biology (Laboratory of Prof. I.Stagljar), University of Zurich, Switzerland; diploma thesis title: Generation of the Genomic Library of Yeast Saccharomyces cerevisiae.
September 2003-December 2007	PhD studies of Molecular Biology at the University of Zurich, Switzerland (under supervision of Prof. P.Schär, PhD adviser Prof. J.Jiricny)

Conferences attended

Poster presentations:	- Swiss Meeting on Genome Stability; Uetendorf, Switzerland 2004 - USGEB Annual Meeting; Fribourg, Switzerland 2004 - Brupbacher symposium; Zurich, Switzerland 2005 - «Responses to DNA Damage»; Brighton, UK 2005
Oral presentations:	- RRR meeting; Zurich, Switzerland 2005 - Swiss Yeast Meeting; Basel, Switzerland 2006

Publications

Scheper W, Thaminy S, Kais S, Stagljar I, Romisch K. (2003): Coordination of N-glycosylation and protein translocation across the endoplasmic reticulum membrane by Sss1 protein; **J Biol Chem 278(39)**: 3798-8003

Hermann G, Kais S, Hoffbauer J, Shah-Hosseini K, Brüggenolte N, Schober H, Fäsi M, and Schär P (2007): Conserved interactions of the splicing factor Ntr1/Spp382 with proteins involved in DNA double-strand break repair and telomere metabolism; **Nucl. Acids Res.35**: 2321-2332

Kais S, Burkhalter MD, Sogo J, and Schär P: DNA double-strand breaks at the ribosomal replication fork barrier are fixed by both homologous recombination and non-homologous end-joining; **in preparation**